CHEMICAL REVIEWS

Review

pubs.acs.org/CR

Nanodiscs in Membrane Biochemistry and Biophysics

Ilia G. Denisov* and Stephen G. Sligar*

Department of Biochemistry and Department of Chemistry, University of Illinois, Urbana, Illinois 61801, United States

ABSTRACT: Membrane proteins play a most important part in metabolism, signaling, cell motility, transport, development, and many other biochemical and biophysical processes which constitute fundamentals of life on the molecular level. Detailed understanding of these processes is necessary for the progress of life sciences and biomedical applications. Nanodiscs provide a new and powerful tool for a broad spectrum of biochemical and biophysical studies of membrane proteins and are commonly acknowledged as an optimal membrane mimetic system that provides control over size, composition, and specific functional modifications on the nanometer scale. In this review we attempted to combine a comprehensive list of various applications of nanodisc technology with systematic analysis of the most attractive features of this system and advantages provided by nanodiscs for structural and mechanistic studies of membrane proteins.

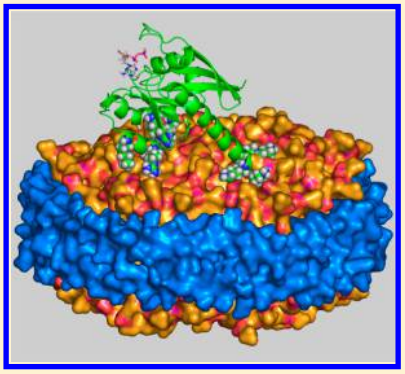

CONTENTS

1. INTRODUCTION TO NANODISCS

Membrane proteins are represented by a tremendous variety of sizes, structures, and functions, including complex supramolecular hierarchical assemblies with dozens of proteins forming sophisticated molecular machines. They perform most

Received: October 10, 2016
Published: February 8, 2017

DOI: 10.1021/acs.chemrev.6b00690
Chem. Rev. 2017, 117, 4669−4713

important cellular functions, including oxidative phosphorylation and proton pumping, ATP synthesis, transport of metabolites, intra- and inter cellular signaling, membrane fusion and communication between cell compartments, the biosynthesis of many compounds including lipids, steroid hormones, and their derivatives, and the breakdown of xenobiotics and internal metabolites. Developmental processes, including cell motility, adhesion, recognition, neuronal patterning, and many other critical events, are all conducted by membrane proteins. Membrane proteins provide the first line of sensing and defense for the cell response to injury, environmental stress, and viral infections and are directly involved in many other processes essential for cell function. The biophysics, biochemistry, structural biology, and cell biology of membrane proteins represent a very broad and significant part of modern life science research. Four Nobel prizes in the last 15 years were awarded for the discoveries in the field of membrane proteins: 2003 and 2012 in chemistry and 2004 and 2013 in physiology and medicine.

Investigations centering on membrane biophysics and biochemistry are vast, and include structural studies using a variety of techniques, efforts to reveal overall dynamics and functionally important motions, defining the affinity and selectivity of ligand binding, both as substrates and allosteric modulators, goals of understanding the chemistry of enzymatic catalysis, the nature of energy transduction, and the generation of motility and the movement of ions and molecules by transporters and channels. Often these critical cellular functions are conducted by supra-molecular complexes of protein, lipid, and nucleic acid, such as those systems in light harvesting photosynthesis, nucleic acid, protein and polymer synthesis, the sensing and motion of bacteria and eukaryotic cells and intercompartmental communication. Some of these properties can be studied using purified proteins in the absence of a lipid bilayer, either in detergents or other nonbilayer mimetics to avoid aggregation. However, many of the aspects critical for membrane protein structure and function depend on the lipid environment.

Most membrane proteins are denatured or display altered activity if removed from their native bilayer. Sometimes specific lipids are required for membrane-centered processes such as the blood coagulation cascade enabled by exposure to an anionic surface. The regulatory role of cardiolipin in the function of some transporters, roles for phosphoinositides in the recruitment of activating proteins that control the formation of focal adhesions in cell migration, and the formation of complex signaling structures mediated by electrostatic factors are a few examples. Appropriate analysis of these systems requires experimental methods that allow measurements in the presence of lipid bilayers or replacing them by various membrane mimetic systems.[1−8] In the past, this has been limited to the use of vesicles and liposomes as they provide an inside vs. outside compartmentalization and a large bilayer area that can allow mobility of multiple proteins and lipids, if diffusion or formation of multiprotein complexes is needed. However, there are many challenges when using vesicle systems. In many cases the resultant samples are turbid, viscous, unstable for extended periods of time, precipitate and have a tendency to segregate into phase separated domains, both in terms of composition and structural heterogeneity. The extensive literature on liposomes and vesicles will not be reviewed in this contribution. Bicelles and similar extended bilayer structures have been successfully used in some NMR applications, although the difficulty in controlling size and avoiding fusion is sometimes problematic.[9,10] It is with these limitations in mind that nanodiscs[11,12] have provided an alternative approach that has enabled molecular investigations and structure−functional studies of membrane proteins. Nanodiscs are now a commonly accepted method of choice for a large variety of biophysical and biochemical studies. In addition, as will be discussed in this review, nanodiscs provide a means for generating a stable library of soluble nanoparticles that faithfully reflect the membrane proteome and thus find use in high-throughput screening and diagnostic applications. By providing a home for recalcitrant membrane proteins, nanodisc technology has also found extensive use in the isolation, purification, and solubilization of membrane proteins for preparative and analytical methods. As will also be described, nanodiscs have also found direct application in therapeutic delivery and in generating controlled immune responses.

2. STRUCTURE AND ASSEMBLY OF NANODISCS

2.1. Nanodisc System

Nanodiscs are composed of phospholipids and an encircling amphipathic helical belt protein, termed a membrane scaffold protein (MSP; Figure 1).

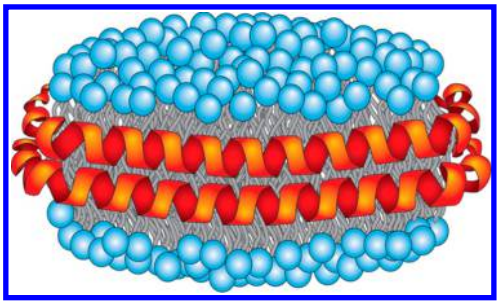

Figure 1. Nanodiscs are discoidal lipid bilayer stabilized by encircling amphipathic helical scaffold proteins termed membrane scaffold protein (MSP). Reproduced with permission from ref 22. Copyright 2014 CRC Press.

The initial MSP sequences used were based on the human ApoA1 protein component of high density lipoprotein particles, although proteins and peptides of similar amphipathic structure can also form discoidal bilayers.[13] These include synthetic amphipathic peptides,[14−16] apolipophorin and other apolipoproteins, such as ApoE3, ApoE4, and ApoCIII.[17−21] We will discuss in detail the optimization of MSPs for generating stable and useful discoidal bilayers of defined size and composition. This review focuses on the evolution of two general, now widely used, applications of nanodiscs: The use as a membrane surface of controlled composition, and in the self-assembly of membrane proteins into the discoidal bilayer that renders the target protein soluble and monodisperse. When we discovered the self-assembly of membrane proteins into nanodiscs over 10 years ago, we initially thought of this as an immediate solution to a roadblock in our own research efforts. Their broad applicability, however, has revealed an amazingly wide range of applications, from blood coagulation and cancer signaling, supramolecular machines located in the membrane for photosynthesis and energy generation, to detailed studies of G-protein coupled receptors, integrins, enzymes, and transporters. In searching the literature we find over 550 publications (through the end of 2016) that use the nanodisc

DOI: 10.1021/acs.chemrev.6b00690
Chem. Rev. 2017, 117, 4669−4713

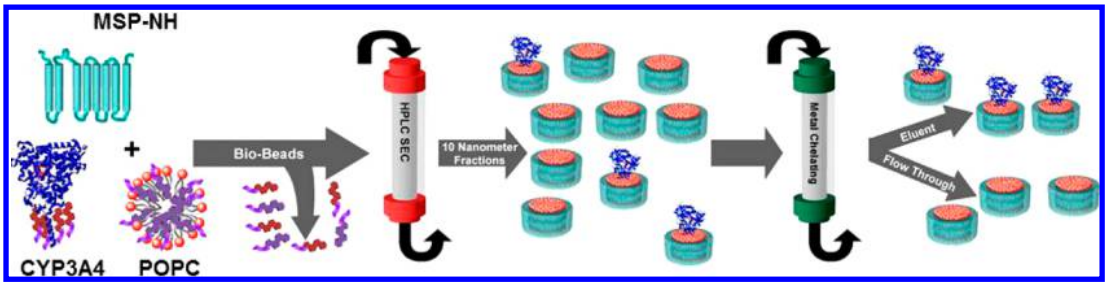

Figure 2. Schematic descriptions of the self-assembly process where detergent solubilized target, lipid, and membrane scaffold protein yield nanodiscs with incorporated membrane protein upon removal of detergent. Reprinted with permission from ref 314. Copyright 2004 Elsevier.

technology to advance the understanding of membrane proteins, and many reviews have discussed various aspects of nanodisc applications.[11,12,22−29] A goal of this review is to provide an entry point to this now vast field of nanodisc applications.

There is a rich literature describing lipoprotein particles formed with a combination of proteins and lipids. The structure, stability and physiological function of human lipoproteins circulating in blood plasma continues to be of major interest in medicine, notably through their involvement in cardiovascular diseases. These particles have a variety of protein, lipid and cholesterol compositions. High density lipoproteins (HDL) consist of lipids and cholesterol and the major apolipoprotein ApoA1, and can assume a variety of structural shapes.[30] From synthesis in the liver, the amphipathic ApoA1 protein associates with lipids and fatty acids, and progresses through a "lipid-free" form, a discoidal bilayer structure to spherical "balls" of lipid, cholesterol and cholesterol esters as it carries out forward and reverse transport functions. The transient discoidal form of HDL offers opportunities as a prototypical nanoscale lipid bilayer that is soluble in aqueous solution, and in the late 1990s we were struck by the potential of using such a system to provide a surface of precisely defined composition. Although doubtful at first, the thought that a membrane protein could also be self-assembled into such a nanometer scale entity that was then soluble in aqueous solution was compelling, as it could be enabling in the investigation of the structure and function of membrane protein targets. A clear bifurcation occurred in these research directions between the path of understanding atherosclerosis and HDL structure on the one hand, and the engineering of the ApoA1 protein to provide homogeneous particles of defined size and composition useful for self-assembling membrane proteins into the bilayer and thus enabling subsequent biochemical and biophysical efforts. Thus these are two separate fields: The structure and function of lipoproteins in cardiovascular areas on the one hand, and the determination of the structure and mechanisms of membrane proteins incorporated into or interacting with nanodiscs of defined composition. This review will not attempt to provide linkages to the former literature, but rather quote relevant experiments with HDL particles that contribute to understanding the structure of nanodiscs.

2.2. Self-Assembly of Nanodiscs

Nanodiscs, along with surfactant micelles, bicelles, liposomes, and many other colloid systems, belong to the interesting class of self-assembled molecular particles with emergent structures which exist in dynamic equilibrium with their environment, potentially exchanging their components with other similar particles. Unlike most of other self-assembled systems, nanodiscs are more stable and structurally better defined due to strong interactions between the scaffold proteins and lipids. The very low solubility of the lipids in water defines a slow lipid exchange between nanodiscs in solution and the stability of the lipid-bound encircling membrane scaffold protein (MSP) amphipathic helix contributes to a resistance of nanodiscs to aggregation at ambient conditions. The self-assembly of nanodiscs is founded on the strong tendency of phospholipids to form bilayers and on the enhanced stability of amphipathic helix structure of scaffold protein due to interaction with lipid acyl chains. Apparently, the nanodisc structure is not the most thermodynamically stable state of the mixture of lipids and scaffold protein in aqueous solution, because lipid and protein components tend to separate irreversibly after prolonged incubation at high temperature.[31] At physiological temperatures, however, even metastable nanodiscs can be used at ambient and physiological temperatures and can be stored for months at 4 °C with minimal aggregation (unpublished observation).

Empty nanodiscs and nanodiscs with incorporated membrane proteins (MP) can be assembled from a detergent solubilized mixture of all components by gradual removal of detergent via adsorption on hydrophobic beads or by dialysis.[11,32] (Figure 2).

This self-assembly protocol is relatively flexible, so that while specific details may vary, the yield and properties of the final product can be optimized by tuning of the important parameters. These include temperature, time, and amount of hydrophobic sorbent used for the amount and properties of the detergent(s) used, as will be discussed. The choice of detergent for incorporating a membrane protein target into nanodiscs depends on the properties of the membrane protein. Thus, the stoichiometric ratio of scaffold protein, lipids and target membrane protein, as well as the mode of incorporation into the bilayer and the preferred monomeric or oligomeric state of the target in the nanodisc needs to be addressed. Finally, the overall solvent composition, the presence of cofactors or substrates for stabilization of the membrane protein, specific metal ions, and agents such as glycerol or other cosolvents are also factors in the control of efficient self-assembly.

Important also is the effectiveness of the isolation and purification methods used to obtain the final product, whether it is chromatography, density ultracentrifugation, electrophoresis, or other methods. With certain proteins and detergents, some atypical difficulties may be faced due to their specific properties. For instance, the binding of some hydrophobic components to BioBeads was reported[33,34] when a cell-free expressed membrane protein was incorporated in nanodiscs, and an alternative sorbent was used to improve the overall yield of incorporated target. The extent of such side reactions may also strongly depend on the relative amount of

DOI: 10.1021/acs.chemrev.6b00690
Chem. Rev. 2017, 117, 4669−4713

all components present, the conditions of assembly, and the time span used for detergent removal. The method of reconstitution of high-density lipoproteins (rHDL) by removal of detergent from the solubilized mixture of lipids and scaffold protein was pioneered and developed by Jonas et al.[35,36] as an alternative to the direct solubilization of liposomes by apolipoproteins. The latter approach is less efficient, may require sonication and heating or cooling to temperatures above or below the temperature of the main phase transition depending on the lipid used, and usually yields a more heterogeneous size distribution of lipoprotein particles. Reproducible detergent-assisted methods are commonly accepted and widely used for structural studies of HDL lipoproteins.[13,37] However, ApoA1 does not produce monodisperse HDL particle sizes[38,39] and by changing the lipid:ApoA1 stoichiometry it was possible to generate rHDL with varying and broad size distributions.[17] This size heterogeneity of reconstituted discoidal HDL particles, as well as the common spherical forms of HDL found in human blood plasma, may be an intrinsic property important for HDL function[40−43] but undesirable as a biophysical tool. On the other hand, using engineered MSP proteins, a very high yield of monodisperse lipoprotein particles can be obtained if one is careful to use the optimal lipid:protein stoichiometry.[11,44]

Reconstituted high-density lipoproteins (HDL) have been studied by various physical and chemical methods in the 1950s and early 1960s, and their general structural characteristics have been extensively reviewed.[45−47] HDL particles contain a single major protein component, ApoA1, and it was established that both lipid and protein are highly accessible to various reactive probes in solution and that the protein becomes predominantly helical in HDL vs the ∼45% helicity in the lipid-free form.[48] Based on the analysis of the ApoA1 helical structure, Segrest et al.[49] suggested that the amphipathic character of these helices played a critically important role in forming protein−lipid interactions. It was also realized that these lipoproteins are very flexible and dynamic entities, with properties strongly dependent on the lipid composition. These early studies are thoroughly reviewed in refs 13, 37, and 50−52, and the physical structure of HDL particles was debated many years, with suggested spherical,[53] ellipsoidal,[54] or discoidal[55−57] models.

Other proteins and apolipoproteins also form amphipathic helices, and discoidal lipoprotein particles have been assembled with apolipophorins[58] and apomyoglobin.[59] Saposins can form small lipoprotein particles and were used to solubilize membrane proteins.[60−63] α-synuclein was shown to have amphipathic sequence and is able to form discoidal lipoprotein particles using DOPS, POPS, sphingomyelin,[64] or POPG,[65] although the presence of well-defined lipid bilayer phase in these particles was not addressed. Besides proteins, shorter oligopeptides also can be used to assemble soluble discoidal particles containing lipid bilayers[66−71] including the recent incorporation of membrane proteins such as cytochrome b5 and P450 CYP2B4.[72]

Using the engineered membrane scaffold protein (MSP) sequences to be described, nanodiscs have been successfully assembled with various synthetic lipids and with mixtures of lipids from natural sources. The most popular synthetic lipids used for nanodisc assembly include phosphatidylcholine (PC-lipids) DMPC,[73−76] DPPC,[77−80] POPC,[44,81−91] as well as mixtures of PC with charged phospholipids such as PS, PG, PE, and PIPs,[92−98] or biotinylated lipids for attachment to avidin-modified glass slides.[99] Multicomponent mixtures of various lipids and cholesterol sometimes are used in studies of membrane interaction and fusion, such as reported,[100] where nanodiscs were assembled with a mixture of POPC, DOPS, cholesterol, PIP2, and biotin−PEG−DSP to probe t-SNARE driven membrane fusion. A mixture of 40% POPC with 25% POPS and 35% L-α-phosphatidylinositol containing 17% arachidonic acid (AA, 20:4) and 13% dihomo-γ-linolenic acid (DGLA, 20:3) was used for nanodisc prepared in the study of lipoxygenase with both AA and DGLA being substrates for the enzyme.[101]

Alternatively, lipid mixtures from natural sources, such as *E. coli* polar lipid[102] or *E. coli* total lipids,[103,104] chicken egg PC lipids,[105,106] soy bean lipids,[107] and others have been used successfully to assemble nanodiscs and incorporate membrane proteins into the resultant bilayer. In addition, nanodiscs can be assembled directly from the cell membranes of the expression system[108,109] or from native tissue membranes[110] by solubilizing them in detergent and adding the appropriate MSP and lipid of choice. Subsequent removal of detergent using common methods, such as dialysis or absorption on hydrophobic sorbents, initiates self-assembly. Such an approach is especially useful for generating soluble libraries of membrane proteins[111,112] and in the analysis of membrane protein complexes.[62,113,114] (Figure 3)

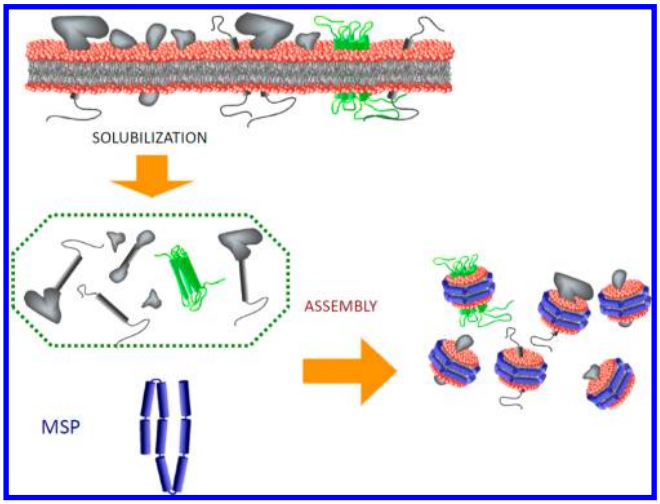

Figure 3. Soluble membrane protein library (SMPL) can be generated wherein membrane proteins can be directly assembled into nanodiscs from intact tissue.

Moreover, direct assembly of nanodiscs from native membranes, such as described for the pig kidney Na^+,K^+ ATPase,[110] provides an active target solubilized in a lipid environment similar or identical to that in a kidney cell and can be isolated as either a monomer or dimer. The first demonstration of this approach was reported when microsomal membranes from Sf9 cells overexpressing cytochrome P450 CYP6B1 from black swallowtail butterfly (*Papilio polyxenes*)[115] were solubilized in cholate and successfully used for nanodisc assembly without preliminary purification of the protein targets. Analysis of the lipid composition of the assembled nanodiscs showed similar fractions of PC, PE, and PI lipids that were present in the original Sf9 insect membranes.[116] Another example of direct solubilization of overexpressed cytochrome P450 CYP73A5 from *Arabidopsis thaliana* and cytochrome

DOI: 10.1021/acs.chemrev.6b00690
Chem. Rev. 2017, 117, 4669−4713

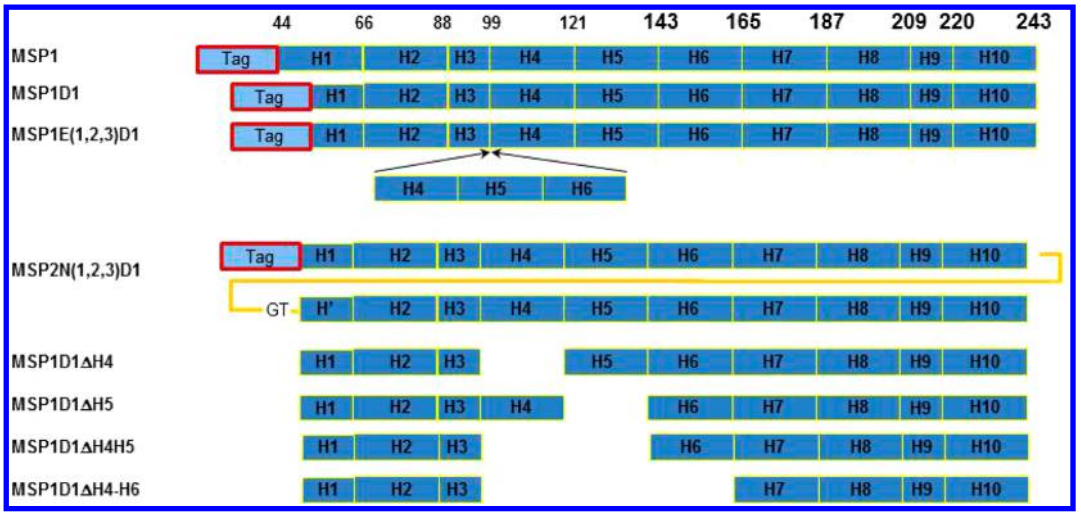

Figure 4. Schematic illustration of MSP sequences described in Table 1,[143] and those designed by Wagner et al.[128] MSP1D1 and extended scaffold proteins with several N-terminal affinity tags, as well as C-terminal modifications with biotin and FLAG-tag are available. Truncated MSP proteins form smaller nanodiscs and are especially useful for enhanced mobility and improved resolution of NMR spectra of incorporated membrane proteins.

P450 reductase from *M. domestica* in nanodiscs using microsomes prepared from Sf9 cells[117] demonstrated the viability of this approach.

Although many of the published examples follow our original protocols of nanodisc assembly from a cholate-solubilized mixture of lipids, MSP and target membrane protein, other detergents and detergent mixtures can be used. Examples of successful nanodisc assembly include cases where all components are solubilized in octyl glucoside,[118,119] Triton X-100,[24,120] β-decyl-maltoside,[121] dodecyl maltoside,[104,122−124] and CHAPS.[125] Refolding of membrane proteins in nanodiscs from an unfolded state via solubilization in SDS detergent was recently demonstrated by successful reconstitution of the homotetramer KcsA channel and bacteriorhodopsin.[126,127] NMR structures of bacterial outer-membrane protein OmpX in detergent DPC and in nanodiscs have been compared and point to the value of the membrane environment in determining structure.[128,129]

Detailed protocols for nanodisc reconstitution and general guidance for incorporation of membrane proteins in nanodiscs are available online at the Sligar laboratory Web site: http://sligarlab.life.uiuc.edu/nanodisc/protocols.html, and in multiple published reviews,[24,28,123,130,131] original papers,[44,73,74,132,133] and corresponding published Supporting Information sections. For example, many useful details are provided in the Methods section and in Supporting Information in ref 108. Several NMR studies have described optimization of nanodisc preparation and protein incorporation.[120,134,135] Preparation of nanodisc incorporated large protein complexes for cryo-EM studies is described in several recent studies.[136−139] An interesting example of direct incorporation of rhodopsin expressed in Sf9 cells by solubilization of membranes and subsequent removal of detergent in the presence of scaffold protein is presented.[109] Informative discussions of various aspects of nanodisc preparation are also provided in recent reviews.[140,141] For modeling purposes a recent version of web-based CHARMM-GUI modeling tool (http://www.charmm-gui.org) includes a nanodisc builder with a choice of nine different MSP proteins.[142]

2.3. Fundamental Structural Features of Nanodiscs

If a major objective is to form highly homogeneous, stable, and monodisperse nanodiscs with controlled size, modification of the original ApoA1 sequence of the amphipathic protein used in assembly is necessary. With this in mind, we undertook an extensive effort to generate variants based on the original human ApoA1 sequence. Although perhaps no longer of relevance to *in vivo* cholesterol transport, this yielded a variety of MSPs for use in providing a membrane surface of precise structure and in incorporating membrane proteins into the bilayer in their native conformation. As an example, we designed a series of extended scaffold proteins with one, two, or three additional 22-mer amphipathic helices inserted in the central part of MSP1 (designated MSP1E1, MSP1E2, and MSP1E3 correspondingly)[44] and studied the self-assembly of discoidal particles with the cylindrical fragment of the DPPC bilayer at the center, surrounded by each of these proteins of different size, as shown in Figure 4 and Table 1.

This work established the existence of an optimal molar lipid/MSP stoichiometric ratio, which is specific for a given pair of lipid and scaffold protein and determined by the mean surface area per lipid in the bilayer and the length of encircling MSP helical belt.[44] We thus established a well-documented method that provides a high yield of monodisperse lipoprotein particles, if assembly is performed at the optimal lipid/MSP ratio. If this ratio is lower or higher than optimal, the size and composition distributions of the resulting nanodiscs are broader, and their stability is compromised. In addition, the bilayer in under-lipidated lipoprotein particles may significantly deviate from planar structure and form saddle-shaped layers.[144,145] The lipid/MSP stoichiometry is also critical when incorporating membrane proteins into nanodiscs. In such cases, the number of lipids displaced by the target membrane protein from the nanodiscs bilayer must be estimated and subtracted from the initial number of lipids in the corresponding empty nanodiscs. This can be estimated using known properties of the components, or experimentally in small-scale preparations using various lipid/protein ratios. In the end, a high yield of monodisperse nanodiscs can be obtained, as quantitated by numerous methods including size-

DOI: 10.1021/acs.chemrev.6b00690
Chem. Rev. 2017, 117, 4669−4713

Table 1. Labels and Amino Acid Sequences of Membrane Scaffold Proteins Used for Self-Assembly of Nanodiscs[a]

Abbreviation	Description	Amino Acid Sequence
H1	Helix 1	LKLLDNWDSVTSTFSKLREQLG
H1Δ(1−11)	Truncated Helix 1	STFSKLREQLG
H1Δ(1−17)	Truncated Helix 1	REQLG
H2	Helix 2	PVTQEFWDNLEKETEGLRQEMS
H3	Helix 3	KDLEEVKAKVQ
H4	Helix 4	PYLDDFQKKWQEEMELYRQKVE
H5	Helix 5	PLRAELQEGARQKLHELQEKLS
H6	Helix 6	PLGEEMRDRARAHVDALRTHLA
H7	Helix 7	PYSDELRQRLAARLEALKENGG
H8	Helix 8	ARLAEYHAKATEHLSTLSEKAK
H9	Helix 9	PALEDLRQGLL
H10	Helix 10	PVLESFKVSFLSALEEYTKKLNTQ
FX	Original N-terminus	MGHHHHHHIEGR
TEV	Modified N-terminus	MGHHHHHHH DYDIPTTENLYFQG

Scaffold protein variant	Abbreviated name[b]	Composition
1	MSP1	FX-H1-H2-H3-H4-H5-H6-H7-H8-H9-H10
2	MSP2	FX-H1-H2-H3-H4-H5-H6-H7-H8-H9-H10-GT-H1-H2-H3-H4-H5-H6-H7-H8-H9-H10
3	MSP1E1	FX-H1-H2-H3-H4-H4-H5-H6-H7-H8-H9-H10
4	MSP1E2	FX-H1-H2-H3-H4-H5-H4-H5-H6-H7-H8-H9-H10
5	MSP1E3	FX-H1-H2-H3-H4-H5-H6-H4-H5-H6-H7-H8-H9-H10
6	MSP1D1	TEV- H1Δ(1−11)- H2-H3-H4-H5-H6-H7-H8-H9-H10
7	MSP1D2	TEV- H2-H3-H4-H5-H6-H7-H8-H9-H10
8	MSP2N1	TEV-H1Δ(1−11)-H2-H3-H4-H5-H6-H7-H8-H9-H10-GT- H1Δ(1−11)- H2-H3-H4-H5-H6-H7-H8-H9-H10
9	MSP2N2	TEV- H1Δ(1−11)- H2-H3-H4-H5-H6-H7-H8-H9-H10-GT- H2-H3-H4-H5-H6-H7-H8-H9-H10
10	MSP2N3	TEV-H1Δ(1−11)-H2-H3-H4-H5-H6-H7-H8-H9-H10-GT- H1Δ(1−17)- H2-H3-H4-H5-H6-H7-H8-H9-H10

[a]Reproduced with permission from ref 143. Copyright 2010 Oxford University Press. [b]Design of the membrane scaffold proteins. abbreviated names: (**1**) MSP1, membrane scaffold protein 1 with N-terminal hexa-histidine tag, followed by Factor X recognition site. (**2**) MSP2, fusion of two MSP1 molecules with short Glycine-Threonine linker and N-terminal hexa-histidine tag, followed by Factor X recognition site. (**3**−**5**) MSP1E1, MSP1E2, MSP1E3, extended membrane scaffold proteins, obtained via insertion of one (residues 56−77 of original MSP1), two (residues 56−99), or three (residues 56−121) extra 22-mer amphipathic helices after the residue Q55 into original MSP1 (**1**) sequence, as described (**10**). All have N-terminal hexa-histidine tag and Factor X recognition site. (**6**) MSP1D1, MSP1 with the first 11 N-terminal amino acids removed which contains the N-terminal hepta-histidine tag and TEV protease recognition site with linker. (**7**) MSP1D2, MSP1 with the first 22 N-terminal amino acids removed contains the N-terminal hepta-histidine tag and TEV protease recognition site with linker. (**8**−**10**) New MSP2 proteins based on MSP1 deletion mutants rather than original MSP1. All three have the same first MSP1D1 molecule, but vary in extent of truncation in the second MSP.

exclusion chromatography,[44] free-flow electrophoresis,[146] mass spectrometry,[147,148] and electron microscopy.[149]

Direct measurements of the lipid−protein stoichiometry in these particles demonstrated the dependence of this ratio on the length of the scaffold protein as dictated by the discoidal structure of the particles. The experimentally determined number of lipids in nanodiscs of different sizes is found to be proportional to the area of the circle inside the toroid belt formed by the helical MSP.[28,44] Similar results were obtained subsequently for nanodiscs prepared with other lipids and lipid mixtures using radioactively labeled lipids[92] or analysis by mass spectrometry.[147,150] In order to further optimize the formation of a unique size of nanodisc, we undertook a series of experiments where an increasing number of amino acids were deleted from the amino terminal of the parent MSP1 sequence.[44] By determining the resultant sizes of nanodiscs formed with the truncated proteins, it was learned that some of the N-terminal amino acids were not taking part in forming the encircling "belt" that stabilizes the bilayer in solution. This result was unanticipated given the extensive literature on related experiments with human apolipoproteins and pointed toward a rational engineering of membrane scaffold proteins for forming phospholipid nanostructures. A new series of MSP of various sizes and tags were generated where in all cases the first 11 residues were deleted (e.g., MSP1D1). The genes for bacterial expression of these constructs are made available through AddGene (https://www.addgene.org). Further structural studies confirmed that the length of MSP determines the diameter of nanodiscs and their size homogeneity. The details of this correlation strongly suggested that the MSP formed "belts"[13,56] rather than a "picket fence"[151] which was confirmed subsequently by solid state NMR,[152] electron microscopy, and other techniques.[153] A "belt" configuration of the membrane scaffold protein in nanodiscs, as well as in the analogous form of HDL particles, is now universally accepted. Very recently this "belt" configuraion of MSP was confirmed in the first high-resolution structure resolved using solution NMR of nanodiscs assembled with MSPΔH5 and DMPC.[154]

The cooperative formation of amphipathic helices upon the interaction of MSP with lipids contributes to the overall stability of nanodiscs, including their dynamics, as virtually no exchange of MSP between preformed nanodiscs is detected over a period of days to weeks (unpublished observation). Other scaffolds, such as the inherently polydisperse styrene maleic acid (SMA) polymers, or shorter amphipathic peptides[16,70,71,155] cannot maintain monodisperse size distribution, and these solubilizing agents dynamically exchange between particles.[16,156,157] Nanodiscs of various sizes can be assembled using MSP with appropriate length. Longer MSPs can be used to assemble nanodiscs up to ∼17 nm diameter.[143] Although even larger diameter discoidal bilayers could potentially be formed, these larger aspect ratio entities are much less stable, often collapsing to spherical aggregates. Optimizing and extending earlier studies, shorter MSPs with one or more helices deleted were designed by Wagner and colleagues for successful solution NMR studies, with the smaller nanodiscs displaying faster tumbling rates and improved spectral resolution.[120,128] A summary of the structure and composition of nanodiscs with various MSPs is provided in Table 1. Equation 1, based on the circular model of nanodisc[44,143] provides a quantitative relation between the length of the MSP protein "belt" and the number of lipids per one bilayer N, which is associated with the mean surface area per lipid S which is a function of the lipid type and phase transition temperature.

$$M = 2(\pi r + \sqrt{\pi N S})/L \quad (1)$$

DOI: 10.1021/acs.chemrev.6b00690
Chem. Rev. 2017, 117, 4669−4713

In this equation, M is the number of residues in the MSP helical belt around the lipid bilayer, r is the mean radius of MSP α-helix, estimated as 5.5 Å, and L is the helical pitch per MSP residue, taken to be 1.5 Å.[158] Excellent agreement of available experimental data obtained with DPPC and POPC with this model was obtained in ref 44 (Figure 5). Subsequently we demonstrated that results with larger nanodiscs also are in a good agreement with this equation.[143]

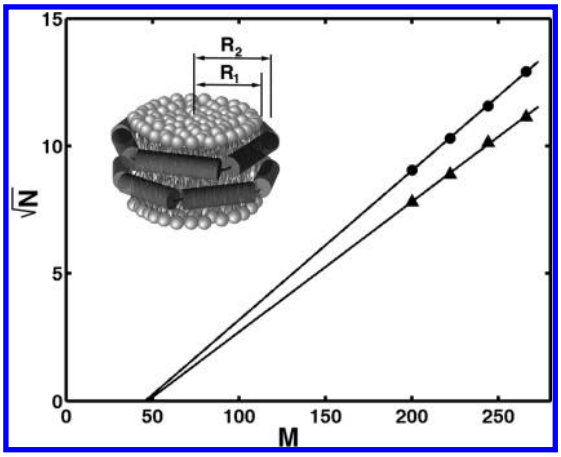

Figure 5. Experimentally determined number of optimally assembled lipids in nanodiscs (N), either DPPC (circles) or POPC (triangles), is correlated with the number of residues (M) in the encircling scaffold proteins. This demonstrated that the first portion of helix 1 was not involved key protein−lipid interactions. See eq 1, Table 1, and Figure 4.[143] Reprinted with permission from ref 143. Copyright 2010 Oxford University Press.

Although there is no X-ray structure of assembled nanodiscs, they have been characterized using multiple structural methods. Early transmission electron microscopy (TEM) often revealed stacked rouleau structures,[57,159] most likely because the heavy metal staining agents induced aggregation.[160] Multiple cryo-electron microscopy (cryo-EM) studies[149,161] and TEM studies[162] showing discoidal particles were reported. These studies provided clear images of single nanodiscs and allowed determination of precise size distributions.[162] Atomic force microscopy (AFM) provides another way to measure sizes and size distributions of nanodiscs absorbed on atomically flat surfaces, such as mica or gold.[77,78] Although one needs to be aware of potential tip artifacts, this method was used early on to demonstrate the heterogeneity of ApoA1 assembled discs.[78] Small angle solution X-ray (SAXS) and neutron (SANS) scattering have proven to be a powerful tool to reveal the structure of nanodiscs, with or without incorporated membrane proteins. Analysis of SAXS and SANS with various structural models is useful for monitoring the size and shape of nanodiscs in solution under various conditions. For example, SAXS was successfully used for establishing the structure of HDL particles[54] and nanodiscs[31,44] as a circular fragment of lipid bilayer enclosed by the amphipathic helical apo-lipoprotein or engineered membrane scaffold protein (MSP). A challenge with solution scattering methods is that one cannot directly apply an inverse Fourier transform to the experimental data to directly yield a 3D-structure, a model is necessary. More recent efforts have used exactly solvable continuum shell models that improved the fitting of SAXS/SANS data to yield shapes varying from circular discs to elliptical bilayers.[15,163−167] In addition, structural parameters of nanodiscs formed with DMPC/DMPG mixtures and pure DPPC or DMPC were obtained using neutron scattering from nanodiscs monolayer formed at water−air interface.[168,169] In all cases, the experimentally determined shape of self-assembled nanodiscs depends critically on the details of self-assembly, such as the exact lipid/protein stoichiometry and the temperature at which nanodiscs are assembled and characterized. Size exclusion chromatography is commonly used in protocols for the preparation of nanodiscs, as this simple method can provide a good estimate of size and polydispersity. Free flow electrophoresis can also be used as a preparative or analytical tool, combining separation by size and charge.[146,170] Other methods include dynamic light scattering and analytical ultracentrifugation,[171] and also fluorescence correlation spectroscopy.[27]

2.4. Physical Properties of Nanodiscs

Nuclear magnetic resonance (NMR) has been widely used to investigate the structure of nanodiscs and, as will be discussed, of membrane proteins inserted in the bilayer. Various NMR methods have been used to study empty nanodiscs. Solid state NMR (ss-NMR) revealed the detailed structure of the encircling MSP,[152] details of lipid-MSP interactions[172] and some of the physiologically important interactions of lipid head-groups with cations in solution.[95] In the first ss-NMR experiments, MSP was uniformly labeled with ^{13}C and ^{15}N, and nanodiscs assembled with unlabeled DMPC were precipitated using polyethylene glycol. High quality two-dimensional ^{13}C-^{13}C correlation spectra were measured using magic angle spinning (at a frequency of 10−12 kHz)[95,152] at various temperatures and with optimized experimental conditions.[152] The results of these investigations established the high conformational homogeneity of MSP in the assembled nanodiscs and revealed a predominantly helical conformation of the MSP. The configuration of the protein backbone was consistent with the "belt" model of MSP, rather than the "picket fence" configuration proposed in the earlier literature for rHDL particles.[151]

Further experimental studies addressed lipid dynamics in nanodiscs assembled using POPC, which has the main thermotropic phase transition at ∼270 K. By monitoring 1-D proton NMR spectra of lipids at various temperatures, one can observe this phase transition in nanodiscs at 276 K as a steep increase in the transverse relaxation time T_2. The slightly higher transition temperature in nanodiscs over that of larger vesicles is attributed to the restrictions imposed by the scaffold protein on the bilayer and was also observed in SAXS studies of the phase transition in nanodiscs formed with DPPC and DMPC.[31,173] It was also possible to measure $^{1}H-^{13}C-^{13}C$ 3D spectra with magnetization transfer between lipid acyl chain protons and solvent water to carbon atoms of MSP.[172] Partial assignment of signals from the MSP residues distinguished between residues in close contact with lipids (<4 Å) and those hydrated by solvent water. In agreement with the expected nanodisc structure, the charged and polar amino acid residues were on the preferentially hydrated surface of MSP, while hydrophobic residues were in contact with lipids on the internal side of the amphipathic helix.

Another important result was obtained using a combination of ssNMR and molecular dynamics simulation of the interactions of POPC/POPS mixed bilayers with solution cations such as Ca^{2+}.[95] The advantage of using nanodiscs for

DOI: 10.1021/acs.chemrev.6b00690
Chem. Rev. 2017, 117, 4669−4713

these studies is not only due to the fact that they form discs of well characterized lipid composition but also in their stability at physiological Ca^{2+} concentrations, even at high content of anionic lipid up to 90% PS. Vesicles with a fraction of PS lipids higher than ~30% undergo aggregation and fusion, making such experiments impossible. Divalent cations such as Ca^{2+} and Mg^{2+} often mediate protein−lipid interactions such as those involved in blood coagulation.[92,95,174] For example, it was demonstrated that, in the presence of Ca^{2+}, the head-groups of PS lipids specifically interact and form small dynamic domains.[95] In these domains PS head groups adopt well defined conformations, as shown by well resolved distinct NMR spectra, characteristic of two conformers, while the acyl chains are not restricted and retain mobility.[95] Dynamics and perturbation of lipids by proteorhodopsin incorporated in nanodiscs as measured by solid-state NMR study are described in an informative study.[34] Here, an increased order parameter of the DMPC acyl chains was found in nanodiscs as compared to liposomes both above (T = 300 K) and below (T = 270 K) the phase transition temperature.

Solution NMR experiments using HDL particles have been extensively reviewed,[175] including insights on rHDL structure and stability. HDL reconstituted with recombinant and ^{13}C-^{15}N labeled ApoA1 grown in D_2O were purified and the lipid-poor and lipid-saturated fractions characterized by circular dichroism (CD) under denaturation with GndHCl. An extensive purification was necessary to obtain monodisperse HDL for structural studies, and issues of complete size homogeneity may result in misinterpretation.[176] Other authors prepared rHDL from ApoA1 and POPC in the presence of cholesterol and characterized the size and composition at several stoichiometric ratios of ApoA1 and POPC.[177] In all cases significant poly dispersity was detected with the most homogeneous fraction of 9.6 nm rHDL particles being only 33% of the sample. This polydispersity of rHDL has been extensively documented using NMR and native gel electrophoresis.[39,178,179]

The rotational correlation times for nanodiscs assembled using MSP1D1 in aqueous solution at 45 °C were estimated to be ~55−60 ns,[180] thus making possible measurement of NMR spectra of membrane proteins in nanodiscs using TROSY pulse sequences and NMR spectrometers operating a fields of 800 MHz or higher. Even so, smaller nanodiscs would provide significant advantage for high-resolution NMR spectroscopy by increasing rotational mobility. Such modified nanodiscs were first introduced by Wagner and co-workers, who designed truncated MSPs by deleting up to three helices (66 amino acids) in the middle of the scaffold protein sequence.[128] These shortened scaffold proteins assembled ~7 nm nanodiscs with only ~10 DMPC molecules per leaflet.[128] Although the shape and overall size homogeniety may be less than ideal, this factor may be unimportant for structural studies of inserted membrane protein targets. The truncated MSPs used for the smallest nanodisc assembly has a length of 123 amino acids, i.e., a physical length of a corresponding helix ~18.45 nm, corresponding to a radius of the enclosed lipid circle ~2.45 nm, enough for optimal packing of ~27 lipids per leaflet (calculated using data provided at http://hydra.nat.uni-magdeburg.de/packing/cci/). These smaller nanodiscs were also significantly less stable than those constructed of the full length MSPs, and aggregated with time forming larger lipoprotein particles.[128] Perhaps, there is a limit for the smallest number of lipid molecules that is necessary to form a stable fragment of the lipid bilayer, which may be determined by some minimal number of lipid molecules inside this fragment. As schematically illustrated in Figure 6, with 27 lipids in smaller

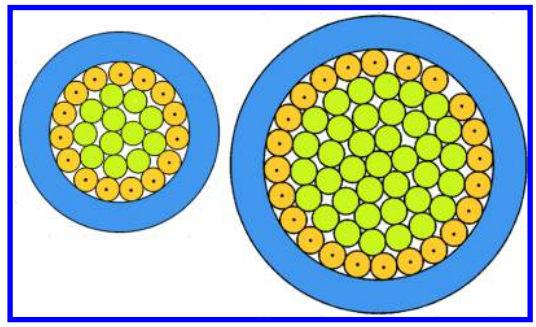

Figure 6. Lipid packing in small nanodiscs (27 lipids and 123 amino acids MSP) and the regular nanodiscs sized (60 lipids, 189 amino acids in MSP1D1). Boundary lipids interacting with MSP are marked with dots. See text for discussion.

nanodiscs, 55% are at the protein−lipid interface and 45% in the bulk lipid phase. For ~60 lipids in the normal nanodiscs, less than 40% interact with the MSP and more than 60% are in the bulk. Another contributing factor may be the limits of the bend radius of an α helix. With 22-mer helices in the MSP, there may be distorted regions at the helical junctions, which compromise stability. The goal of generating homogeneous nanodiscs of smaller size may be enabled by using amphipathic helices of shorter length between the Gly/Pro breakpoints found in the original ApoA1 sequence.[140]

Recently a large set of lipid mixtures were incorporated in nanodiscs in order to measure the total charge and electrophoretic mobility with various lipid compositions and ionic strengths (Na concentrations from 50 to 250 mM), four different pH values, and three temperatures.[96] Results obtained with MSP1D1 (126 lipids per disc, 63 per monolayer) and MSP1E3 (250 and 125 lipids per leaflet, respectively) are comparable. Nanodiscs with pure POPC and mixtures with POPS (10%, 30% and 70%), POPA (10%, 30% and 70%), POPE, and PIP2 (both 10% in POPC) were assembled at pH 7.4 in 50 mM Tris buffer containing 100 mM NaCl and studied in the presence or absence of 3 mM Ca^{2+} or 3 mM Mg^{2+}. This study provided a large amount of previously unavailable information about the polyelectrolyte nature of the charged head groups on lipid bilayers and the contribution of monovalent (Na^+) and divalent (Ca^{2+} or Mg^{2+}) counterions to the total electrostatic properties of mixed nanoscale lipid bilayers. Unlike the small effects observed with Na^+, specific interactions of divalent metal cations with the lipid head groups were observed, with the total charge of nanodiscs formed with POPC and POPS being perturbed significantly more by Ca^{2+} than by Mg^{2+}. The interaction of Ca^{2+} with POPA nanodiscs resulted in their partial aggregation, while no aggregation was observed in the presence of Mg^{2+}. An opposite effect was observed with nanodiscs containing PIP2 lipids, where aggregation was observed with Mg^{2+}, but not with Ca^{2+}. Overall, the electrostatic properties and charge measured in nanodiscs are in agreement with earlier results obtained using lipid vesicles, although a negative charge measured on POPE lipids was unexpected, and consistent with the behavior of PE lipids.[181] An important contribution of this study is the quantitative measurement of polyelectrolyte effect of the charged lipid bilayer surface in nanodiscs and the resulting deviation of measured total charge from that estimated by

DOI: 10.1021/acs.chemrev.6b00690
Chem. Rev. 2017, 117, 4669−4713

composition alone. For 30% and 70% POPS, total lipid charges were measured as −24.4 and −42.3, respectively, versus calculated values of −38 and −88. For 10% PIP2 nanodisc, the measured and compositional charges are −25.6 and −39, respectively.[96] This polyelectrolyte effect is stronger at high concentration of anionic lipids and is due to electrostatic interactions between charged groups which are separated by distances comparable to the Bjerrum length, which is ∼7 Å under conditions used in this study.

Free flow electrophoresis can be used for preparative or analytical separation of nanodiscs with various lipid compositions and also with incorporated membrane proteins. Application of this method was described using nanodiscs assembled with three scaffold proteins, MSP1D1, MSP1D1(-) without the His-tag, and MSP1E3D1, having slightly different pK_a, and hence charge, at neutral pH.[146] Nanodiscs containing pure POPC and either 10% or 25% POPG were well separated in a laminar flow with the electric field applied at 90 ° to the flow direction. Separation of two membrane proteins, cytochrome P450 reductase (78 kDa, calculated pI 5.06 and −22.9 charge at pH 7.0) and plasma membrane ATPase (100 kDa, pI 6.48, charge −3.5) incorporated in nanodiscs was very efficient, particularly for separation of nanodiscs with P450 reductase from empty nanodisc assembled with neutral POPC. This method offers a complementary approach from standard size-exclusion chromatography. For the ATPase, which is essentially neutral at pH 7.0, incorporation into nanodiscs containing 40% POPG resulted in displacement of charged lipids from the bilayer, and improved separation from the highly charged empty nanodiscs.

Native mass spectrometry of intact nanodiscs was first described in ref 147 and has been further developed.[150] Samples of nanodiscs, formed from either DMPC of POPC lipids, in ammonium acetate buffer were infused into a Fourier transform ion cyclotron resonance mass spectrometer with both collisionally activated and electron capture dissociation.[147] Multiple peaks observed in the experimental spectra were fitted using a model with various numbers of lipids per nanodisc. The results of 155 ± 2.4 DMPC molecules and 141 ± 2.6 POPC molecules per nanodisc are both in a good agreement with previously published data.[11,32,44,92] An additional parameter used in fitting mass spectrometry data is the number of tightly bound water molecules or ammonium cations (both having molecular mass 18 Da). These were on average six or five for DMPC or POPC nanodiscs, respectively. These results validate the application of native mass-spectrometry to the analysis of nanodiscs and membrane proteins in nanodiscs, with all parameters obtained for nanodiscs in the gas phase closely matching those observed in solution. In addition, by gradually increasing the voltage of the collisional activation step, it was possible to remove individual lipids from nanodiscs without complete dissociation of the lipoprotein complexes. This exciting result suggests the possibility of analyzing the boundary lipid surrounding membrane proteins incorporated in nanodiscs as well as potentially reveal functional domains within the nanobilayer.

Nanodisc mass spectrometry has been further advanced with incorporated membrane proteins.[113,148,182,183] Heterogeneous nanodiscs assembled with mixed lipids were analyzed for lipid composition by a combination of dual Fourier transform of the mass spectra and further deconvolution of m/z ratios into mass and charge coordinates during variation of the collisional activation voltage. A new algorithm developed for data analysis allowed automatic deciphering of multiple overlapping components with minimal user intervention.[148] Results demonstrated that, at low collision energy, nanodiscs assembled with DMPC and POPC in the gas phase have mass and collision cross-section energies very similar to the values known from solution studies. A different approach was used by Klassen and colleagues, who assembled smaller discoidal particles termed "picodiscs" using saposin as a scaffold protein[61,62,184,185] in order to analyze specific interactions of soluble proteins with glycosphingolipids in nanodiscs. Application of such discs for probing protein−lipid interactions will be described later in this review.

2.5. Molecular Dynamics Simulations of Nanodiscs

Insight into the mechanisms of nanodisc formation and the structural parameters of the lipid bilayer and encircling scaffold protein are provided by molecular dynamics (MD) simulations. A series of early 4.5 ns simulations of nanodiscs with 80 DPPC lipids per monolayer and three MSP proteins with different lengths found the most stable assemblies for the (Δ1−11) scaffold proteins MSP1D1 and (Δ1−22) MSP1.[186] These models were built using MSP protein helices arranged in a belt configuration, in agreement with available experimental data.[44] All of these simulations demonstrated stable lipoprotein discoidal complexes with main differences due to different lipid packing densities. The MSP1 nanodiscs with 200 amino acids in the MSP surrounding 80 DPPC lipids per leaflet showed a notable decrease of the mean surface area per lipid over the simulation time, indicating nonoptimal packing. On the other hand, nanodiscs assembled with (Δ1−11) and (Δ1−22) scaffold proteins were more stable in time and reproduced the experimentally determined surface area per lipid of 0.53 nm^2.[44] This again shows the importance of lipid packing in generating homogeneous discoidal particles. The first MD simulation of an incorporated membrane protein, bacteriorhodopsin (bR), in nanodiscs used an initial model built from the final equilibrated 4.5 ns (Δ1−11) MSP1 nanodisc simulation.[186] After placement of bR in the center of nanodiscs and removal of 20 lipids the entire complex was equilibrated for an additional 4.5 ns. Although the lipid bilayer remained flat with no out-of-plane deformation, the nanodisc structure gradually evolved from circular to more square shape (Figure 7).

The pathway of assembly and disassembly of nanodiscs with cholate was explored early on using coarse-grained (CG) simulations,[187,188] with initial results described in two previous publications.[189,190] Here the MSP models used in the assembly simulation corresponded to (Δ1−11) and (Δ1−22) MSP1

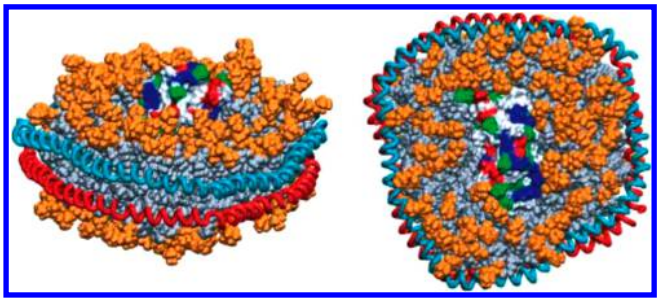

Figure 7. Molecular dynamics simulations of DPPC nanodiscs with incorporated bR monomer. Reprinted with permission from ref 186. Copyright 2005 Elsevier

DOI: 10.1021/acs.chemrev.6b00690
Chem. Rev. 2017, 117, 4669−4713

with 160 DPPC lipids per nanodisc. After detergent was removed in the simulation, the lipids collapsed as a single cluster, which then gradually rearranged into a bilayer fragment surrounded by two scaffold proteins. In one simulation, formation of a nearly ideal double-belt configuration of MSP was achieved, while in another a portion of one MSP did not contact lipids even after 9 μs.[187] In a separate work, solubilization of a preformed nanodisc by cholate was modeled by adding various numbers of cholate molecules (from 5 to 320 per nanodisc) to the simulation, and results were compared to experimental data obtained by small-angle X-ray scattering (SAXS).[188] Incorporation of cholate into nanodiscs in coarse-grained (CG) simulations reached equilibrium in 1- 2 μs. Both experimental and CG modeling results show that 5 or 10 molecules of cholate can be easily accommodated in one nanodisc without significant perturbation of the flat discoidal shape, and only minor increase in overall diameter of the disc. However, the addition of 50 molecules of cholate resulted in a significant increase in the nanodisc diameter, an opening of the scaffold protein belt and gradual transition to an out-of-plane distorted shape. This became more pronounced at 100 molecules of cholate per nanodisc. Experimental SAXS results at high cholate concentrations also showed a disappearance of the signature feature of the lipid bilayer and an increase in the measured radius of gyration. Finally, at 320 cholate molecules of cholate, nanodiscs are transformed to a spherical cluster of lipid and detergent all surrounded by MSP with an approximate diameter of 13.3 nm. Inspection of these structures in reverse order provides useful insight as to the potential sequence of structures occurring during the self-assembly of formation of discoidal nanodiscs from the spheroidal detergent micelles and vesicles.[188] These results were extensively reviewed in the context of the broad picture of the MD simulations of nanodisc and HDL structures, dynamics and function.[191−193]

Subsequently, several course grain (CG) molecular dynamics simulations of nanodiscs were used to compare discs of various structures and bicelles.[194−196] Useful observations were made based on comparison of all-atom and CG simulations of nanodiscs assembled with (Δ1−22) MSP1 and DMPC.[194] Both simulations revealed a high ordering of lipids in nanodiscs and lower configuration entropy as compared to liposomes under the same conditions, in agreement with NMR experimental data.[34] More ordered lipids were found in the center and perturbation of lipid conformations for those annular lipids due to the contact with scaffold protein was noted. A simulation of nanodisc self-assembly was also performed in a similar manner as in earlier work[187] but on a longer time scale (42 μs), with equilibrium reached within the first 20 μs.[194] Another study compared DMPC/DHPC bicelles and DMPC nanodiscs using CG simulations, and also included incorporation of an α-helical trans-membrane peptide KALP21 and a GPCR (rhodopsin) dimer.[196] In these simulations, the lipids in nanodiscs had smaller solvent accessible surface area than in bicelles, but slightly higher than in pure bilayers, indicating the presence of perturbation and of higher hydration at the MSP−lipid interface. When rhodopsin is incorporated into the lipid bilayer, the residence time of lipids in contact with the GPCR was significantly longer than in bicelles, in some cases reaching 1 μs, the limit of the simulation. Lipids at the dimer interface (involving the TM1, TM2, and TM7 trans-membrane helicies of rhodopsin) remained bound for longer times, indicating the presence of specific lipid−protein interactions and suggesting a possible matching of lipid size with cavities at the protein−protein interface. In addition, binding of DHPC to rhodopsin in bicell simulations was also observed at the regions exposed to solvent and not interacting with lipid, indicating potential artifacts for protein solubilized in bicellar systems.[196]

Recently, a new method for CG modeling of nanodiscs using extended MSP proteins and incorporated targets was developed by Tielemans group.[195] This work provided a method for efficiently building nanodiscs with MSP1 (200 amino acids), extended MSP1E1 (222 amino acids), and MSP1E2 (244 amino acids), with or without incorporated membrane proteins. These models can be used for equilibration and CG or all-atom simulations with a facile transition between the two systems of modeling. The number of lipids per disc, the mean surface area per lipid, and structure of the scaffold protein are three main input parameters that can be taken from experimental data. If two parameters are known, the third one can be predicted with reasonable precision. POPC, DMPC, and GM1 ganglioside lipids were used to model empty nanodiscs, and bR, OmpX, and the glucose transporter were incorporated in some models. Equilibrated structures of nanodiscs can be built based on the known structural parameters rather than obtained as a result of modeling the self-assembly process as the latter may be determined by metastable intermediates trapped at the kinetically stable local minimum of the energy landscape. Multiple simulations with varied input parameters gave a range of sizes and structures of nanodiscs depending on the length of MSP and number of lipids and is entirely consistent with the experimental results reported earlier.[44,73] Boundary lipids in contact with the scaffold protein are perturbed more than lipids in the center, and the average thickness of the bilayer is found to be higher in the center of nanodiscs, with the difference reaching more than 30% in some simulations (Table 1 in ref 195). Therefore, the mean area per lipid is larger at the periphery than in the center, and the average area per lipid is expected to be higher in smaller nanodiscs, because of the larger fractions of structurally perturbed boundary lipids. In all modeling exercises, both all-atom and CG simulations gave stable structures of MSP and incorporated membrane proteins and confirm the main conclusions derived from experimental data.

Importantly, all modeling studies reported perturbed circular structures, which in most cases can be approximated with slightly distorted polygons, and sometimes as elongated ellipsoidal shapes (see Figure 6B in ref 195), which were used for fitting SAXS results in the recent experimental publications.[15,164,165,197] While ellipsoidal shell models provide analytically solvable solutions which fit experimental SAXS and SANS results better than an ideal circular model, real nanodiscs are more likely to have slightly irregular centrosymmetric shapes with pronounced kinks at the proline residues separating helical fragments, as it can be seen in the recent NMR structure (pdb file 2N5E[154]). One study used a series of all-atom molecular dynamics (MD) simulations in parallel with experimental measurements to evaluate the immediate lipid environment of the heterodimer TAP (transporter associated with antigen processing) complex in nanodiscs assembled using *E. coli* polar lipids.[102] For model building, a mixture of POPE/POPG at a ratio of 3:1 approximates the native *E. coli* lipid composition, and a reference simulation was performed with TAP in POPC/POPG 3:1 bilayer. Both experimental and MD modeling results show that 22 lipids surrounding 12 trans-membrane helices of the TAP heterodimer are enough to form

DOI: 10.1021/acs.chemrev.6b00690
Chem. Rev. 2017, 117, 4669−4713

a lipid environment sufficient for fully functional transporter. Electron microscopy of TAP in nanodiscs was used for structural characterization of these assemblies.

The first all-atom MD simulation on the rHDL lipoprotein particle used a prearranged "picket-fence" model (since shown to be incorrect) and equilibrated it to evaluate the resulting structural parameters of truncated (Δ1−47) ApoA1 used in the model.[151] Theoretical modeling of HDL particles assembled with various derivatives of ApoA1 and other apolipoproteins was thoroughly reviewed by Pan and Segrest.[198] These authors provide an extensive list of references related to structural studies defining all stages of lipoprotein maturation starting from lipid-poor particles to the discoidal HDL particles containing mostly phospholipids and finally to spheroidal lipoprotein particles rich in cholesterol esters and triglycerides. This excellent review[198] should be referred to as a primary source of information on modeling of lipoprotein particles formed with natural lipoprotein as opposed to the engineered scaffold proteins covered in this review.

2.6. Overall Dynamics and Stability of Nanodiscs

The dynamics of lipid free MSP1D1 and MSP1D1 in nanodiscs assembled with DOPC was probed by hydrogen/deuterium exchange at 21 °C, pH 7.4 (pD 7.0).[199] MSP1D1 in nanodiscs showed much slower exchange than lipid-free scaffold protein on the short time scale, from 10 s to 30 min. However, a major fraction MSP1D1 reached the same level of H/D exchange after 2 h. The most protected fragments of MSP1D1 in nanodiscs contain residues 72−83, 115−126, and 127−137 (in the amino acid notation used in ref 199), which includes the His-tag and TEV protease recognition sequence. These residues correspond to numbers 61−82, 104−115, and 116−126 in the original Δ(1−43) ApoA1 sequence, and correspond to helices 4 and 5, and helices 6 and 7. The C-terminal helices 9 and 10, as well as the remaining part of N-terminal helix 1, were more dynamic and less protected from exchange by interacting with lipids in assembled nanodiscs, as compared to the lipid-free MSP1D1. Many local unfolding events were identified by analysis of H/D exchange kinetics of MSP1D1 in nanodiscs, and the extent of dynamic disordering was correlated to the proposed salt-bridges in the double-belt MSP1D1 structure.[199]

The thermodynamic stability of nanodiscs has been studied using differential scanning calorimetry (DSC), the state of the lipid bilayer by laurdan fluorescence, and the overall discoidal size by SAXS.[31] The presence of a clearly observed lipid phase transition in DMPC and DPPC nanodiscs confirmed the intact bilayer structure surrounded by the helical scaffold proteins. The lipid melting temperature T_m was slightly higher than in liposomes, which was attributed to the extra lateral pressure provided by the scaffold protein at elevated temperatures, where protein helices had to extend following thermal expansion of the bilayer. In addition, the thermodynamic properties of a significant fraction of lipids were perturbed due to their interaction with the scaffold protein at the perimeter of nanodiscs. On average, the structure of these lipids is slightly different from the bulk lipids at the center of nanodisc bilayer, as noted earlier in describing MD simulations[31,186] and NMR measurements.[95] Subsequently, SAXS measurements were repeated at various temperatures to probe the lipid phase transition in more detail and with much larger nanodiscs assembled with MSP2 scaffold proteins.[143] These experiments confirmed the presence of a fraction of lipids with perturbed properties at the protein−lipid interface. In larger nanodiscs the relative fraction of these lipids is significantly smaller, and the phase transition is considerably sharper, consistent with the general explanation suggested in the earlier work.[31]

Lipid packing and mobility in nanodiscs was examined using Laurdan fluorescence, with on average less than one fluorescent probe per nanodisc in order to minimize perturbation caused by the dye. Laurdan fluorescence is sensitive to dipolar relaxation of the solvent molecules on the nanosecond time scale and is commonly used as a sensitive probe for dynamic properties of lipid bilayers.[200,201] These results demonstrated that DMPC and DPPC lipid nanodiscs undergo the same thermotropic transition as observed in vesicles, thus indicating the full-scale transition from the strongly restricted dynamics below T_m to the highly mobile and fully hydrated state above T_m.[31,173] Comparison with literature data[202] confirmed the presence of an intact bilayer fragment in nanodiscs with the structural and dynamic properties very similar to the properties of lipid vesicles with the same composition. Note that lipid nanoparticles solubilized using styrene-maleic acid (SMA) copolymers (SMALP) did not show such well-defined phase transition as monitored by DSC,[203,204] the mobility of spin-labels,[204] or by Laurdan fluorescence measurements.[156] Specifically, in SMALP particles, no sharp increase in lipid mobility could be observed at temperatures above T_m, suggesting that most of the lipids in these particles interact with SMA copolymer and do not form a bulk lipid bilayer with dynamic properties similar to those observed in liposomes and vesicles. The strong interactions of SMA with lipids and absence of free polymer even at high polymer content in SMALPs[205] also suggest that a major fraction of the lipids are involved in direct interactions with the SMA copolymer and cannot form a fragment of unperturbed lipid bilayer.

Various aspects of nanodisc structure, stability, and other properties were systematically studied by assembling nanodiscs with varying mixtures of neutral and charged lipids. The stability of nanodiscs with respect to thermal unfolding and prolonged storage was compared for discs with binary mixtures of zwitterionic DMPC, negatively charged DMPA or DMPG, and with the synthetic cationic lipid DMTAP.[206] A high yield of nanodiscs could be obtained for all mixtures of DMPC and DMPG, but DMPA at higher than 25% fraction and DMTAP at more than 10%, destabilized nanodiscs and precipitated at high concentrations. On the other hand, 25% DMPG stabilized nanodiscs with respect to prolonged storage and to thermal denaturation probed as by DSC.

Lipid exchange between nanodiscs assembled with MSP1E3D1 and bicelles was studied using DMPC/DHPC bicelles and nanodiscs containing lipids with FRET donors and acceptors.[207] Lipid transfer was monitored by gradual disappearance of FRET, and Arrhenius dependence of rate revealed a high activation energy, 28 kcal/mol, measured between 20.5 and 33.2 °C. FRET dependence on DHPC concentration was also studied in order to take into account this side reaction. Interestingly, sigmoidal time-dependence of mixing was observed in most experiments, which is similar to the "lag phase" observed in liposome fusion experiments.[208] This feature, together with the similar high activation barriers observed in fusion pore formation, suggests the same mechanism for lipid exchange between nanodiscs and bicelles.[207]

The specific effects of various lipids on incorporation of membrane proteins in nanodiscs and their functional properties and stability were addressed in several studies.[209−212] POPC-

DOI: 10.1021/acs.chemrev.6b00690
Chem. Rev. 2017, 117, 4669−4713

POPG at 3:2 mixtures, supplemented with cholesterol hemisuccinate (CHS), were used for incorporation of the GPCR human A_{2A} adenosine receptor.[213] Nanodiscs containing the GPCR and empty nanodiscs were characterized using analytical ultracentrifugation and SEC, and highly homogeneous samples with an estimated content of 75 lipids and one GPCR monomer per nanodisc were obtained. The effect of CHS content on the conformational equilibrium of another GPCR, the leukotriene B4 receptor, was probed using nanodiscs.[214] Binding properties of β_1-adrenergic receptor as a function of lipid composition in nanodiscs was systematically investigated.[215] The same group described the effects of specific lipids on the activity of the MraY translocase[216] and screening for optimal lipid requirements for cell-free expression of membrane proteins with direct incorporation in nanodiscs.[217] In order to study the effect of various lipids on the conformation and dynamics of the multidrug pump LmrP it was assembled in nanodiscs with PE with a varied degree of methylation of the amino group, specifically DOPE (no methylation), DOPE$(Me)_2$ (two methylations), DOPC (fully methylated) and with constant fractions of DOPG (23%) and cardiolipin (10%) in a *E. coli* polar lipid extract.[218]

Often incorporation in nanodiscs is used in the process of membrane protein isolation and purification from expression system or from native tissue. Incorporation in nanodiscs early in the solubilization process improves the stability of proteins and extends their functional lifetime. This method is commonly used in GPCR studies where, for example, the β_2-adrenergic receptor was incorporated into nanodiscs and used in various binding experiments.[219−222]

3. USE OF NANODISCS FOR STRUCTURAL STUDIES OF MEMBRANE PROTEINS

One of the first questions often asked is: Can nanodiscs be used to determine the structure of membrane proteins? As we will clearly see in this section, important structural information can indeed be gleaned using a variety of biophysical techniques. Obtaining critical structural data, ranging from quaternary information, protein−protein and protein−lipid recognition to detailed molecular pictures of membrane proteins is most certainly enabled by nanodisc technology. We separate the discussion as to the structural methodologies utilized.

3.1. Nanodiscs and X-ray Crystallography

One immediate query relates to the usefulness of nanodiscs for determining the crystal structure of membrane proteins. Here the answer is more complicated. Being in a native-like bilayer environment, membrane proteins assembled in nanodiscs are inherently more stable and display full functionality. An important utility of nanodiscs, therefore, is in collecting substantial quantities of target material that is needed for X-ray crystallography and other biophysical investigations. Many investigators have taken advantage of the fact that the target of interest is active and monodisperse in nanodiscs and stable to storage and procedures for concentration. Thus they use assembly into nanodiscs to store and collect active materials for subsequent investigation and functional studies.[220,221,223] The direct crystallization of proteins in the nanodisc has been more challenging. Although nearly a decade ago, crystals of bacteriorhodopsin in nanodiscs were grown in the Kossiakoff laboratory, they diffracted very poorly (unpublished observation). There are several obvious problems. First, an inserted membrane protein is azimuthally disordered in the discoidal bilayer. In addition, if the temperature is above the gel-liquid phase transition, the protein is also mobile[73] which makes crystallization difficult even though, with careful attention to detail, the nanodisc population can be made highly homogeneous and monodisperse. A second complication is that the encircling MSPs are orientated antiparallel to each other and are stabilized by interhelical salt bridges.[198,224] Because of the similarity in the amino acid sequences of the 22-mer helical repeat topology, even though there is a global energy minimum, there could be rotational disorder in the MSP configuration, which could inhibit crystallization. An alternate strategy may be operational for those integral membrane proteins that have large globular domains on each side of the bilayer or where specific antibodies can be used to provide a larger site for crystal contacts to form. Another approach could be to engineer the scaffold proteins to form a two-dimensional lattice that would be of use in depth profiling structure determination by X-ray or electron scattering.[225] Thus, we are optimiztic that a high-resolution crystal structure of a membrane protein self-assembled into a nanodisc will be forth coming. With this caveat, we turn to the successful and extensive use of nanodiscs using other structural tools such as NMR, EPR, and electron microscopy (EM).

3.2. Nanodiscs in Cryo- and Negative Staining Electron Microscopy

The high degree of size homogeneity of nanodisc preparations have been enabling for beautiful high-resolution structures of membrane proteins using EM. For example, integrins self-assembled into nanodiscs allowed the first structural definition of the conformational changes responsible for inside-out signaling.[226,227] This effort also used the concept of using nanotube assemblies to provide multiple orientations of a membrane protein in nanodiscs. Dramatic advances in cryo-electron microscopy, led by technical breakthrough in both source and detector, have allowed atomic resolution images to be obtained. For membrane proteins, nanodiscs have provided a means to avoid aggregation, preserve target function and structure as well provide immunity to freezing and mounting. Full three-dimensional reconstructions have yielded high-resolution images of membrane proteins in nanodiscs. Examples include the ryanodine receptor which revealed the ordering of trans-membrane helices[228] (Figure 8) and the structure of the TRPV1 ion channel in the unliganded, agonist-bound, and antagonist-bound states at resolutions of 3.2, 2.9, and 3.4 Å, respectively.[229]

The structure of the *Tc* toxin at an average resolution 3.46 Å in POPC nanodiscs resolved for the first time the trans-membrane fragment, and the mechanism for direct insertion of ten helices was presented based on comparison with the prepore structure.[230] Helices rearrange in the membrane with interhelical loops forming a funnel for the entrance to the pore. Others have utilized nanodiscs in electron microscopic investigations of lipoxygenase,[231] drug efflux pumps,[232] a magnesium channel,[138] AMP dependent protein kinase,[94] the ribosome-SecYE complex[233] and other membrane proteins.[120,161] Thus nanodiscs and electron microscopy have become a mainstay for the structural determination of membrane proteins and their interactions to form supramolecular complexes involved in signaling, energy transduction and transport.

There are many more examples of successful application of nanodisc incorporation for characterization by

DOI: 10.1021/acs.chemrev.6b00690
Chem. Rev. 2017, 117, 4669−4713

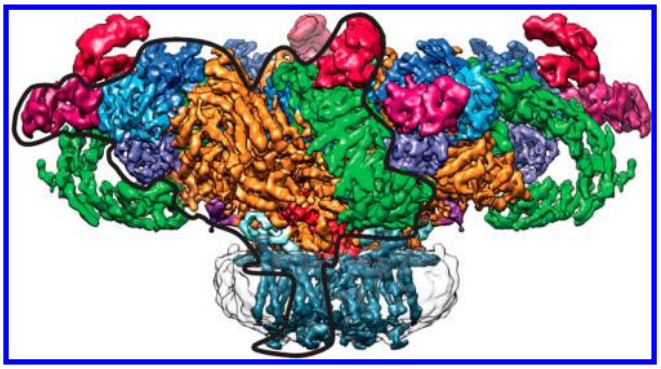

Figure 8. Structure of the ryanodine receptor in nanodiscs as determined by cryo-electron microscopy.[228] A contour of a most probable protomer is outlined with thick black line. Reprinted with permission from ref 228. Copyright 2015 Macmillan Publishers Ltd.

EM.[80,136,137,149,227,234−236] The HIV envelope glycoprotein precursor, gp160, was incorporated in POPC MSP1D1 nanodiscs with various stoichiometries, one, two, or three per one nanobilayer.[91] The native-like homotrimer in nanodiscs was separated and studied using cryo-EM to monitor the binding of the cognate receptor CD4 and with antibodies. A fully functional trimer in nanodiscs was stable for 2 weeks at 4 °C or up to 8 weeks at −20 °C and could be used as an immunogen for analytical or production purposes. Separately, the role of the membrane-proximal external region (MPER) and trans-membrane three-helix bundle was also probed by incorporation of this part of gp160 protein in nanodiscs and binding studies with specific antibodies.[237] Based on the fact that the presence of membrane and formation of trimer are necessary for efficient binding with neutralizing antibodies, a structural model of the MPER fragment was suggested.[237]

Recently a capture of virus entry into the cell using cryo-EM was reported for a complex of nanodiscs containing coxsackie-adenovirus receptors with human pathogen coxsackie virus B3 (CVB3).[238] The entry intermediate was resolved using single-particle data collection with multiple orientations to 7.8 Å without or to 3.9 Å with imposed icosahedral symmetry, due to the size homogeneity and small diameter of nanodiscs. An asymmetric approach to analysis of EM data allowed the authors to identify an extension of electron density near nanodisc membrane and formation of channel in the surface of virus capsid. Moreover, the RNA density was found to be delocalized toward the opening in the capsid suggesting reorganization of genome for exit. Very recently another cryo-EM study demonstrated interaction of poliovirus with nanodiscs.[239]

3.3. Nanodiscs and Structure Determinations by Magnetic Resonance Spectroscopy

Nuclear magnetic resonance (NMR) has long been used to obtain structural information on soluble proteins.[240−242] Solution methods have traditionally limited the size of the protein target, although more recently these barriers have been surpassed with advances in pulse sequences.[243,244] The inherent tendency for aggregation when membrane proteins are removed from their native bilayer environment limited early NMR investigations. Assembling a membrane protein into nanodiscs with defined stoichiometry, however, has opened the door to numerous high-resolution studies. Solid state NMR (ssNMR) provided an alternate approach to investigate large macromolecular objects.[245−249] The first ssNMR spectra of nanodiscs were reported by Rienstra and colleagues and yielded their unambiguous determination that the membrane scaffold proteins were orientated in the "belt" configuration.[152] The past few years has witnessed an explosion in the use of both solution and solid state NMR methods with nanodiscs to reveal critical details of membrane protein structure and function.[9,34,72,126,135,180,250−256] For example, the complete three-dimensional structure of OmpX in nanodiscs by solution NMR demonstrated the value in revealing subtle conformational differences when in the native bilayer environment[257] (Figure 9).

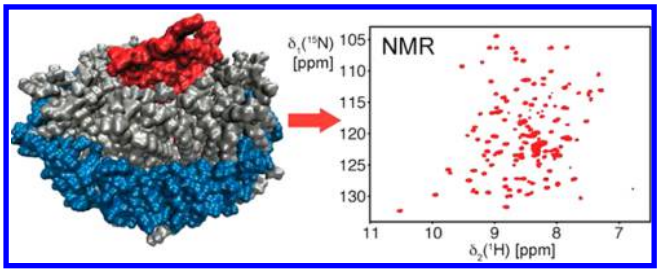

Figure 9. Structure of the membrane protein OmpX in nanodiscs is determined by solution NMR spectroscopy. Reprinted with permission from ref 128. Copyright 2013 American Chemical Society

Indeed, a recent NMR investigation of the oncogenic protein KRas4b showed that the conformation of this important drug target was altered when bound to a nanodisc membrane surface, thus illuminating the need for a membrane bilayer in understanding the conformational changes of membrane proteins as they interact with lipid surfaces.[250] The structural features of other membrane proteins involved in signaling at the membrane surface have been reported, such as the neurotrophin receptor in nanodiscs[135] and numerous beta-barrel systems.[257,258] A direct comparison of the membrane protein BamA in different membrane mimetics[259] and a review of nanodiscs in NMR applications[128] illustrated the enablement of this approach for structural determination. Structures of the antiapoptotic BCL-2 family protein BCL-XL, a significant anticancer drug target, were compared for the soluble form and for the full-length form with the C-terminal fragment incorporated in nanodiscs.[98,260] Results show that the C-terminal tail forms an α-helix in the membrane, but retains significant mobility and may be susceptible to proteolysis in soluble form. The mobility of the C-terminal helix may be related to a functional role of this protein in the apoptosis process and in conformational modulation of the globular domain.[98]

Various membrane mimetics have also been compared in a search for optimal conditions for NMR structural studies of the neurotrophin receptor p75NTRc from rat.[135] This protein contains an extracellular domain, a single-span trans-membrane helix, and an intracellular domain, which in turn consists of two domains and a linker. Based on extensive experimental probing of several separate fragments expressed in a cell-free system in *E. coli* and assembly in nanodiscs of various sizes using original and truncated MSP proteins or in DMPC/DHPC bicelles, optimal conditions for solution NMR spectroscopy were evaluated by varying the lipid:protein stoichiometry and lipid composition. Among many useful observations described in this work, the importance of the membrane protein interaction with bilayer was indicated by nontrivial dependence of the intensity

DOI: 10.1021/acs.chemrev.6b00690
Chem. Rev. 2017, 117, 4669−4713

of the DD domain NMR signals and the size of MSP forming nanodiscs. Truncated MSP designed by the Wagner group[128] were used in order to improve the signal from incorporated proteins, but no such effect was observed. This unexpected result is explained by the predominant effect of the conformation of the intracellular domain on the mobility of nanodiscs with these proteins, which may reach ~20 nm in size. As a result of a more compact conformation of this domain in larger nanodiscs, due to interactions with anionic lipids and higher mobility, MSP1 and the presence of anionic lipids provided the best conditions for the NMR study of the structure and dynamics of the intracellular domain of p75NTR. nanodiscs were also useful for the investigation of the possible specific dimerization of DD domains, by incorporation of several monomers in one nanodisc.[135] In a detailed comparison of the results obtained for various stoichiometric ratios of this domain in nanodisc, up to 6:1, no stable and specific association was observed under reducing conditions, i.e., in the absence of disulfide bond formation. Nanodiscs are thus especially useful for studies of membrane proteins possessing only one transmembrane helix, because they avoid the presence of detergents that often can interact in an undesirable way with the extramembrane domain. At the same time the presence of nanodisc bilayer provides a native-like membrane for the transmembrane fragment and can be adjusted for mimicking necessary protein−lipid interactions by choice of lipid composition.

Another optimized strategy for using nanodiscs in solution NMR spectroscopy was described for a different class of proteins, the GPCRs, which usually face various experimental challenges that limit resolution.[214] Monomeric leukotriene B4 receptor (BLT2) was selectively isotopically labeled and assembled in nanodiscs using partially deuterated DMPC and protonated cholesterol hemisuccinate (CHS) as lipids and protonated MSP1D1 as the scaffold protein. Comparison of NMR results obtained in nanodiscs with various CHS content (3%, 43%, and 98%) showed a redistribution of the BLT2 receptor between four conformational substates observed in the absence of the ligand. These conformational changes are associated with ligand-dependent G protein activation, with one specifically assigned as the active state at high CHS concentration. Population of this state also is maximized in the presence of the natural agonist LTB4 and increases to a lower extent when weaker synthetic agonist is used instead. In addition, allosteric coupling between CHS and ligand induced conformational transition toward an active conformer was observed, which may suggest an important role in the signaling properties of this GPCR.

Short of complete structure determination, nanodiscs can be used to define specific distances and orientations of a membrane protein in a native-like bilayer environment. Examples include conformational changes induced by ligand binding to the maltose transporter,[261,262] critical structural motions of G-protein coupled receptors[263] and the revelation of multiple conformations of SNARE proteins in diverse prefusion states.[264] Dynamics and transitions between inactive and active conformations of β_2-adrenergic receptor in nanodiscs were characterized by NMR of selectively deuterated receptor, and found to be on millisecond scales,[265] slower than in the detergent dodecyl maltoside (DDM). Here the population of the active state was higher in nanodiscs than in DDM. Dynamic transitions between closed and multiple open states monitored by NMR signals from methionine residues provided insight into a possible structural mechanism of biased signaling of a μ-opioid receptor.[266] The improved stability of nanodisc incorporated chemokine receptors CCR1 and CCR5, coupled with recently developed methods of NMR spectra analysis, provided necessary resolution for assignment of binding interface between these receptors and their ligand MIP-1α.[267] These results will help in evaluating the effect of two known sites of single nucleotide polymorphism of MIP-1α on the progress of autoimmune disease regulated by these chemokine interactions. The distinct advantages of the nanodisc platform for investigating GPCR structure and function are obvious.

3.4. Nanodiscs in Single Molecule Structural Investigations

Since nanodiscs are monodisperse, are highly homogeneous, and can be readily affixed to surfaces without loss of function, they are immediately applicable to single molecule studies. Atomic force microscopy and single molecule optical and fluorescence spectroscopy are completely compatible with membrane proteins self-assembled into nanodiscs. Ligand binding, protein dynamics, and questions of molecular recognition events in protein−protein interactions have used the nanodisc technology applied to enzymes,[27,99,268] electron transfer proteins,[269] and G-protein coupled receptors.[270] In the case of GPCRs, the ability to selectively control the number of the target protein in a nanodisc of controlled size allowed the first clean documentation of the inherent activities of monomer and dimer in receptor signaling.[81,271]

Incorporation in nanodiscs provided a new way to study the dynamics of the homotetrameric K^+ channel protein using single molecule fluorescence resonance energy transfer (FRET) in solution.[272] Confocal in-solution alternating laser excitation microscopy allowed probing femtoliter sample volumes and distinguished between donor and acceptor fluorescence. The dynamic response of the channel as a function of pH, presence of PIP_2 lipid and an activating mutation revealed conformational changes consistent with a "twist-to-shrink" structural model of opening and closing movements. Using nanodiscs is critical for such experimental design, as they provide a combination of the native-like lipid bilayer environment and solution-based sampling.

Stepped rotation of the F_0F_1 ATP synthase from *E. coli* incorporated in nanodiscs was directly observed monitoring the signal from an avidin coated gold nanorod attached to the biotinylated c-ring.[273] Stability of the ATP synthase was greatly improved in nanodiscs, as compared to the detergent solubilized preparations, which allowed acquiring single-molecule data for sufficiently long time to achieve the required signal-to-noise ratio. A further study used the same approach to resolve the question on the mechanism of the overall clockwise torque overcoming the counterclockwise forces generated by the F_1 ATPase at high concentrations of ATP.[274] The results of this work revealed more a detailed picture of interactions between the F_1 and F_0 subunits that are responsible for the ATP synthase activity.

Multiple conformations of a SNARE complex reconstituted between two nanodiscs were resolved by single molecule FRET and site-directed spin labeling EPR.[264] Two major conformational states were identified as fully assembled (45%) and a half-zipped complex with the C-terminal half of v-SNARE synaptobrevin mostly in a random coil state (39%). A third state (16%) was not characterized structurally, and exhibited FRET at an intermediate level. A three-state structural model proposed based on these results suggests the main structural

DOI: 10.1021/acs.chemrev.6b00690
Chem. Rev. 2017, 117, 4669−4713

transitions are localized at the C-terminal domain, while the N-terminal half remains in a folded coiled coil structure. Later a single-molecule FRET study of SNARE proteins similarly assembled between two nanodisc membrane patches allowed detection of a large conformational change at the C-terminal part in the presence of complexin, while no changes were observed at the N-terminal region.[100] This suggests the mechanism for inhibition of SNARE-dependent membrane fusion by complexin via separation of C-terminal helices and prevention of their zippering.

Single-molecule force spectroscopy of membrane proteins incorporated in nanodiscs provides advantages over alternative methods, as described in the study comparing mechanical unfolding and force spectroscopy of bacteriorhodopsin (bR) in native purple membranes and in DMPC nanodiscs.[275] Nanodiscs with bR were homogeneously distributed and densely packed as a single layer on mica, while the distribution of purple membrane fragments was heterogeneous and not perfectly flat. An AFM tip was attached to the C-terminus of the protein in most cases, and force−distance curves were analyzed based on the known fold of the bR molecule. The unfolding mechanism and population of unfolding intermediates were similar for bR in nanodiscs and in purple membranes, indicating a stable bR trimer assembled in nanodiscs.

Although not formally applying a single-molecule technique, the study of the monomeric SecYEG translocon complexes in nanodiscs by a combination of fluorescence correlation spectroscopy and FRET-based assay of translocon activity was used to establish functional competence of the monomer.[276] Based on the observed high activity, this work suggests that formation of dimers and higher oligomers is not required for active translocon function, unlike earlier proposals.[277] In the further development of these methods, the lipid dependence of binding affinity of SecA ATPase to the SecYEG translocon and functional competence of ATP-dependent translocation was addressed using nanodiscs with various sizes and lipid compositions.[278] The presence of large lipid surface in nanodiscs with ∼30 nm diameters formed with ApoE resulted in very high affinity for SecA binding, and high content of anionic lipids was critically important, while binding to SecYEG in smaller 13 nm nanodiscs formed with MSP1E3D1 was 10 times weaker.

Single-molecule fluorescence was also used to monitor binding of the substrate Nile Red and the resultant allosteric effects with CYP3A4 in nanodiscs immobilized on surface.[27,99] Total internal reflection fluorescence microscopy (TIRFM) was used with Nile Red dye as a model substrate to monitor the residence time in the active site or at the peripheral site formed at the protein−membrane interface. A short residence time of 0.66 ms was assigned to the Nile Red binding to the lipid bilayer, while slower residence time of 33 ms was attributed to the binding of Nile Red at the active site of CYP3A4. This was confirmed by elimination of the slower phase by inhibitor miconazole, which blocked substrate binding to the active site. Dissociation of the substrate from active site was further slowed in the presence of an allosteric effector.

One of the first applications of nanodiscs for membrane protein studies was realized by obtaining information on the positioning of cytochrome P450 CYP2B4 and cytochrome P450 reductase (CPR) on the membrane surface.[77,79] Nanodiscs with or without P450 or CPR were absorbed on mica, and atomic force microscopy (AFM) was used in the scanning mode for mapping surface and localize proteins on top of the bilayer. Tapping mode was used to measure the height of CYP2B4 over the background level of DPPC nanodiscs,[79] and this information was used to evaluate the mode of incorporation according to the available structural models, before the X-ray structure of any eukaryotic P450 enzymes was resolved. The results of this work are consistent with the current knowledge of P450 positioning in the membrane.

The incorporation of CPR in nanodiscs improves the stability of this flavoprotein and enables application of single-molecule studies of activity using the model substrate resazurin and monitoring formation of the resorufin product by fluorescence.[269] Results of this work revealed the presence of at least two distinct conformational states of CPR with dramatically different activity levels. This observation is consistent with the presence of two domains containing FMN and FAD and the existence of two forms, open and closed, known from earlier studies. Results obtained using single-molecule techniques provide detailed information on the population of these conformational states and the effect of ionic strength on large-scale dynamic transitions on millisecond scale. Multimode AFM was also used for the detection of cholera toxin binding to nanodiscs containing GM1 gangliosides (molar ratio GM1/DMPC 5:95) immobilized on a microcantilever.[76] Binding could be quantitatively estimated by monitoring te deviation of the cantilever because adsorption of the toxin with molecular mass 87 kDa resulted in higher deviation of the cantilever at higher toxin concentrations. Control experiments with 100% DMPC nanodiscs showed no binding.

3.5. Structural Studies Using Nanodiscs as a Membrane Surface

Communication between the inside and outside of a cell or organelle requires interaction with the membrane surface. Indeed the composition of the membrane, including the nature of the lipid present, factors such as cholesterol and connecting points to intra- and extra-cellular frameworks, are involved in modulating and controlling the activity of multiple membrane proteins. Nanodiscs have proven invaluable as they provide a means for precisely controlling the composition of a membrane area, avoiding, for instance, complications due to ″patching″ in vesicles. Systems investigated include the blood coagulation cascade, with recent work the structure of lipid−protein interfaces[279] and revelation of critical protein−protein interactions,[280] as well as the recruitment of signaling molecules such as talin and the activation of integrin signaling.[93,97] In the former case, studies have revealed, at atomic resolution, the changes in structure and dynamics of membrane domains induced by divalent metals in the recruitment of clotting factors that provide valuable insight into the role of the membrane surface in blood clotting. Strong specific effects of phosphatidylinositol-4,5-bisphosphate (PIP2) lipid head-groups were revealed for talin binding to, and F3 domain interaction with, the membrane surface. Activation of inside-out signaling was found to critically depend on regulation of the autoinhibited form of talin by PIP2 lipids.[97]

A proteomics approach with isotopic labeling combined with nanodisc technology can be used to identify soluble interacting partners of membrane proteins by pull-down assay and mass-spectrometric analysis.[281] This method was applied to the protein-conducting channel SecYEG complex, maltose transporter $MalFGK_2$ complex and membrane integrase YidC assembled in nanodiscs, and several proteins specifically binding to these targets were identified.[281] Nanodiscs have

DOI: 10.1021/acs.chemrev.6b00690
Chem. Rev. 2017, 117, 4669−4713

also enabled several useful strategies toward targeting specific lipid−protein interactions, as described in our earlier review.[282] For instance, ganglioside incorporation in nanodiscs was used to probe interactions of cholera toxin[76,184,283] and other toxin proteins.[62,284−286] Interactions of granuphilin with PIP2 lipids in nanodiscs studied by NMR provided necessary information for evaluating the structural model of PIP2 binding site in the common membrane binding C2A domain.[287]

3.6. Molecular Spectroscopy of Membrane Proteins in Nanodiscs

Spectroscopic methods are a mainstay for determining critical functional aspects of many membrane proteins. As has been noted before, in the absence of bilayer environment, many membrane proteins do not display native properties, are aggregated and often inactive. Self-assembly into nanodiscs restores the native state.[288,289] There are a plethora of spectroscopic investigations that have successfully used nanodiscs. Nanodiscs provided especially significant advantages for spectroscopic investigations due to their lack of turbidity and low viscosity. This allows the direct application of fast mixing methods to monitor structural and functional properties of the incorporated membrane protein by optical methods. The previously mentioned electron spin resonance spectroscopies have been widely used, including EPR, DEER, ELDOR, ESEEM, and PALDOR,[103,124,218,261,262,290−293] and the stability nanodiscs at cryogenic temperatures has enabled the trapping of membrane protein intermediates and their characterization by resonance Raman, optical, and EPR spectroscopy.[12,24,83,88−90,294−296] Manifestations of the lipid effects upon the functional properties of membrane proteins are ideally investigated using nanodiscs, which allow the precise control of the lipid composition. Published work includes documenting shifts in redox potential of heme and flavoproteins due to local membrane electrostatics,[297,298] and the critical role of cardiolipin in the assembly, activity, and stability of the mitochondrial respiratory complex II.[210]

The orientation of cytochrome P450 CYP3A4 in nanodisc POPC membrane was measured experimentally using linear dichroism spectroscopy of nanodiscs absorbed on an optical glass waveguide.[299] Polarized absorption of the heme provides a strong chromophore with the known from (X-ray structure) orientation with respect to the protein globule. This orientation was compared to a molecular dynamics (MD) simulation of CYP3A4 using a highly mobile membrane mimetic model,[300−302] and good agreement (±6°) was found between experimental and simulation results. After an additional all-atom simulation was performed with a full representation of the lipid acyl chains, even better agreement (within 2°) with experiment was realized. Clearly the details of a membrane protein interacting with the core bilayer region can be critical in determining orientation and function. Later interactions of another human cytochrome P450 CYP2J2 with nanodisc lipid bilayer were probed by introduction of charged residues at the protein-membrane interface.[303] No difference was found experimentally with neutral POPC lipids; however, with 30% and 60% POPS the F-G loop in the native CYP2J2 was inserted in the bilayer significantly deeper than in mutant proteins, which showed only minor changes. The extent of membrane insertion was measured by fluorescence quenching of Trp235 residue interacting with the membrane by pyrene incorporated in the lipid bilayer.[303]

The effect of anionic lipid on the photocycle intermediates in bR was thoroughly studied using nanodiscs with a variable doping of DOPG or DMPG in nanodiscs assembled with DMPC and DOPC.[212] Incorporation was performed under conditions yielding monomeric bR in nanodiscs, which was confirmed by CD spectroscopy. The kinetics following the recovery of the 560 nm absorbance band after excitation at 532 nm were significantly faster when the DOPG or DMPG lipid fraction was 50% or higher, indicating an important contribution of anionic lipids in the protonation of the Schiff base. In addition, the recovery was slower in DMPC/DMPG nanodiscs as compared to DOPC/DOPG, correlating with the much higher main transition temperature of saturated lipids. Similarly, reconstitution of proteorhodopsin as a monomer in nanodiscs revealed dependence of basic spectral and photophysical properties on lipid composition and confirmed that oligomerization is necessary for the fast photocycle.[304] For rhodopsin monomer in nanodiscs, the kinetics and intermediates observed on a microsecond−millisecond scale are very similar to those formed in native membranes.[305] Late intermediates in the photocycle also could be observed in nanodiscs, unlike in rhodopsin solubilized in the detergent lauryl maltoside. This made possible further study of constitutively activating mutations in opsin, the ligand free form of rhodopsin, using site-specific fluorescent labeling.[306] Specific movements of trans-membrane helix-6 were probed using a M257Y mutation, and Arrhenius analysis of the temperature dependent kinetics revealed a lower activation barrier for the mutant opsin when in detergent versus nanodiscs, although more constraints and a lower population of the active form was present in the lipid phase. Similar results were obtained in another study,[307] which compared the proton pumping function of bR in nanodiscs assembled using charged lipids, with compositions varying from 100% to 10% DOPG (negatively charged) to 10% DOTAP (positively charged) in a POPC (zwitterionic, overall neutral) background. The fraction of all-trans retinal and rate of recovery was reduced in DOTAP/DOPC nanodiscs, while with 50% DOPG the amplitude of transient absorption and rate of recovery significantly increased, and in 100% DOPG both increased even more. Surprisingly, the photocurrent measured in a 10% DOTAP bilayer was higher than in DOPG, where proton may be temporarily trapped and not released from negatively charged head-groups as quickly as from positively charged ones.

Two cytochrome c oxidases were incorporated in MSP1E3D1 nanodiscs using soy bean lipid. The microsecond kinetics of proton coupled electron transfer was found to be faster in nanodiscs as compared to a detergent solubilized form.[308] The same acceleration of proton transfer in nanodiscs was observed in the reaction with O_2 in flow-flash experiment. A clear advantage of nanodiscs over liposomes for such experiments is the optical transparency and exposure of both sides of the membrane to soluble reagents. A novel approach to the direct measurement of proton 2D-diffusion on nanoscale at the water-membrane interface using nanodiscs was recently described by Brzezinski, Widengren and collaborators.[309] Using fluorescence correlation spectroscopy (FCS) they monitored the pH-dependent kinetics of fluorescence fluctuations of individual fluorescein molecules in DOPG nanodiscs. Fluorescein was either attached to DOPE lipids or to cytochrome c oxidase incorporated in DOPG nanodiscs. The results of this work show anomalously fast 2D proton diffusion on the scale of single nanodiscs membrane, 8−12 nm, which determines

DOI: 10.1021/acs.chemrev.6b00690
Chem. Rev. 2017, 117, 4669−4713

approximately 100 times faster protonation rate of fluorescein in DOPG membrane than in aqueous solution. Even stronger acceleration of fluorescein protonation was observed by these authors earlier in DOPG vesicles.[310] A microscopic mechanism describing 2D and 3D diffusion under conditions of low and high buffer concentrations is proposed to explain these differences.[309]

3.7. Solution Scattering Reveals the Structure of Membrane Proteins in Nanodiscs

X-ray and neutron scattering has been extensively used to characterize membrane proteins in nanodiscs. For example, small-angle X-ray scattering (SAXS) of several MPs in nanodiscs has been used to demonstrate topology within the lipid bilayer and to provide information on the orientation of the target protein. Examples include the formation of functional trimers of bacteriorhodopsin (bR),[73] Curdlan synthase[311] and cytochrome P450.[197] Further advances have been realized by adding small angle neutron scattering (SANS) to the structural toolkit. An important advance has been the creation of a "silent nanodiscs" where lipid and scaffold protein are contrast matched so only the target protein is observable in a SANS experiment.[312,313] Deuterated lipids were obtained from *E. coli* grown in D_2O with deuterated glycerol and partially deuterated choline chloride and characterized by ^1H NMR. SANS of nanodiscs assembled with deuterated MSP1D1 and deuterated PC lipids in D_2O buffer approached almost zero forward scattering, thus providing an optimal media for structural studies of membrane proteins in such "stealth" nanodiscs by SANS.

SAXS of membrane proteins incorporated in nanodiscs were reported for cytochrome CYP3A4,[197,314] bR,[73] and the rhodopsin monomer.[81] Furthermore, X-ray and neutron reflectometry have been recently used to quantitate conformational changes of membrane proteins in nanodiscs, such as the redox-dependent movement needed for efficient electron transfer from NADPH cytochrome P450 reductase to cytochrome P450[315] and the structural changes of visual rhodopsins following photon activation as monitored by wide-angle X-ray scattering in nanodisc preparations.[316] Very recently, X-ray scattering in combination with solution NMR was used to follow the assembly of G-protein α-subunits with a GPCR on membrane surfaces of defined composition.[317]

3.8. Determining the Structure of Oligomers and Multi-Subunit Proteins

Because of their small size and stable incorporation of membrane proteins, nanodiscs are the best tool for analysis of the oligomeric state of functional protein assemblies and for probing for effect of oligomerization as one can cleanly make a sample containing a defined number of target proteins. This is especially important for such classes of proteins as the 7-transmembrane receptors, such as GPCRs, which usually exist as dimers or higher oligomers.[318−323] Isolation of GPCR monomers in nanodiscs and comparison of their properties with oligomers in nanodiscs under identical conditions were performed in several studies.[73,81,271] Incorporation of the bR trimer in nanodiscs of various sizes and determination of the spectral properties as a function of the number of lipids surrounding the protein demonstrated that a layer of at least two lipids is necessary for functional trimer reconstitution.[73] A rhodopsin monomer isolated in nanodiscs was found to efficiently activate transducin in a 1:1 complex and generate the metarhodopsin-II intermediate, while only one rhodopsin monomer in the dimer can form this metarhodopsin-II−G-protein complex.[81] In addition, the rhodopsin dimer is only 49% active in catalyzing GTPγS exchange as compared to the monomer. It was thus proven that only one monomer in the rhodopsin dimer is catalytically active due to steric restrictions, resolving a long-standing question in the field. In later experiments, arrestin was also found to bind to the monomeric phosphorylated rhodopsin in nanodiscs as well as that which occurres in native membranes.[271] An even higher affinity of arrestin binding to monomeric rhodopsin in nanodiscs than to rhodopsin oligomers in liposomes was reported.[324] Furthermore, negatively charged POPG enhanced arrestin binding to rhodopsin. Similarly, the POPS dependence of arrestin mutant binding demonstrated that removal of the negatively charged C-terminal tail from the membrane facilitated complex formation between arrestin and rhodopsin.[271] The conformational changes in visual arrestin caused by binding to phosphorylated rhodopsin monomer incorporated in nanodiscs have been probed by DEER with distance mapping via site-specific labeling.[325] This experiment provided direct evidence of a 1:1 complex of arrestin and monomeric rhodopsin in nanodiscs, with the same conformational changes observed in this small model system as for arrestin complexes with rhodopsin in the native disk membranes.

Nanodiscs provided a very fruitful experimental approach to studies of functionally important oligomerization of bacterial chemotactic Tar receptors from *E. coli*[130,132] (Figure 10).

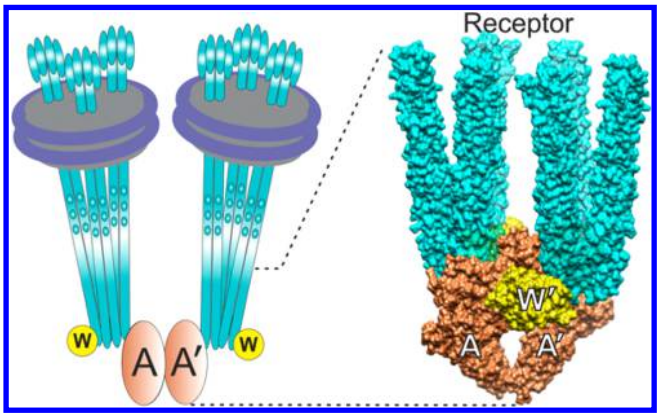

Figure 10. Schematic representation of the bacteria chemotactic receptor Tar in nanodiscs illustrating the CheA kinase dimer, AA′, and the coupling protein, CheW. Left panels shows two trimers of Tar dimers incorporated in separate nanodiscs and interact to form a fully functional unit.[326] The right panel shows a space-filling model of the lower half of this complex with two sets of three dimers indicated in blue. Reproduced with permission from ref 326. Copyright 2014 PNAS.

These homodimer helical trans-membrane receptors form "trimers of dimers" and higher oligomeric clusters with unknown functional implications. Assembly of one or several dimers in nanodiscs with total *E. coli* lipid extract provided a clear picture of "trimer of dimers" formation with emerging ability to activate the chemotaxis histidine kinase CheA. Isolated dimers were competent in trans-membrane signaling but showed a very low level of chemotaxis activation, demonstrating that the trimer of dimers is a fully functional signaling unit. Later, a more detailed study of the isolated dimer in nanodiscs established the functional competence of dimers in translating ligand binding events through the membrane and

DOI: 10.1021/acs.chemrev.6b00690
Chem. Rev. 2017, 117, 4669−4713

confirmed the presence of conformational changes related to partial signaling.[327] Full-scale activation of CheA by three neighboring Tar dimers was experimentally confirmed by separation of nanodiscs with different numbers of dimers per nanodisc.[328] The fully functional unit of two trimers of dimers interacting with two molecules of histidine kinase CheA and one coupling protein CheW was isolated in nanodiscs and demonstrated the same activity as isolated arrays of complexes in the native membrane.[329] Interestingly, a strong dependence on the lipid composition in nanodiscs was observed for Tar receptors with respect to the extent and rate of adaptational modification.[209] The most successful functional incorporation among synthetic lipids was achieved with phosphatidyl ethanolamine (PE) lipid mixtures, which constitute the largest fraction in *E. coli* membranes. Optimal mixtures included ~7−10% of anionic lipids. Lipids with fully saturated chains were unfavorable for functional reconstitution, independent of the headgroup identity. A strong lipid effect on the functional properties of Tar receptors is somewhat surprising, because only 10% of the receptor is integral to the membrane bilayer, and long helical bundles extend far from the lipid head groups. More detailed information on the structure and dynamics of Tar helices in dimers was recently reported using site-specific labeling with spin probes and continuous wave EPR spectroscopy.[291,292] Well-developed protocols for nanodisc incorporation and isolation of various populations of Tar receptor dimers with controlled stoichiometry provided a basis for evaluating allosteric mechanisms in core chemotaxis signaling complexes.[326] Trimers of dimers of the *E. coli* aspartate chemoreceptor Tar and serine receptor *T*sr were assembled as homotrimers and both 2:1 and 1:2 heterotrimers. Soluble core signaling complexes containing two such trimers of dimers, each in separate nanodisc, as well as one CheA dimer and two CheW proteins were assembled and probed for functional activity. The experimentally observed partial kinase inhibition was inconsistent with initially considered simple models. A more complex structural model for the coupling pathway combines incomplete allosteric coupling in an isolated core signaling complex with improved coupling in arrays of core complexes.[326]

Most recently a novel understanding of the functional properties and structural arrangement of the large multisubunit light harvesting complexes (LHCII) was achieved by comparison of their spectral properties in a monomeric state in nanodiscs[330] and diluted in proteoliposomes at high lipid:protein ratio (up to 7000:1) with aggregated LHCII complexes (trimers and higher) in thylakoids and in liposomes at low lipid:protein ratio (from 30:1 to 600:1). While the lipid environment did not alter the properties of LHCII as compared to those observed in a detergent solubilized system, aggregation and clustering of these complexes in the membrane changed the lifetime of the excited state, which explains the shorter lifetimes observed in native membranes.[331]

Nanodiscs enabled sophisticated bioengineering efforts toward directed incorporation of assemblies of membrane proteins with a given stoichiometry and topology. A prototype study employed complementary DNA scaffolds of membrane proteins in order to enforce their coincorporation with a given stoichiometry in a single nanodisc.[332] Dimers and trimers of the voltage-gate anion channel VDAC were assembled in MSP1E3D1 nanodiscs with 3:1 DMPC:DMPG lipid mixture with high enrichment over control reactions with untagged proteins. This method significantly improved the yield of incorporation comparing to the earlier study from the same group, where a relatively broad distribution of VDAC channel oligomers was observed by electron microscopy.[333] In addition, the DNA scaffold facilitated incorporation of protein monomers with desired orientation, providing an auxiliary handle for directed self-assembly of multimeric protein complexes in nanodiscs. DNA oligomers were covalently connected to the cysteine residue on the protein using a bifunctional succinimide−maleimide linker. Dimers or trimers of DNA-modified VDAC proteins were first formed in detergent-solubilized solution followed by subsequent mixing with the nanodisc assembly mixture in Triton X-100 and subsequent detergent removal on BioBeads. Formation of heterotrimers was accomplished by using three different DNA tags, each featuring two regions for complementary base sequences, so that each of three contained one complement for two others.[332] The resulting assemblies were characterized by negative stain transmission electron microscopy and by single-molecule fluorescence using three different AlexaFluor dyes which allowed quantitation of colocalization of dimers and trimers in single nanodiscs.[332]

In summary, nanodisc technology has enabled the structural tools long applied to soluble proteins to be effectively utilized in the investigation of membrane proteins. The wide variety of sizes of nanodiscs (6—17 nm in diameter, and even up to 50 nm[239]) and the control over bilayer composition has opened the door to further high resolution structural studies of lipid and protein interactions.

4. APPLICATION OF NANODISCS IN ANALYTICAL AND FUNCTIONAL STUDIES OF MEMBRANE PROTEINS

The incorporation of membrane proteins into nanodiscs provides several important advantages for multiple experimental methods that are commonly used for quantitative studies of the binding of small molecules, such as substrates, inhibitors and effectors. As already mentioned, homogeneous and stable preparation of the membrane protein with well characterized and controlled oligomerization state is a prerequisite for the precise quantitative and reproducible measurements and for unambiguous interpretation of the experimental data. The separation of specific ligand binding to the target protein from partitioning of the small hydrophobic ligand into the hydrophobic detergent micelles often represents a challenging task.[334−336]

4.1. Binding of Small Molecules to Membrane Proteins in Nanodiscs

Nanodiscs have been critical in the successful monitoring of many protein−membrane association events. For example, solution NMR was used to study the soluble protein complex formation with the nanodisc lipid bilayer. α-Synuclein, an important family of proteins involved in autosomal dominant Parkinson's disease, binds to POPA/POPC nanodiscs and was found to be weaker in the presence of 1 mM Ca^{2+} ions, as detected by $^{1}H-^{15}N$ heteronuclear single-quantum coherence (HSQC) spectra of uniformly ^{15}N-labeled synuclein.[337] This effect is attributed to Ca^{2+} binding to anionic lipids that reduces the affinity of synuclein for the membrane. The binding of granuphilin, a protein that molecularly docks insulin granules to the cellular fusion machinery, to nanodiscs was studied in order to explore the mechanism of specific interaction of the common C2 domain with PIP2 lipids incorporated in a POPC bilayer.[287]

DOI: 10.1021/acs.chemrev.6b00690
Chem. Rev. 2017, 117, 4669−4713

A combination of NMR, isothermal titration calorimetry, and microscale thermophoresis methods allowed the authors to identify single protein residues which form the binding site directly interacting with the PI(4,5)P2 head-groups. Single-point mutations across this site identified five critically important residues essential for PIP2 recognition. Analytical applications of nanodiscs to binding studies of PIP binding domains in several proteins using pull-down assays, fluorescence polarization measurements, and NMR spectroscopy were developed in order to identify residue-specific binding sites.[338] Further application of NMR spectroscopic methods provided more information about the binding mode and orientation of the FYVE domain interacting with PIP3 lipid.[339] Interaction of monomeric class A GPCR neurotensin (NT) receptor incorporated in nanodiscs with agonist NT and with G-proteins was probed at various lipid compositions, and affinity of Gq proteins toward activated receptor increased with increased POPG content.[340] Thus, the presence of negatively charged lipids is essential for fully functional signaling of nonvisual GPCR as well as for rhodopsins.[212]

Some of the most challenging drug targets are the G-protein coupled receptors (GPCRs). Nanodiscs have been widely used for investigating these recalcitrant membrane proteins at multiple stages, from stability improvements in solubilization and purification protocols, to incorporation of purified GPCRs into nanodiscs for biophysical and biochemical studies. As with other membrane proteins, nanodiscs allow one to probe the functional properties of receptor proteins as they exist in a native-like membrane environment, with controllable and known oligomerization state, all in an entity soluble in aqueous solution. This enabled a major success: the comparison of a monomeric GPCR with those of homo- and hetero-dimers.[11] The first incorporation and functional study of a monomeric β_2-adrenergic receptor in nanodiscs was described by the Sligar laboratory in 2006.[341] In this case, heterologously expressed protein was solubilized in detergent, assembled with phospholipid and scaffold proteins and purified by affinity chromatography using a genetically engineered FLAG tag. Receptor incorporated in POPC nanodiscs was used for binding studies with the small ligand antagonist dihydroalprenolol and the agonist isoproterenol, as well as radiolabeled G-proteins. A binding isotherm for the former ligand was obtained by equilibrium dialysis, and the measured dissociation constant of ∼5.5 nM was similar to that previously reported in the literature. Similar results were obtained for the agonist binding to the low-affinity form of receptor (without G-protein). G-protein binding experiments confirmed a fully functional form of the monomeric receptor incorporated in nanodiscs, including demonstration of a 10-fold enhanced binding of G-protein in the presence of agonist.

Discoidal rHDL particles were also used in binding studies of GPCR receptors, including monomeric β2-adrenergic receptor,[221,342] monomeric μ-opioid receptor,[343] and parathyroid hormone 1 receptor.[108] Application of model membranes for functional studies of monomeric and oligomeric GPCR proteins was reviewed in ref 344. In addition, β2-adrenergic receptor incorporated in rHDL was used in pull-down assay to identify previously unknown proteins interacting with this receptor, which provide new information about intracellular signal pathways.[219]

The binding of small ligands (molecular mass ranging from 337 to 428 Da) to the human adenosine receptor A_{2A} (GPCR) incorporated in nanodiscs assembled with mixed POPC-POPG lipids was studied using SPR and a scintillation proximity assay.[213] Possible partitioning of the ligand into the lipid bilayer of nanodiscs was accounted for by placing empty nanodiscs in the reference channel. Results of this work confirmed that label-free monitoring of small molecule binding kinetics of the membrane protein in nanodiscs could be performed using SPR, suggesting a new approach to the measurement of the influence of agonistic or antagonistic ligands on the binding of G proteins or β-arrestin to the extracellular or intracellular sides of the bilayer. Significantly enhanced stability of the receptor incorporated in nanodiscs was also reported as an advantage and interpreted as evidence of a native-like environment. As a note, the scintillation proximity assay was also used to study binding to other membrane proteins in nanodiscs, such as the beta-2 adrenergic receptor[345] and bacterial leucine transporter.[346]

Multiple binding studies performed with proteins incorporated in nanodiscs confirmed that, in many cases, the presence of annular lipids surrounding the target protein is essential for function. In some cases it has been possible to estimate the number of specific lipids needed and to correlate this with lipid−protein structural interactions. As an example, the transporter associated with antigen processing (TAP) requires the presence of approximately 22 lipids to form one annular array in the nanodisc to display the stoichiometric 1:1 high affinity inhibition by the viral TAP inhibitor ICP47.[102] An inhibitor constant of K_i = 0.28 μM was found in the smaller MSP1D1 nanodiscs and roughly the same (K_i∼0.21 μM) in the larger MSP1E3D1 nanodiscs, while in detergent the digitonin inhibition constant is ∼20-fold higher. In addition, in a novel method, microscale thermophoresis was used to measure binding of the substrate C4 peptide to the TAP transporter.[102] The other approach based on the fluorescence polarization assay was used to prove direct interaction of IL-13Rα2 protein with the trans-membrane protein TMEM219 in nanodiscs in the presence of chitinase 3-like-1, which is subsequently activated for regulation of apoptosis, inflammation response, and melanoma metastasis.[347] Binding with high affinity was detected only when both components were present in solution, while no effect was observed with only Chi3l1.

Another example of functionally important interactions with lipids was described for the ABC transporter MsbA, where the binding properties and ATPase activity of the catalytic unit strongly depended on the lipid bilayer properties, even at some distance (∼5 nm) from the target.[348] The rates of ATP hydrolysis were 5 − 10 times faster in nanodiscs than in the detergent DDM, while the binding of the substrate analog ATP-γ-S measured by SPR was 10 − 100 fold tighter when MsbA was incorporated in the larger MSP1E3 nanodiscs than when target self-assembled using the smaller MSP1D1 membrane scaffold protein. In addition, the affinity for a substrate analog was significantly lower when DMPG was used, as compared with pure PC lipids.

ATP-dependent substrate binding and release by an energy-coupling factor (ECF) transporter incorporated in nanodiscs was studied to explore conformational changes during substrate translocation.[103] A biotin transporter from *Rhodobacter capsulatus* was expressed in *E. coli*, purified and incorporated into nanodiscs using a total *E. coli* lipid mixture. In order to successfully incorporate a multisubunit transporter, the extended scaffold protein MSP1E3D1 was used to generate larger nanodiscs. Although reconstruction into liposomes was inefficient, assembly into nanodiscs yielded a complex that was

DOI: 10.1021/acs.chemrev.6b00690
Chem. Rev. 2017, 117, 4669−4713

functional for several days without loss of activity. In this case the ATPase activity in nanodiscs was slightly higher than previously reported for detergent solubilized transporters, and was not stimulated in the presence of biotin substrate. ATP-induced conformational rearrangement between subunits was monitored by electron paramagnetic resonance (DEER) spectroscopy, with site-specific labeling and by cross-linking of cysteine mutants at subunit interfaces using various bifunctional thiol reagents. Results of these experiments indicated that binding of ATP by the ATPase domain induces conformational changes with increased flexibility at the interface between the other subunits. A structural model of this mechanism was also proposed based on these experimental results.[103]

Limited proteolysis of an ATP-binding type I transporter from *Salmonella enterica* was compared in the presence and absence of various cofactors for a complex solubilized in detergent with those reconstituted in proteoliposomes and in nanodiscs prepared using MSP1E3D1 and *E. coli* total lipids.[124] Here the ATPase activity was not stimulated by substrate in detergent solution but was 6-fold accelerated in proteoliposomes. Substrate binding protected all domains, to some extent, against tryptic hydrolysis, with the highest protection observed upon ATP binding. Three conformational states, i.e., open, semiopen, and closed, corresponded to the observed accessibility of the cleavage sites. Interestingly, mutants that bind ATP but are unable to catalyze hydrolysis were considerably more resistant to proteolysis, indicating their preference toward the closed conformation. Overall these results were similar to that of the maltose and histidine transporters, despite significant structural differences between these proteins.[124]

Another recent study of the multidrug transporter LmrP compared protein conformational dynamics in detergent micelles and nanodiscs reconstituted with total *E. coli* polar lipids using EPR spin labels at multiple sites.[218] Measurements performed at various pH revealed a significant lipid headgroup dependence of the apparent transition between conformational states, with p*K* of 6.9 and 7.3 for measurements taken on the extracellular site and on cytoplasmic site, respectively. In detergent solubilized protein, these transitions were observed at the significantly more acidic p*K*s of 4.7 and 5.9. Further experiments using nanodiscs with varied lipid compositions revealed a specific role for methylation of PE head groups in stabilization of the outward-open conformation of the protein at higher pH. In addition, native mass spectrometry was implemented for detection of those lipids that most strongly interact with detergent-solubilized LmrP transporter. A gradual increase of the collisional activation voltage from 225 to 300 V revealed the presence of various cardiolipins, which withstand solubilization in detergent. In addition, DEER experiments at various pH with LmrP in nanodiscs assembled using various fractions of DOPE and DOPG demonstrated that, in the presence of cardiolipin, the conformational equilibrium at the extracellular side was altered, as opposed to that on the intracellular side. This indicated a specific role of cardiolipin, and possibly other lipids, in regulating the large-scale conformational changes necessary for function of this transporter. The possible mechanism of this regulation may involve lipid head groups as proton donors or acceptors, facilitating protonation of protein residues on the extracellular side and favoring closed conformation.[218] In other investigations, the interaction of MalE and maltose triggers coupling of ATPase hydrolysis to translocation in the MalFGK2 transporter.[349]

4.2. Binding of Membrane Proteins to Nanodisc Membranes and to Proteins in Nanodiscs

Nanodiscs also proved to be very useful for binding studies of membrane proteins using surface plasmon resonance (SPR)[92,104,146,213,267,283,284,350−354] and various related methods, such as localized surface plasmon resonance (LSPR)[355] or nanoplasmonic array resonance.[356] Various experimental approaches to the use of SPR-type methods in binding studies of membrane proteins in nanodiscs were described in a recent review.[357] Nanodiscs can be attached to the sensor surface using affinity tags added to the MSP sequence (histidine, FLAG, RGD, etc.) or labels attached to genetically engineered sites on the scaffold protein (e.g., specific DNA sequences, biotin, sulfhydral reactive agents, etc.), making possible label-free detection of nonmodified native membrane proteins. When nanodiscs containing an incorporated membrane protein are attached to the surface of an SPR sensor, both sides of the lipid bilayer are accessible for interactions with partners. This is in contrast to liposomes, where the closed lipid bilayer prevents access to the inside domain of incorporated membrane proteins. In some cases this feature of nanodiscs represents an advantage, providing a straightforward method for observation of trans-membrane signaling, such as release of the UIC2 antibody bound to the P-gp transporter induced by ATP binding to the cytosolic domain on the opposite side of the nanodisc.[357] Another example is the simultaneous interactions of the sensor histidine kinase CpxA with cytosolic partner protein CpxR and the periplasmic protein CpxP.[104] In the latter case, results obtained with SPR were compared with data measured using microscale thermophoresis, and both methods confirmed a 10-fold increase of binding affinity between CpxA in nanodiscs and the regulator protein CpxR in the presence of ATP. Farnesylated and nonfarnesylated versions of full-length cancer signaling protein K-Ras4B as well as peptides corresponding to the hyper-variable region, bind to nanodiscs assembled with DPPC, DOPC, and DOPS (each containing 5% of DOPE) as was monitored using SPR. A slightly higher affinity and strong cooperativity was detected for the farnesylated peptides.[358] Highly cooperative binding that reached saturation at concentrations almost an order of magnitude lower was noted for farnesylated peptides, although the formal dissociation constants measured were not dramatically different. KRas4b binding at different temperatures to DPPC nanodiscs confirmed a strong dependence of cooperativity on the fluidity of the bilayer, with diminishing cooperativity when temperatures increased from 25 to 45 °C.

Advances in SPR methods with a goal of improving sensitivity and multiplexing of membrane protein analysis were reported for CYP3A4 in nanodiscs detected by LSPR on arrays of silver nanoparticles on glass[355] prepared using a nanosphere lithography method.[359] Nanodiscs containing CYP3A4 were covalently attached via a carbodiimide coupling to the silver nanoparticles activated through a self-assembled monolayer of 11-mercaptoundecanoic acid. The binding of substrates or inhibitors to the P450 enzyme is monitored by the shift of the LSPR band. In this case, LSPR provided a higher sensitivity and required less material due to the strong response of the localized plasmon mode upon changes of refraction index in the immediate vicinity of nanoparticle (see reviews in refs 360 and 361). In addition, the response was even stronger if the

DOI: 10.1021/acs.chemrev.6b00690
Chem. Rev. 2017, 117, 4669−4713

plasmon band of the Ag nanoparticles overlaps with the optical absorption band of the target, in this case the heme group of CYP3A4. If the optical spectra of the target changes in response to substrate or ligand binding, the result is a further dramatic increase in overall sensitivity.[362] For CYP3A4 on Ag nanoparticles this effect allowed distinct observation of type I or type II ligand binding by detection of the 2−8 nm blue- or red-shifted plasmon band. This signal could be readily observed from ~10^9 nanodiscs containing CYP3A4 which corresponds to less than 1 femtomole.[355] Incorporation in nanodiscs maintained CYP3A4 in the native and fully functional state and prevented poisoning of the sensor surface.

Another approach to the miniaturization of parallel multichannel sensing was developed by the Bailey group.[363,364] Here, silicon oxide microring resonators were used for sensing refractive index changes for detecting binding events on an array of 30 μm diameter silicon rings. The multichannel chip described in ref 363 contained 32 rings, with the possibility of measuring each independently using a tunable near-IR laser to launch an optically guided mode. Nanodiscs self-assembled with a target protein were physically absorbed on the ring surface, with any nonspecific absorption of analyte blocked by serum albumin. This method allowed multiple binding experiments to be performed simultaneously under identical conditions and from the same sample. Alternatively, the selectivity and cross-reactivity of various targets could be measured by placing nanodiscs containing different membrane proteins on separate rings, on the same chip, and observing the output using the same analyte partner. A proof-of principle experiment showed selective interaction of specific binders with nanodiscs containing 30% POPS (annexin), biotinylated lipid (streptavidin), glycolipid receptor GM1 (cholera toxin) and CYP3A4 (antibody to CYP3A4) in nanodiscs.[363] This method, together with the use of nanodiscs to form libraries of membrane proteins from biological samples, can be used for precision medicine applications and the screening for cancer markers.

Another type of nanoplasmonic sensor, the Lycurgus Cup Array, or nanoLCA, was used in combination with nanodisc incorporated cytochrome P450 CYP2J2 to monitor substrate binding with high sensitivity.[356] A regular array of nanoholes covered with the thin gold layer (final diameter 180 nm, periodicity 350 nm) is used as an optical sensor for substrate binding with CYP2J2-nanodiscs coupled to a self-assembled monolayer of 11-meraptoundecanoic acid.[355] A blue shift of the plasmonic band was observed upon substrate binding, similar to that previously reported in the aforementioned LSPR study.[355] Sensing was also detected based on colorimetric analysis of the bright-field microscope image. Such technology may be used in further development of high-throughput analytical methods.

The binding of various proteins to a membrane surface as a function of membrane composition and the presence of specific lipids can be conveniently studied using nanodiscs assembled with the desired mixtures of lipids. Such studies provide quantitative information on the lipid specificity for protein binding to the bilayer nanodiscs with well characterized composition, thus avoiding possible segregation of lipids and formation of compositionally heterogeneous patches on liposomes. This nanodisc approach was used in binding studies of blood coagulation proteins,[92,174,279,353,365] as their interaction cascade is triggered when negatively charged lipids are exposed and available for interacting with blood clotting enzymes.[174,365] Especially important for this system is the high stability of nanodiscs containing a high fraction of lipids containing carboxyl groups, such as phosphatidylserine, in the presence of 1−3 mM Ca^{2+} cations.[92] Normally these conditions result in aggregation and fusion of liposomes of the same composition.[95] The coagulation factor X binding to nanodiscs assembled with POPC/POPS mixtures of different compositions, from 0 to 90% PS lipid, showed that maximum affinity is reached at 80% PS, and the maximum rate of Factor X activation by the complex of tissue factor and Factor VIIa is observed at 70% PS.[92] This observation confirmed the idea of preferential activation of Factor X on PS-rich clusters, the formation of which may be favored by the presence of divalent cations.[279]

The activation of monoacyl glycerol lipase interacting with nanodiscs formed with POPC:POPG mixed lipids and with pure POPC discs was observed with a K_m decreasing and V_{max} increasing, as compared with activity measured in Triton X-100 micelles, with no enhancement due to the negative charge of POPG lipids.[366] Hydrogen−deuterium (H/D) exchange measurements were used to identify two helices interacting with the lipid bilayer, which apparently form the entrance to the substrate binding pocket. Conformational changes and dynamics of the enzyme were also probed by these authors and suggest possible conformational changes leading to substrate entrance from the membrane side.

In other studies, the interaction of cholera toxin proteins with glycosphingolipids (GSLs) and glycolipids included in nanodisc bilayers were studied by electrospray ionization mass spectrometry[184,286] with a new "catch-and-release" method.[62] This method combines two steps of collision-induced dissociation of the complex formed by carbohydrate-binding protein with glycosphingolipid in nanodiscs. In this approach, the first step breaks down interactions between lipids in nanodisc and releases a complex of protein and GSLs, which is then subjected to another collision induced dissociation where the target protein is analyzed and identified. Further development of this approach with pico-discs[61,62] formed using saposin instead of membrane scaffold proteins[63] provided a proof-of-principle background for screening of specific lipid−protein interactions. Another approach used two-step analysis with nanodiscs containing GSL ganglioside GM1 immobilized on an SPR surface for monitoring protein binding from an *E. coli* extract.[283] Subsequently, the protein was identified by mass-spectrometry as the enterotoxin LTB. These and other applications of nanodiscs containing target membrane proteins for binding specific high-affinity ligands with detailed analysis using various proteomics methods has recently found further success as summarized in several publications.[111,112,182,219,281,367]

Surface immobilization of rhodopsin in nanodiscs using the His-tag on the scaffold protein was used for the application of matrix-assisted laser desorption ionization − time-of-flight (MALDI-TOF) mass-spectrometry to monitor interactions with soluble transducin.[368] The fully functional state of immobilized rhodopsin was confirmed by light-activated binding, while control experiments in the dark showed no association of the effector protein. Rhodopsin − transducin complexes were dissociated when treated with the non-hydrolyzable inhibitor nucleotide GTPγS. Viability of quantitative analysis of bound protein without fluorescent or radioactive labeling made this technique attractive for analytical and screening studies.

DOI: 10.1021/acs.chemrev.6b00690
Chem. Rev. 2017, 117, 4669−4713

5. ONE EXAMPLE OF NANODISC USE IN MEMBRANE PROTEIN INVESTIGATIONS: CYTOCHROME P450

It is beyond the scope of this review to extensively discuss the results from the numerous systems that have benefited from using nanodisc technology. In this section we have chosen on particular multicomponent membrane protein system that can serve as an example of the depth of knowledge which can be obtained that would be difficult or impossible without the use of nanodiscs. Here the membrane is a key partner and plays a critical role in determining the correct structure of the protein needed for function.

These benefits of nanodisc applications can be clearly illustrated by multiple successful studies of human cytochromes P450. Cytochromes P450 represent an important superfamily of heme enzymes involved in multiple biochemical networks, including the biosynthesis of steroid hormones and other regulatory compounds, as well as providing the major pathway of xenobiotic metabolism and decomposition. In prokaryotes these enzymes are soluble, while in eukaryotes they are incorporated in the membrane via single N-terminal helical anchor. Additional interaction with the membrane is realized by incorporation of a hydrophobic patch on the P450 protein surface between the head groups of membrane lipids.[79,299,369−373] The membrane bilayer also serves as a template for the productive association with required redox partners such as the membrane anchored flavoprotein cytochrome P450 reductase (CPR) and small heme protein cytochrome b_5.[72,374−377] All three proteins, cytochrome P450, CPR, and cytochrome b_5 are held and oriented in the appropriate mode in order to form the functionally competent complexes.[72,376]

The complexity of the multiprotein P450 systems and the availability of multiple spectroscopic probes of structure and function provide an excellent demonstration of the value of studying membrane proteins in their native bilayer environment. Purified mammalian P450 heme enzymes and CPR exist in solution mostly in aggregated forms and hence have historically been studied in solubilized forms using mixed micelles consisting of mild detergents and/or lipids[378−380] with addition of glycerol. Other investigators have incorporated the P450 protein in lamellar vesicles.[381−383] Nanodiscs have presented a system where the precise stoichiometry of protein components can be controlled, where potential lipid specificities can be provided and where the proteins are in the correct conformation for functionality.

5.1. P450 Substrate Binding

The advantages provided by nanodisc incorporation of monomeric human P50 were demonstrated by several studies of the main human drug metabolizing enzyme, P450 CYP3A4.[27,85,99,297,314,384−392] The first incorporation of eukaryotic cytochrome P450 in POPC nanodiscs demonstrated the potential of this system for understanding cytochrome P450 function.[314] Unlike other studies, which did not use nanodiscs,[393−396] incorporation of CYP3A4 into nanoscale lipid bilayers ensures clear UV−vis spectral monitoring of substrate binding and avoids aggregation that inhibits substrate access to the active site. This difference is clearly noted in the nearly complete shift of heme iron spin state from low-spin to high-spin form, the so-called "Type-I spectral shift" characteristic for cytochrome P450 substrate binding.[295,314,385−389,397] Titration of CYP3A4 with the substrate testosterone was shown to reach a high degree of high-spin conversion (~96%) at concentrations higher than 200 μM, with a clearly sigmoidal shape of the titration curve and apparent Hill coefficient of ~2.2.[314] Careful analysis of spectral titration indicated that it is impossible to fit the observed titration curves using a model with only one or two binding sites. For testosterone (TST), at least three molecules of the substrate bind to a monomeric CYP3A4 in nanodiscs. These results demonstrated for the first time the critical importance of a reconstitution system, which provides a well characterized membrane surface with control of target protein oligomerization state. Complete spin shift upon substrate binding critically depends on the subtle conformational changes of P450 heme enzyme and upon access of water to the heme-oxygen catalytic site, thus indicating fully functional form of CYP3A4 in nanodiscs.

Subsequent *in vitro* titration experiments demonstrated an almost complete transition of the type-I spectral change (monitoring the low-spin to the high spin conversion) of CYP3A4 in nanodiscs with other substrates.[87,386,388,397] These observations indicate complete accessibility of all P450 molecules in the sample when incorporated in nanodiscs, and saturation could be achieved in an equilibrium titration with several ligands including testosterone, progesterone and bromocriptine.[87,314,386,387,397,398] On the other hand, only partial spin-shift is usually observed with the same substrates when using other solubilization conditions, i.e., with detergent micelles or in liposomes.[393,394,399] In some cases, however, a complete spin shift has been reported for truncated CYP3A4, which is more soluble and less prone to aggregation.[400] In addition, >90% monoexponential binding kinetics with these substrates confirm the functional competence and homogeneity of CYP3A4 preparations in nanodiscs. Similar results were obtained with other cytochromes P450, such as CYP19A1 and CYP17A1 self-assembled in nanodiscs.[83,86] In these cases, substrate binding measurements revealed a 90% - 98% spin shift with substrates such as pregnenolone and progesterone, yet with only partial conversion with the 17-hydroxylated metabolites. This has provided a useful base of comparison for the relative ability of a given substrate to fit the binding pocket and to induce the functionally important spin-state changes. Having established 100% functional competence and homogeneity with respect to the native substrates with some P450 enzymes (e.g., CYP17A1 and CYP19A1) or various model substrates for CYP3A4, it is becoming possible to use the amplitude of the fractional spin shift as a reliable probe for functional substrate positioning in the enzyme active site. This structural and functional homogeneity of membrane bound P450 enzymes in nanodiscs allows one to differentiate between modes of substrate positioning, which relate to functional conformers required for activity. An example is the use of resonance Raman spectroscopy to reveal control of regio- and stereo-specificity of catalysis, which would be impossible with a highly heterogeneous or aggregated sample.[83,87,88,90]

Monomeric human CYP3A4 incorporated in nanodiscs was also used to realize the first mechanistic description of the allosteric properties of this enzyme by single-molecule methods,[27,99] as already discussed earlier in this review. Comparison of the fast binding of fluorescent model substrate Nile Red to empty nanodiscs with a slower binding to CYP3A4 enabled estimation of the binding rate via nanodisc bilayer as ~5 s^{-1}.[99] In this case a homogeneous monodisperse preparation of CYP3A4 in nanodiscs provided the basis for determining the kinetic heterogeneity in terms of several kinetic processes and ruled out possible contribution of protein

DOI: 10.1021/acs.chemrev.6b00690
Chem. Rev. 2017, 117, 4669−4713

oligomers. Another substrate binding study used CYP3A4 in POPC nanodiscs to explore the effects of partitioning of various P450 substrates into the lipid bilayer.[392] The intrinsic fluorescence of 6-(p-toluidino)-2-naphthalenesulfonic acid (TNS), α-naphthoflavone (ANF), miconazole, and bromocriptine was used to monitor partitioning of these substrates into the lipid bilayer of nanodiscs, while binding to the CYP3A4 was observed by optical spectroscopy and spin shift changes. Some substrates, such as bromocriptine and miconazole, bind more tightly to CYP3A4, while ANF preferentially partitioned into the membrane.

An important regulatory role of substrate binding in P450 catalysis and the type-I spin-state shift is the coupled shift of the ferric heme iron redox potential to more positive values.[401−403] This shift significantly accelerates electron transfer from the redox partner CPR for reduction of cytochrome P450 heme iron from Fe^{3+} to Fe^{2+} state, which enables binding of atmospheric oxygen (O_2) to the prosthetic group. The rate of P450 reduction strongly depends on the redox potential of both cytochrome P450 and CPR. Experimental assessment of these rates in eukaryotic P450 enzymes is not easy, and direct measurements are sparse and produce highly scattered numbers, as reviewed in refs 404 and 405. Because of the much higher stability and homogeneity of nanodisc incorporated monomeric cytochromes P450, redox potential measurements can be performed using spectro-electrochemical titration in solution in order to explore the effects of substrate binding as well as the changes of redox potential caused by charged lipids. Results of these experiments demonstrated that in CYP3A4 upshift of redox potential is proportional to the fraction of high-spin shift caused by substrate binding,[297] similar to the earlier results obtained using soluble bacterial cytochrome P450 CYP101A1.[406] For CPR in nanodiscs the effect of incorporation in the lipid bilayer was probed by measuring midpoint potentials of both flavins in pure POPC nanodiscs (zwitterionic head-groups) and with 50% POPS (negatively charged lipids). Membrane incorporation shifted both flavin midpoint potentials to positive values in a POPC bilayer, while negatively charged POPS lipids caused negative shifts that favor accelerated electron transfer to the P450 heme.[298]

The binding of small molecules to proteins perturbs the energy landscape and alters functionally important motions. Since membrane proteins inserted in nanodiscs result in a native-like environment, this method can be used to quantify these parameters. The conformational dynamics of CYP3A4 in nanodiscs, both with and without the inhibitor ketoconazole bound, were investigated using hydrogen/deuterium (H/D) exchange.[407] This work provided the first account of structural and dynamic changes of membrane bound cytochrome P450 caused by small molecule binding. Several previous studies of H/D exchange in the mammalian P450 enzymes CYP46A1,[408,409] CYP19A1,[410] and CYP2B4[411,412] were performed in a solubilized form without the presence of a lipid bilayer. In agreement with modeling studies of CYP3A4 in the membrane,[299,372,373,398] exchange rates were low for the F′ and G′ helices, which are embedded in the lipid bilayer, and much higher for F and G helices, indicating their exposure to the solvent. The binding of ketoconazole resulted in significant stabilization of the A and G helices and other fragments, including a middle portion of I-helix in the catalytic site. Surprisingly, the C-helix and J-helix and the loop preceding J′-helix became less protected.[407] These results indicated the presence of global changes in the dynamic landscape of membrane bound P450 enzymes upon the presence of substrates or inhibitors, with specific features not reported in similar H/D exchange studies of soluble counterparts.[413,414] Comparison of CYP3A4 in nanodiscs and in 0.1% detergent Emulgen revealed similar exchange rates, with the exception of the F and G helices, which are significantly less exposed to the solvent in nanodiscs,[407] even though they do not directly interact with the membrane.

Substrate binding to another mammalian P450, CYP2J2, in nanodiscs was studied by optical spectroscopy,[415−417] and results were compared using several N-terminally truncated samples with different truncation lengths. No effect of truncation was observed in binding the natural substrate arachidonic acid (AA) and one drug Ebastin, which is also metabolized by CYP2J2.[415] Further work compared the binding of AA with the closely related endogenous substrates anandamide and 2-arachydonyl glycerol.[416] This work utilized direct observation of type I spectral changes in the Soret band and indirect probing by competitive perturbation of equilibrium and kinetics of CN^- binding in the presence of substrates. These indirect measurements provide more sensitive probe for the presence of substrate at the binding pocket or at the access path for the diatomic ligand. Results of binding studies, together with turnover in a reconstituted system, demonstrate variations in rates and product distributions linked to the substrate structure. A separate study explored effect of N-terminal truncations of CYP2J2 on the functional interaction with CPR in nanodiscs and discovered that the full-length CYP2J2 is reduced ∼200 faster than the same P450 with the truncated N-terminal.[417]

A nonclassical cytochrome P450, the human thromboxane synthase, CYP5A1, was also incorporated in nanodiscs and the binding of two substrate analogs were studied using optical spectroscopy.[418] The effect of mutations at position I346 on the I-helix, which corresponds to highly conserved threonine (T252) in the widely studied bacterial CYP101A1, was also probed using I346T and I346S mutants, and variations in the spectral response and in binding affinity were reported. Cyanide binding was also used with CYP5A1, as with CYP2J2, to probe substrate binding.[419] Additional investigations of substrate binding to P450s in nanodiscs were undertaken by many laboratories and include the isozymes CYP5A1,[418,419] CYP2J2,[303,356,415−417] and CYP5A1.[418−420]

5.2. Intermediate States of Membrane Protein Catalysis: The Oxy Complex of P450 and Its Reactivity

Many oxidase and oxygenase systems operate at a membrane surface and involve complex catalytic cycles that involve redox input and diatomic ligand binding. An important advantage provided by homogeneous and stable reconstitution of monomeric cytochromes P450 in nanodiscs involves spectroscopic investigation of ternary complexes of the enzyme with substrates and dioxygen liganded to the active site heme iron. P450 catalysis is based on utilization of atmospheric oxygen O_2 for oxidative transformations of substrates, and spectroscopic studies of the oxy complex and further iron-oxygen intermediates in the catalytic cycle provide indispensable information about mechanism of these enzymes.[402,403,421] Although several recent EPR investigations of P450 CYP11A1 and CYP2B4 intermediates were made with the protein outside a membrane environment,[422−425] in general due to aggregation and diffusional limitations, the presence of side reactions with detergents and the inherent instability of oxy

DOI: 10.1021/acs.chemrev.6b00690
Chem. Rev. 2017, 117, 4669−4713

complexes in P450 enzymes, properties of these important intermediates in eukaryotic P450 enzymes have not been investigated to the same level as in their soluble prokaryotic counterparts. The application of nanodiscs has enabled isolation and stabilization of these transient oxy complexes in human P450 in a membrane environment. New details of P450 catalytic mechanism were revealed by resonance Raman and other spectroscopic characterizations of transient intermediates in the human cytochromes CYP17A1 and CYP19A1 in the presence of various substrates.[24,83,89,90]

In studies of the steroid biosynthetic pathways, Raman spectra of the oxy complex in human CYP17A1 self-assembled into nanodiscs were measured in the presence of four substrates.[83] Two of them, progesterone (PROG) and pregnenolone (PREG), undergo a hydroxylation at the C17 position that is catalyzed by the "compound I" intermediate thought to be involved in most alkane hydroxylation reactions.[426,427] The corresponding products, 17-hydroxy-PROG and 17-hydroxy-PREG are also substrates for the subsequent step in androgen biosynthesis, a C17-C20 bond cleavage. The mechanism of this second lyase step in CYP17A1 catalysis was debated for many years (see reviews in refs 426 and 428), and two alternative pathways have been suggested. One is the usual P450 alkane functionalization by a higher valent compound I intermediate. The other is a very different chemistry involving the peroxo-anion intermediate prior to protonation and formation of compound I.[421,426,427,429] Raman spectra of the CYP17A1 oxy complex, which is the direct precursor of the peroxo-ferric states, revealed drastic difference between the ν(Fe-O_2) and ν(O-O) modes for 17-hydroxy-PROG and 17-hydroxy-PREG bound CYP17A1. While these modes are at 542 and 1131 cm^{-1} with the former substrate, they are observed at 526 and 1135 cm^{-1} with the 17-hydroxylated PREG, revealing a previously unseen downshift of both ν(Fe-O_2) and ν(O-O) modes as compared to those observed when PREG and PROG are bound, at 535−536 cm^{-1} and at 1140 cm^{-1}, respectively. This unprecedented downshift of both modes in the 17-hydroxy-PREG complex can be attributed to hydrogen bonding between 17-hydroxyl group and the proximal oxygen atom of the Fe-O-O intermediate. This is distinct over that normally seen where hydrogen bonding occurs to the distal oxygen atom of the peroxo state.[83] A similar unusual perturbation of the Fe-CO Raman spectra of the carbonmonoxy form of CYP17A1 in nanodiscs in the presence of 17-hydroxy-PREG was subsequently reported.[89] Recently a combination of cryoreduction and resonance Raman spectroscopy, using nanodiscs to avoid aggregation and precipitation, allowed direct characterization of a new hemiacetal intermediate thus strongly supporting the peroxo-anion driven catalytic mechanisms reaction.[88] Here, the oxy complexes of CYP17A1 in nanodiscs with PREG and 17-hydroxy-PREG were frozen and reduced at 77 K by γ-irradiation from a ^{60}Co source to form peroxo-ferric complex stabilized in the frozen glycerol-buffer matrix, as reviewed in refs 294, 421, 430, and 431. Optical absorption and resonance Raman spectra measured at gradually increasing temperatures were used to identify a new previously unseen intermediate with a Soret band at ~ 407 nm and vibrational ν(Fe-O_2) and ν(O-O) modes at 579 and 791 cm^{-1} respectively with 17-hydroxy-PREG substrate.[88] No such intermediate was observed with PREG bound. Structural assignment of this intermediate as a peroxo-hemiacetal Fe-O-O-C, with the intact $^{16}O-^{16}O$ or $^{18}O-^{18}O$ bond originating from $^{16}O_2$ or $^{18}O_2$ used for preparation of precursor oxy complex, is confirmed by the correctly observed isotope shifts and the absence of any H/D solvent isotope dependence in spectra measured in H_2O or D_2O.

The oxy complex in CYP19A1 was also characterized by resonance Raman (rR) spectroscopy in the presence of two substrates, androstenedione (AD) and 19-oxo AD,[90] and no significant variation in the anticorrelation between the ν(Fe-O_2) and ν(O-O) modes was detected. With AD these modes were measured at 538 cm^{-1} and 1130 cm^{-1}, while with 19-oxo AD they are at 534 cm^{-1} and at 1132 cm^{-1}. In addition, low-frequency Raman spectra for the ferric CYP19A1 were measured with excitation at 356.7 nm, and an Fe-S mode was observed at 349 cm^{-1} with both substrates. Unlike that observed in CYP17A1,[83] the absence of an unusual H-binding pattern and virtually no changes in the heme modes are consistent with a compound I mechanism of catalysis for CYP19A1 in both hydroxylation with AD as substrate and the subsequent lyase reaction with 19-OH AD.

In addition to substrate binding, an equally important step in P450 catalytic cycle is dioxygen binding to the ferrous protein, resulting in the formation of the oxy-ferrous complex, which has partially ferric-superoxide character.[402,403,432] Understanding the structure and stability of this ternary complex of the heme enzyme is critical for correct mechanistic description of efficient P450 catalysis.[402,421] Experimental studies of P450 oxygen binding kinetics and autoxidation revealed similar advantages when the target protein is in nanodiscs. Experimental studies of CYP3A4 in nanodiscs[386] allowed one to characterize the stability of oxy-ferrous complex in a human cytochrome P450 as a function of the substrate present in the active site. The kinetics of formation and auto-oxidative decay of the oxy complex was monitored by UV−vis absorption spectrophotometry in stopped-flow experiments at various temperatures. In addition, the absorption spectra of this unstable intermediate in CYP3A4 was measured for the first time in the substrate-free form (maximum at 417 nm) and in the presence of saturating amounts of testosterone (425 nm) and bromocriptine (420 nm). These results revealed a high sensitivity of the oxy complex Soret band to the presence of substrates of various structure and polarity in the CYP3A4 active site, which is replicated in other human cytochromes P450.[83,86,296] Similar to the case of substrate binding, the kinetics of oxygen binding and autoxidation, with or without substrates, could be successfully described by monoexponential curves, indicating a high degree of CYP3A4 sample homogeneity in nanodiscs. The kinetics of cyanide binding to CYP3A4 were also found to be monoexponential for substrate-free and substrate saturated enzyme. Here, however, superposition of two kinetic processes was observed in autoxidation and cyanide binding experiments when CYP3A4 was only partially saturated with substrate, and different intermediates were present.[387] This is in contrast to the more complex kinetics observed in substrate binding[399,400,433,434] and electron transfer,[384,435] when CYP3A4 is partially aggregated. In addition, detergents can also bind as pseudosubstrates of solubilized P450 enzymes and compete for active site.[400] On the other hand, with CYP3A4 in nanodiscs, the kinetics of substrate binding monitored by the absorption spectra in Soret range (380−420 nm) can be well described by single exponential process with the rates significantly faster than those reported for detergent solubilized or aggregated CYP3A4. The significant acceleration of substrate binding to cyto-

DOI: 10.1021/acs.chemrev.6b00690
Chem. Rev. 2017, 117, 4669−4713

chromes P450 incorporated in nanodiscs is likely due to their monomeric state and lack of aggregation, although variations in the solvent composition (particularly, the presence of 15−20% glycerol that is present in many P450 samples) can also play important role in binding kinetics.

The rates of CYP3A4 autoxidation of in nanodiscs is very high, from 2.6 s^{-1} with bromocriptine and 20 s^{-1} with testosterone (TST) bound, rising to ∼500 s^{-1} in the substrate-free CYP3A4 at 37 °C. This suggests that autoxidation is the major nonproductive pathway in this P450, and that the presence of various substrates can significantly stabilize the oxy complex. Analysis of the temperature dependence of autoxidation rates based on the Eyring equation revealed unusually high activation energy, ∼15−18 kcal/mol, significantly higher than those reported for autoxidation of model porphyrin systems. High barriers for autoxidation in cytochromes P450 suggest that large-scale conformational dynamics are contributing to the rate-limiting step, which determines the rate of superoxide ligand release from CYP3A4 interior.[387,402] Similar results were obtained in carbon monoxide (CO) flash-photolysis experiments and in geminate rebinding of CO to CYP3A4 bound with substrates.[387] The same conclusions were also reached recently based on kinetic analysis of the nitric oxide synthase (NOS) reaction cycle.[436] Autoxidation rates measured for the human CYP19A1 and CYP17A1 in nanodiscs measured in the presence of the native substrates androstenedione[86] and PROG and PREG are slower than in CYP3A4, apparently indicating tighter substrate binding and less dynamic structure of substrate bound steroidogenic CYP19A1 and CYP17A1.

5.3. Use of Nanodiscs to Trap Membrane Protein Intermediates at Low Temperature

The use of low temperatures to stabilize and characterize enzyme intermediates is well-known.[437,438] The application of nanodiscs was critical for mechanistic studies of steroidogenic human cytochromes P450 using cryo-radiolysis. These experiments require preparation of a homogeneous oxy complex of the enzyme saturated by a substrate of choice. Both oxygen binding and substrate binding must be near saturation in order to resolve the spectra of the cryo-reduced intermediate. As described earlier in this section, these conditions can be achieved using CYP17A1 or CYP19A1 incorporated in nanodiscs at ambient conditions by stopped flow mixing. However, the lifetime of the oxy complex in these enzymes at room temperature is in the range of 2−10 s, which is not enough time for freezing as a transparent glass in aqueous-glycerol buffer solvent matrix.[294,439] The use of glycerol or ethylene glycol as cryo-solvent is preferable for these applications, as these organic solvents cannot dissolve lipids and preserve intact nanodiscs, as opposed to alcohols or dimethyl sulfoxide. Alternatively, the P450 oxy complex in nanodiscs can be prepared by mixing a concentrated solution of anaerobically reduced P450 saturated with substrate with oxygenated 85% glycerol/buffer containing the same substrate concentration at −40 to −50 °C. At these temperatures, stability of oxy complex is significantly higher, so that the sample can be thoroughly mixed and cooled to liquid nitrogen temperature to stabilize the ferrous dioxygen intermediate. Thus, oxygenated cytochromes P450 can be characterized by low-temperature spectroscopic methods, including UV−vis absorption and resonance Raman scattering.[24,83,88−90,296,397] Using this approach, the UV−vis spectra of oxygenated human CYP3A4, CYP19A1 and CYP17A1 incorporated in nanodiscs in the presence of various substrates were measured both by stopped flow spectroscopy at ambient conditions in aqueous buffers[86,386] and by cryo-spectroscopy in aqueous-glycerol buffer solutions.[295,296] In general, the positions of the main absorption bands are not altered, displaying the typically split Soret with a main band at 418−430 nm, and higher-energy component at ∼355 nm. Also observed are overlapped α- and β-bands at 550 and 575 nm, similar to the spectra of the oxy complexes observed with soluble cytochromes P450 and chloroperoxidase.[403,432,440] In P450 CYP3A4 and CYP17A1, the positions of the Soret band in the oxy complex vary in wavelength, depending on the substrate bound.[294,295,386] This variation can be used in combination with the rR data to investigate the positioning and orientation of substrates with respect to the oxygen bound heme iron catalytic site. In analogy, additional information of this type can be obtained from spectral studies using carbon monoxide (CO) or cyanide (CN^-) in the presence and absence of substrates and inhibitors.[87,89,397]

Cryo-spectroscopy has also been used to measure the rate of autoxidation in CYP19A1 in nanodiscs, over a broad temperature range, for evaluating the overall energetics of the catalytic cycle.[296] Based on the results of this work, a new application of temperature-derivative spectroscopy[441] was realized. This method allows deriving the activation barriers of irreversible reactions in one scan over the entire temperature range available for a given system.[442] For example, the value of activation energy for the autoxidation of CYP19A1 bound with its native substrate androstenedione was calculated as 18.5 kcal/mol, similar to the barriers measured for other cytochromes P450.[386,387] In order to study other intermediates in the P450 reaction cycle, a frozen sample of oxygenated CYP17A1 or CYP19A1 in nanodiscs was irradiated with γ-rays from a cobalt-60 source, generating the peroxo- or hydroperoxo-ferric complexes with good yield as discussed in the original publications and reviews.[294,430,431,439] Using this approach, unstable intermediates present in cytochrome P450 catalysis can be observed, which was not possible by other methods.[24,83,88−90,294−296,417,443] Note that these methods were initially developed for studies of soluble bacterial P450s[294,402,421,430,444−448] and later applied to the membrane bound mammalian P450s using the nanodisc platform.[24,88,89,296]

The binding of cytochrome b_5 to CYP2B4 assembled in nanodiscs using amphipathic 22-mer peptides instead of the normal MSP were recently probed by NMR.[72] Previously authors measured the binding of Cyt-b_5 and CYP2B4 in DLPC bilayers (K_d = 0.008 μM) and in solution (K_d = 0.14 μM) and found that the mutual affinity of the two proteins is substantially higher when the complex is incorporated in a membrane.[376] In addition, in nanodiscs it is more stable than in bicelles, where it starts to precipitate in 3 days, while in nanodiscs it is stable for more than a week, as judged by the same size chromatographic elution profile after 10 days at room temperature.[72] 2D $^1H-^{15}N$ TROSY heteronuclear single-quantum coherence (HSQC) spectra of ^{15}N labeled Cyt-b_5 with and without CYP2B4 in nanodiscs were compared in order to identify residues on Cyt-b_5 participating in direct interactions with cytochrome P450. In addition to several previously known residues, L75 was also identified as a part of Cyt-b_5−CYP2B4 interface. This difference between nanodisc results and those obtained using bicelle incorporation[449] is

DOI: 10.1021/acs.chemrev.6b00690
Chem. Rev. 2017, 117, 4669−4713

attributed to possible variations in membrane incorporation modes in these two model systems, or to the presence of detergents in bicelle samples. The binding of P450 reductase (CPR) to human cytochrome P450 CYP3A4 incorporated in POPC nanodiscs was also studied by size exclusion chromatography with monitoring of catalytic activity by the rate of NADPH reduction.[390] A comparison of the reduction kinetics of CYP3A4 in nanodiscs and liposomes by the reductase domain from CYP102[435] and by dithionite[384] clearly demonstrated essentially full completion in nanodisc samples, while oligomers formed without a membrane present resulted in only 55% reduced CYP3A4,[435] and a slower reduction in the aggregate.[384]

In addition, the interactions of CPR with full-length and truncated CYP2J2 were monitored by the kinetics of NADPH supported reduction in the first electron transfer step.[417] Binding constants of CPR to CYP2J2 were estimated by direct titration of CPR into the solution of CYP2J2 in POPC nanodiscs monitoring the small optical signal originating from the spin shift caused by interaction with CPR. Here the binding of CPR was significantly tighter in the presence of the transmembrane N-terminal fragment of CYP2J2 ($K_d \approx 0.12$ μM), as compared to 0.58 μM for truncated CYP2J2. Reduction of CYP2J2 by CPR was also much faster for the full-length heme enzyme than for truncated CYP2J2 when CYP2J2 and CPR were mixed from different syringes, but not faster when CYP2J2 and CPR were mixed and incubated together before adding NADPH. This suggests that even truncated cytochrome P450 can form a functionally competent complex with CPR on the nanodiscs membrane, although with lower affinity and kinetic stability.

The CYP725 from plant *Taxus cuspidate*, a key enzyme in biosynthesis of the anticancer compound Taxol, was also incorporated in nanodiscs for functional studies.[450] Comparison of *in vivo* and *in vitro* metabolic profiles established the inherent substrate promiscuity and multiple products observed for this enzyme even when incorporated in nanodiscs as a clean monomeric species. Notably, this cytochrome P450 from plant was active in a complex with cytochrome P450 reductase from rat liver, as well as with plant reductases. Results of this study highlighted the application of nanodiscs for scaffolding complexes of two or more proteins as a supra-molecular functional unit. Such application of nanodiscs for the isolation and characterization of two cytochromes P450, CPR and one more soluble enzyme as a complex assembly termed "metabolon"[451,452] was proposed by the Møller laboratory.[453]

Other examples are worth mentioning. The activity of CYP5A1 in nanodiscs was compared with various lipid compositions, and significant activation was observed in the presence of the anionic lipids POPS and POPE, as compared to zwitterionic POPC.[419] Several additional P450 enzymes from plants were incorporated in nanodiscs for functional studies[117,453,454] as well as their redox partners P450 reductases.[117,269,315,453] The cyclooxygenase homodimer (Cox-2) was also incorporated in nanodiscs assembled with POPC, POPS, DOPC, or DOPS lipids.[211] Surprisingly, the activity of Cox-2 did not depend on the lipid composition of the nanodiscs. The functional incorporation of monoamine oxygenase (MAO) in nanodiscs showed improved substrate binding ($K_m \approx 3-6$ fold lower for two different substrates) and stability, as compared with detergent solubilized preparations.[455] The binding of proteins and small molecules to nanodiscs or to membrane proteins in nanodiscs changes the mobility and hydration of lipoprotein particles, so that these changes can be used for label-free detection of binding events and even for quantitative measurement of a binding isotherm. Experimental methods sensitive to such changes include NMR, fluorescence spectroscopy, and recently developed methods such as microscale thermophoresis.[456−458]

5.4. Mechanistic Enzymology of Cytochromes P450 in Nanodiscs

Applying the nanodisc system to the study of membrane bound cytochromes P450 has enabled significant advances toward understanding the molecular mechanisms of this important class of enzymes involved in drug metabolism and steroid hormone biosynthesis. Many of these enzymes metabolize hydrophobic substrates that can be localized in the membrane and have active sites that are at the membrane interface. Thus, the specific conformational landscape of the protein that is critical for function demands that P450 be in a bilayer environment. By allowing control over protein oligomerization state and membrane composition, the nanodiscs have proved to be indispensable for studies of P450 structure and function. The advantages for investigations into substrate binding events, which can be dramatically altered in detergent or aggregated states, has been discussed earlier in this review. The reproducibility of the nanodisc environment provided a basis for extending the classical measurements of catalysis as a function of substrate(s) concentration to include a global analysis of multiple parameter readouts. By examining product formation, pyridine nucleotide oxidation and spectral response in separate experiments and simultaneously fitting the data sets it was possible to separate binding cooperativity from differences in the functional properties of P450 CYP3A4 with one, two, or three substrates bound.[385] This analysis not only explained the highly unusual pyridine nucleotide oxidation kinetics commonly observed but also showed that the lag in response at low substrate concentrations was not due to binding cooperativity manifested through interaction free energy coupling but rather due to the lack of catalysis when only one substrate was bound at the enzyme active site.[385,459−461] Extending this work to the case when multiple substrates are present provided a new way to understand the critical human drug−drug interactions mediated by P450 CYP3A4.[388] Subsequent work involved studies of many drug pairs and the resulting heterotropic cooperativity[389] and has been reviewed.[460] Further mechanistic insight has been found by coupling experimental results with molecular dynamics calculations.[398]

A related aspect of P450 catalysis is the high degree of "uncoupling" or the nonproductive release of reducing equivalents as superoxide, peroxide, or water during the reaction cycle.[421] Not only are these processes wasteful in energy utilization, they can result in the production of deleterious reactive oxygen species. Such uncoupling is pronounced in enzymes involved in drug metabolism where large active sites are needed to accommodate multiple substrates but also in the difficult carbon−carbon lyase reactions involved in steroid biosynthesis. By providing a stabilizing membrane environment, the nanodisc system has been helpful in understanding the mechanisms of these uncoupling reactions in the case of hepatic human CYP3A4[85,385,387] and in CYP17A1 catalyzing androgen synthesis.[82,462] Detailed mechanistic investigations involving the mechanisms of hormone biosynthesis have likewise been aided

DOI: 10.1021/acs.chemrev.6b00690
Chem. Rev. 2017, 117, 4669−4713

by use of the nanodisc system, including measurements of kinetic solvent isotope effects[84,462] and the trapping of transient intermediates at low temperatures.[24,88]

6. NANODISC APPLICATIONS IN BIOTECHNOLOGY AND MEDICINE

6.1. Cell-Free Expression Using Nanodiscs

Various applications of nanodiscs for cell-free expression of membrane proteins have been realized by multiple groups[311,463−467] and have proven to be useful alternative for expression in conventional recombinant systems, such as *E. coli*, mammalian, yeast, or insect cells, where overexpression of the alien protein often results in inhibition of cell growth and low yield. Especially difficult is production of isotopically labeled membrane proteins for NMR studies due to the slow growth on minimal media and very low expression levels. Unlike growth in cell culture, cell-free expression in a lysate of bacterial or eukaryotic cells provides significant advantages in terms of increased tolerance to various additives that are used for stabilizing membrane proteins and allows site specific labeling and the incorporation of non-native amino acids reflective of post-translational modifications.[253,288] Nanodiscs can be added to the cell-free expression system in order to provide a necessary solubilizing environment for the expressed membrane protein, with the expressed membrane proteins directly incorporated into the preformed nanodiscs added to the mixture,[289,352,467] absorbed on the nanodisc bilayer surface,[463] or assembled afterward using additional lipids and MSP. Comparison of the yield of correctly folded membrane proteins in the presence of detergent micelles, liposomes, bicelles, and nanodiscs demonstrated significantly improved results when nanodiscs were present in concentrations 0.05−0.15 mM, and equimolar or 2-fold excess of synthesized membrane protein per nanodisc is provided.[467] An additional advantage of using nanodiscs in cell-free expression is the availability of subsequent affinity purification of the expressed native membrane protein, thus avoiding using the His-tag on the scaffold protein. For some proteins, such as the homodimeric trans-membrane domain of human receptor tyrosine kinase ErbB3, successful incorporation of correctly folded protein depended on the lipid composition.[467] Such dependence was specifically addressed in a screening study optimizing the lipid composition of nanodiscs for the cell-free expression of proteorhodopsin and phospho-MurNAc-pentapeptide (MraY) translocase.[217] While proteorhodopsin was efficiently solubilized with all combinations of lipid and scaffold protein tested, the best result for MraY was achieved only with 0.1 mM nanodiscs prepared using MSP1E3 and DOPG, while DMPC discs could not fully incorporate this protein. In addition to potential lipid specificity, differences in the phase transition temperature of the nanodiscs should be considered. Screening for optimal lipid composition was also performed in another study from the Bernhard group.[216,468] Here, the lipid preference and specificity of several MraY homologues from various bacteria was explored. All enzymes obtained from Gram-negative bacteria required negatively charged lipids for correct functional folding, while the same MraY protein from Gram-positive *B. subtilis* was much less sensitive to lipid composition and tolerated detergent solubilization. An interesting result of using the nanodisc approach in a cell-free expression system was realized by monitoring the folding of an expressed membrane protein *in situ*.[289] Nanodiscs assembled with DMPC were immobilized using the scaffold protein His-tag on a Ni-NTA modified thin gold surface used in the surface enhanced infrared absorption spectrometer operated in an attenuated total reflection mode. Cell-free expression of bacteriorhodopsin (bR) using an *E. coli* system with a direct contact between the gold surface and a monolayer of nanodiscs was used. Time-dependent infrared spectra were observed, so that gradual increase of the amide I and amide II bands allowed detection of synthesized bR in nanodiscs. Within 10−60 min, both the amide I and amide II bands shifted from 1645 to 1673/1655 cm^{-1} and from 1557 to 1549 cm^{-1} indicating formation of a predominantly α-helical structure. Later in time, from 60 to 260 min, two amide I bands merged into one band at 1663 cm^{-1} typical for a bundle of α-helices, which was taken as a sign of the correctly folded tertiary structure of bR. Functional competence of cell-free expressed bR folded in nanodiscs was demonstrated by observing the intact photocycle, including appearance of the M intermediate with kinetics similar to that previously reported.[469] The presence of retinal, and the method of administration to the cell-free system strongly affected the rate of folding and the final yield of correctly folded bR. In the absence of retinal, the secondary structure did not appear to the full extent, and addition of retinal at the end of the reaction did not result in complete folding. If retinal was incorporated into nanodiscs before the start of expression, the overall folding was faster, and appearance of the α-helical bundle signature 1660 cm^{-1} band was observed within 10 min. Folding was also much slower if retinal was administered to the expression media, indicating diffusional limitations for retinal binding to the partially folded bR. All of these observations indicate novel opportunities provided by a combination of cell-free expression of membrane proteins with nanodiscs used for solubilization and folding with simultaneous observation of this process. On the other hand, it was shown[470] that fragments of bacteriorhodopsin separately synthesized in the cell-free expression system and incorporated in nanodiscs do not exchange between lipoprotein particles after mixing and cannot associate to form the native bR molecule. However, if bicelles are added to this mixture, association of these fragments was detected by disulfide cross-linking, indicating a potential dynamic equilibrium.

6.2. Solubilization and Delivery of Drugs and Contrasting Agents for Imaging

The specific labeling of membrane scaffold protein (MSP) by covalent attachment of a dye molecule at the N-terminus mediated by sortase A and intracellular imaging of HeLa cells with direct uptake of labeled nanodiscs was recently described.[471] In this case, labeling was conducted using preformed nanodiscs where the His-tag had already been removed, so that the N-terminal glycine, which is mostly efficient for Sortase A action, is formed after TEV protease cleavage. Labeling was done using fluorescein-depsipeptide, and fluorescent spots were observed in HeLa cells after a 4 h incubation. This observation suggests that labeled nanodiscs can be used as a probe for immunostaining organelles in various cell lines, although results of this work do not distinguish between uptake of intact nanodiscs and penetration of labeled MSP into the cell. An earlier study demonstrated that HeLa cells absorb lipids labeled with a Gd^{3+} chelating complex from nanodiscs by lipid exchange,[472] which may suggest that nanodiscs could disassemble, at least partially, during this process. In this latter work, nanodiscs with rhodamine tag on MSP were assembled together with a maximum content of

DOI: 10.1021/acs.chemrev.6b00690
Chem. Rev. 2017, 117, 4669−4713

monomeric Gd^{3+}-chelating lipids corresponding to ~48 Gd^{3+} (38%) per disc. These nanodiscs proved to be very efficient contrasting agents in T_1 magnetic resonance imaging at the highest tested field (7 T), as they are easily absorbed with long retention times (up to 72 h) by HeLa and MCF7 cells and allow signal accumulation for sufficiently long times.[472] Nanodiscs with trimeric Gd^{3+}-chelates also were assembled with 28% loading (137 Gd^{3+} per disc) but were less efficiently absorbed to cells, as judged by fluorescently labeled MSP. Interestingly, cellular proliferation experiments with cells labeled with Gd^{3+}-loaded nanodiscs show no decrease in the growth rate and high retention of Gd^{3+} in the cell culture. Nanodiscs thus offer a multimodal platform for *in vivo* imaging and delivery.

The distribution of nanodiscs modified with chelated ^{64}Cu was studied in cancer tumor bearing mice using positron emission tomography (PET).[166] MSP1E3D1 was covalently modified at the lysine amino groups by chelating agent DOTA with an average of 5 modified lysines per MSP. Nanodiscs were successfully formed with this scaffold protein and POPC as lipid. Chelating with the radioactive isotope ^{64}Cu was performed by incubation of the modified nanodiscs in a $CuCl_2$ solution at pH 7.5 for 45 min, with chromatographic analysis showing efficient labeling in the peak nanodisc fraction. Stability *in vitro* was tested by incubation of labeled discs in mouse plasma at 37 °C, and a gradual decrease of radioactive nanodiscs concentration with concomitant growth of the fraction of small radioactive particles was observed with approximately 50% labeled nanodiscs remaining intact after 48 h. PET images showed a biphasic clearance, with the fast phase attributed to renal excretion. Blood levels of ^{64}Cu dropped 7-fold from 1 to 12 h and remained steady till 48 h after intravenous injection of ^{64}Cu-labeled nanodiscs, while tumor accumulation significantly increased from 1 to 24 h and stabilized after 48 h.[166] This suggests that labeled nanodiscs remain in circulation for the time of experiment. Liver, intestine, lungs and other organs also showed some accumulation of radioactive label. Low accumulation in spleen was mentioned as particularly important as it may suggest a low immunogenicity of nanodiscs *in vivo*. It has long been known that various nanocrystals or nanoparticles can be solubilized in high density lipoprotein (HDL) fractions and used for *in vivo* imaging via computerized X-ray tomography (gold), MRI (iron oxides or gadolinium), or optical imaging (quantum dots) of aortic walls for arteriosclerosis diagnostics[473] or *in vitro* imaging of macrophage cells.[474]

The small size, stability, and high capacity for solubilization of hydrophobic molecules suggests a high potential for nanodisc application for *in vivo* drug delivery.[475,476] There are several successful examples of therapeutic application of nanodiscs loaded with various biologically active compounds. Direct delivery and positive therapeutic effect of the pulmonary surfactant POPG in nanodiscs was demonstrated *in vivo* by intranasal administration to mice infected with respiratory syncytial virus.[477] Control experiments with POPC nanodiscs show no effect in suppression of the viral plaque formation *in vitro*. Suppression of interferon gamma production in mice after a single inoculation was as efficient with POPG administered in nanodiscs as with liposomes. Turnover measurements showed that the half-life of POPG nanodiscs in mice is 60−120 min, as judged by the disappearance of the membrane scaffold protein. Although this is a relatively narrow therapeutic window in mice, extrapolation to humans suggests a plasma lifetime greater than ~10 h.

These results with nanodiscs build on an extensive literature where reconstituted high density lipoprotein particles (rHDL) are used as vehicles for drug delivery, as is thoroughly described in a recent review.[478] The high solubility of nanodiscs and HDL and their stability *in vivo*, combined with the ability of lipid phase to absorb lipophilic compounds, constitutes a potential advantage for delivery of hydrophobic drugs. This is especially true for such poorly soluble drug as Amphotericin B, which was recently incorporated in rHDL[476,479] with a formulation successful in the treatment of *Leishmania* infection in mice.[480] All-trans retinoic acid also was loaded into nanodiscs,[476,481] and efficient inhibition of HepG2 cell culture growth was observed. Targeted delivery can be achieved by using chimeric proteins, combining scaffold protein and specific binding protein, as was described[482] by fusing ApoA1 and an antibody fragment. Nanodiscs formed with this protein could bind specifically to the surface of corresponding non-Hodgkin lymphoma cells with subsequent delivery of fluorescent compound curcumin into the cells.

Several studies demonstrated highly promising results in loading rHDL or nanodiscs with various therapeutics for drug delivery. Modified drugs, such as acyclovir palmitate, can be incorporated in HDL and administered to rats with more than 70% of the dose recovered in liver[483] demonstrating a potential in the treatment of hepatitis B infection. *In vitro* tests showed a much higher anti-HBV inhibition activity of HDL incorporated acyclovir palmitate as compared to the same derivative or acyclovir in liposomes. Recently, another example of *in vivo* targeted mouse delivery of simvastatin loaded into discoidal rHDL particles was described.[484] Labeled HDL particles were found in liver, kidney and spleen, with no toxic effects were observed even at high dose within a week. *In vivo* MRI experiments and tissue analysis demonstrated pronounced accumulation of labeled HDL particles in blood vessel walls and in atherosclerotic plaques. Low-dose treatment inhibited plaque inflammation, while high-dose treatment can be applied for rapid prevention of inflammation in advanced plaques.[484]

6.3. Nanodiscs in the Development of Vaccines and Therapeutic Antibodies

The incorporation of various antigens and their fragments, including viral proteins, in nanodiscs is considered as a means for vaccine development and the generation of specific antibodies to membrane protein targets. A recent publication described the success using the HIV envelope spike proteins and their fragments.[91,237] The small size of nanodiscs and their stability in plasma improved antigen lifetime *in vivo* and may prove to be a most useful approach in vaccine development. Viability of this concept is supported by the recent successful production of antibodies in phage display for several proteins that were self-assembled in nanodiscs.[105,485,486] In this screening approach, the target protein is incorporated in nanodiscs and attached to the surface of streptavidin magnetic beads using biotinylated-MSP nanodiscs. Particles with strong binders are washed with selection buffer and reapplied to the next selection round as described.[486] Synthetic antibody fragments generated using this method were used for crystallization of an archaeal DUF106 protein having conserved YidC fold of the Sec61/SecYEG translocon component protein.[485]

DOI: 10.1021/acs.chemrev.6b00690
Chem. Rev. 2017, 117, 4669−4713

An *in vivo* study suggests a new approach to the antigen-specific down-modulation of antibodies in mice by intravenous injection of nanodisc incorporated acetylcholine receptor (AchR) from *Torpedo californicus*.[487] In control experiments with bare AchR, the level of anti-AChR increased, which was explained by the presence of antigen in a non-native and/or aggregated form. Empty nanodiscs had no effect. This approach can be further developed for the treatment of human autoimmune diseases such as myasthenia gravis, if recombinant human AChR is used in analogy with the ND-AChR result. Similarly, enhanced immune response and protective effect in a mouse model were demonstrated for the hemagglutinin (HA) from influenza vaccine incorporated in nanodiscs.[488] Both intranasal and intramuscular deliveries of HA-nanodiscs were as efficient in triggering immune response as in a commercial vaccine formulation. Comparison of hemagglutination activity of nanodiscs with various numbers of HA monomers revealed higher activity of HA trimers in nanodiscs as compared to pure HA in solution, suggesting that HA in nanodiscs has structure similar to the original protein in viral envelope.

6.4. Nanodiscs for Generating Libraries of Membrane Proteins and Molecular Screening

Nanodiscs can be useful for high-throughput screening methods with membrane proteins as targets. The inner membrane protein DsbB from *E. coli* was incorporated in nanodiscs and immobilized to screen compounds with potential for development of fragment-based drug discovery.[489] Proteins immobilized in nanodiscs retained full functionality and were used for affinity screening of 1071 compounds. In this method, a mixture of fragments of a potential drug is added to the target and reference cells and binding is detected by monitoring the disappearance of a high resolution ^{1}H NMR spectrum of the small molecule due to its of loss of mobility. This "target immobilized NMR screening" has an advantage of multiple usage of the same protein target sample (up to 200 times[490]) thus limiting the required amount of the membrane protein to ~25 nmol.[489] Comparison of the results of two experimental series performed using DsbB in nanodiscs and in dodecyl phosphocholine (DPC) revealed that more hydrophobic fragments preferentially bind to DsbB in nanodiscs, while more hydrophilic fragments were identified as binders to DsbB in DPC micelles. The overall hit rate for DsbB was 8.7%, or 93 fragments from the library, as compared to a 0.6% obtained with the reference sample containing the OmpA membrane protein. Overall, this method eliminates the difficulties caused by nonspecific binding in detergent micelles and can be used in the similar fragment-based screening studies with less stable membrane proteins, such as GPCRs.

Our earlier work demonstrated the validity of generating "soluble membrane protein libraries" (SMPL) where faithful representation of the membrane proteome of *E. coli* could be formed by incorporation into nanodiscs.[111] Membranes were resuspended in octyl glucoside or in SDS with subsequent removal of insoluble membrane fraction by centrifugation. Nanodiscs were assembled from the mixture of solubilized *E. coli* membrane proteins with MSP1E3 and POPC in cholate by removal of detergent on hydrophobic beads at 4 °C and purified by Ni-NTA affinity chromatography using His-tag on the scaffold protein. Proteins were identified by mass spectrometry of trypsin hydrolyzed membrane proteins separated by SDS-PAGE. Overall, it appeared that a large fraction of the initial membrane proteome was represented in the library. 28−29 bands were identified on gels from detergent extract and from raw membranes respectively, and 25 bands were represented in high yield in the nanodisc library. Several important membrane proteins were identified by a proteomics analysis of the SMPL, including the outer membrane proteins OmpA and OmpW, which are monomeric in native membranes, and OmpC and maltoporin, which exist as trimers. Several inner membrane proteins, such as the ATP synthase and chaperone DnaK were also identified. A similar procedure was described later for the soluble library created with the proteins from the metastatic human osteosarcoma cell line 143B.[491] In this work four different lipid mixtures added to the original solubilized membrane for nanodisc assembly were compared for efficiency of membrane protein incorporation. The mixture of POPC, POPS and cholesterol (72:20:8 molar ratio) was found to be more efficient than pure POPC or 80% POPC with 20% POPS, and significantly more efficient than 80% POPC with 20% cholesterol. In addition, there was a significant preference in the solubilization of various classes of membrane proteins depending on the lipid composition used. For instance, the fraction of GPCRs solubilized in a mixture of POPC, POPS, and cholesterol was much higher than in other lipids, while the more structural proteins favored POPC/POPS nanodiscs. These findings suggest that direct solubilization of cell membranes for analytical and screening purposes can be tuned and optimized by selection of lipid mixtures used to support generation of a nanodisc library.

The same SMPL method was applied to a high-throughput screening for potential receptors of amyloid beta oligomers (AβO) using libraries prepared from rodent synaptic membranes.[112] Synaptic plasma membranes from rat cerebral cortex were used to prepare synaptosomes, which were solubilized in the detergent DDM and used for nanodisc assembly with MSP1E3D1 and POPC. After removal of detergent on hydrophobic beads, nanodiscs were purified by Ni-NTA affinity chromatography using the His-tag on MSP. The binding of AβO detected by a chemiluminescence assay was specific with respect to some synaptic proteins and selective for the high molecular weight oligomers. An inhibitor of AβO binding to the nanodisc library was identified through screening 2700 drug-like compounds for antagonist activity. This was confirmed with animal tissue slices. Overall this work established viability of creating libraries from native membranes for proteomics or screening against target functionally specific binders.

Screening for potential binding ligands in a 12-mer phage display peptide library was accomplished using bacteriorhodopsin as a model membrane protein.[492] bR was expressed in a cell-free system and incorporated in nanodiscs assembled with DMPC lipids. The samples as well as a control of empty nanodiscs were immobilized in 96-well microtiter plates for screening with the library of random peptide 12-mers. These investigators identified 69 phage clones interacting with intracellular loops AB and EF, but not with the CD loop, of bR. In general, incorporation of a membrane protein in nanodiscs provides a direct and robust approach to the phage display screening for the clones binding to the nonlinear epitopes.

The soluble library approach also provides new information about functional assemblies of many different membrane enzymes, as demonstrated by the isolation and characterization of a P450 metabolon catalyzing conversion of L-tyrosine to the defense compound dhurrin in sorghum plants.[493] Microsomes

DOI: 10.1021/acs.chemrev.6b00690
Chem. Rev. 2017, 117, 4669−4713

prepared from sorghum seedlings were directly solubilized using SMA copolymer generating particles with sizes ranging from 10 to 25 nm. Target particles containing complexes of P450 enzymes, together with their redox partner flavoprotein P450 reductase, were separated by 2′5′-ADP affinity chromatography using the NADPH binding site on the reductase. Two cytochrome P450 enzymes constituting the metabolon were identified by mass spectrometry in these particles, indicating statistically significant assembly of these three proteins *in vivo*. Functional analysis was performed using reconstituted system in liposomes, because similar experiments with SMALP particles did not show enzymatic activity.[493] This study demonstrated the potential of using the metabolon approach in synthetic biology and biotechnology for production of high-value biologics.

Another screening of protein − lipid interactions has been realized for soluble proteins which specifically bind lipids in nanodiscs or "picodiscs"[61,62,286] with detection based on catch-and-release electrospray ionization mass spectrometry. The method was developed using a homopentamer of the cholera toxin CTB5 B subunit and a fragment of toxin A from *Clostridium difficile* as soluble proteins which bind to gangliosides incorporated in picodiscs assembled using saposin A and POPC.[61,63] Selective binding of six gangliosides was detected for CTB5, and of five gangliosides for Toxin A, consistent with the earlier reported specificities. Screening of lipid mixtures from porcine brain and human epithelial cell line against CTB5 identified the binding of several isoforms of GM1 and fucosyl-GM1. Performance of this screening was compared for picodiscs formed with saposin A and POPC and nanodiscs formed with MSP1E1 and DMPC.[62]

6.5. Nanodiscs and Nanomaterial Engineering

Negatively charged nanodiscs assembled using MSP1D1 and DMPG lipids were used as templates for making composite nanoparticles by electrostatic absorption of positively charged 1.4 nm amine coated gold nanoparticles.[494] Deposition of colloidal Au particles resulted in rapid lateral growth of nanodiscs during the first few minutes. At the same time, appearance of optical absorption in the near-UV region below 440 nm was observed. After two minutes the characteristic plasmon optical absorption band for gold nanoparticles at 550 nm appeared and increased with time. After 20 min, the size of particles did not change, due to the depletion of gold in solution, as also because of a lateral restriction provided by the scaffold protein. The mean height and diameter of the discoidal polycrystalline Au-nanodiscs determined by AFM and EM were 4.7 and 15.5 nm respectively. Raman spectroscopy demonstrated significant enhancement of lipid modes, indicating possible application of such discoidal particles as promising substrates for surface enhanced Raman spectroscopy applications.

Numerous reports were published describing various composite nanoparticles resembling spherical HDL, which used apolipoproteins and lipids coating Au nanocrystals, iron oxide nanoparticles or quantum dots.[474,495,496] As the lipids in these particles usually do not form bilayers, they cannot be formally termed nanodiscs, although they are formed by similar self-assembly methods and take advantage of the solubilizing power of apolipoproteins interacting with lipids. MSP also can be used for the purpose of solubilizing nanocrystalline inorganic structures. Semiconductor nanoplatelets with CdSe core and with or without CdS coating with dimensions 42 nm by 12 nm and thickness 3 nm were coated by monolayers of DMPC or POPC on the flat sides and perimeter of MSP1E3D1.[497] These colloidal particles were stable in solution for more than one month, had very strong fluorescence and were readily absorbed by live human carcinoma cells, so that imaging using confocal microscopy clearly revealed localization of these particles in endosomal vesicles. Such particles can be used for intracellular imaging and for fluorescent labeling and tracking cells. Sometimes nanodiscs are assembled with lipids containing highly specific modifications on the head groups for selective binding of targets. For example, biotinylated lipids were incorporated into nanodiscs for selective binding of quantum dots coated by streptavidin.[351]

Many nanostructures can be built using nanodiscs, guided by a suggestion of protein based nanoelectronic surface assemblies proposed by Salemme and Sligar.[498] One-dimensional stacks of nanodiscs were formed using complementary DNA oligonucleotides conjugated to the lipid head groups.[499,500] Dioctadecyl lipids with covalently attached oligonucleotides were mixed with POPC nanodiscs assembled with MSP1D1 with an average of 4 or 6 DNA tags per nanodisc. A mixture of two populations of nanodiscs with complementary DNA tags is briefly warmed to 60 °C (above the DNA melting temperature) and then slowly cooled to room temperature with the rate of 0.1 °C to allow assembly of stacked superstructures of nanodiscs via DNA hybridization.[499] Long ∼10 μm stacked structures termed BioNanoStacks[499] were visualized using optical microscopy and Rhodamine-lipid staining. The negative staining TEM measured periodicity was 5.6 ± 0.3 nm, with cryo-EM measuring 5.7 ± 0.4 nm and a diameter of 11.9 ± 1.8 nm. Taking into account the length of DNA spacers, these measurements indicate a slightly tilted orientation of nanodiscs in stacks. When 23-mers of DNA were used instead of 13-mers, the spacing increased, consistent with the expected extra 10 base-pairs. Reversible thermal melting of BioNanoStacks at various ionic strengths (from 30 to 100 mM NaCl) was observed and the same stacking structures were assembled using nanodiscs with 1:1 POPC/POPS mixtures, but with lower melting temperatures due to the electrostatic repulsion of the negatively charged POPS bilayers. In a subsequent study,[500] histidine tags on the scaffold protein in BioNanoStacks were used to bind 5 nm Au Ni-NTA coated nanoparticles to form one-dimensional arrays as observed by transmission electron microscopy. With two His-tags per disc, the observed pattern of Au-nanoparticles binding on both sides of nanodisc stacks indicated opposite orientation of MSP C-termini, or simply preferential binding in this orientation. Statistical analysis of the binding pattern revealed deviations from purely random binding, which may be partially attributed to the steric effects due to the similar sizes of nanodiscs (5.7 nm) and the Au nanoparticle (5 nm). Highly regular nanoparticle patterning could be achieved by manipulation of nanoparticle diameter, nanodisc size and spacing. In general, this method provides a new and highly promising method for design of supramolecular composite structures on the nanometer scale.

A notable example of supra-molecular engineering was achieved by assembling of photosynthetic reaction centers (RC) from *Rhodobacter sphaeroides* incorporated in nanodiscs on the surface of single-wall carbon nanotubes.[501] Complexes of nanodiscs with RC on nanotubes were isolated from background components by density gradient ultracentrifugation using fluorescence for detection of the RC, Laurdan labeled lipids and nanotubes. A parallel arrangement of nanodiscs along

DOI: 10.1021/acs.chemrev.6b00690
Chem. Rev. 2017, 117, 4669−4713

the nanotube was confirmed by atomic force microscopy. Assembly of these complexes on nanotubes was reversible, and multiple cycles of assembly and disassembly were demonstrated by the addition and removal of sodium cholate. Remarkably, the RC demonstrated photoelectrochemical activity in the assembled state under laser illumination at 785 nm, which also could be reversed and regenerated by addition and removal of cholate. This result suggests a new approach toward design of solar energy conversion complexes by incorporating protein components stabilized in nanodiscs into nanoscale inorganic structures.

Another prototype device based on coupling of olfactory receptors from mice incorporated in nanodiscs with nanotube transistors was developed for sensing volatile compounds.[502] In this goal of generating an "artificial nose", several different receptors were incorporated in nanodiscs and attached to the nanotube using His-tag engineered on the receptor. Nanodiscs provided a more stable environment for receptors as compared to detergent, where activity was irreversibly lost in 5 days, while in nanodiscs the receptors remained functional for as long as 4−10 weeks. A relatively fast characteristic sensing time (10−50 s) and ability for electronic multichannel readout demonstrated the high potential of this new technology. In summary, self-assembly offers a powerful tool for engineering complex structures. The facile and faithful formation of nanodiscs from two scaffold proteins and hundreds of lipids can be used to generate even more complex entities with defined optical and electronic properties.

7. SUMMARY AND FUTURE DIRECTIONS

We have endeavored in this review to summarize the broad use of the nanodisc technology for investigating the structure and function of membrane proteins and the use of this nanometer mimetic as a soluble lipid bilayer surface of controlled composition and size. Specific references that provide inroads for other systems involving nanometer scale lipoprotein particles, micelles, bicelles, and other entities are noted. Developing any broadly applicable tool for studying membrane proteins requires an intimate knowledge of physical chemistry and structure. Much work remains to precisely understand the mechanism of self-assembly whereby hundreds of lipids come together with an amphipathic stabilizing protein to generate discs of precise size and composition. Self-assembly is poorly understood, and the balance of thermodynamic and kinetic factors is not known. The various factors affecting overall yield must be explored, including the possible role of various detergents in the mixture. While general guidelines have been described, the physics that determines the branch point deciding successful incorporation of an integral membrane protein into the nanodisc bilayer versus nonspecific aggregation events needs significant attention Such knowledge is crucial to maximize the yield of target incorporated nanodiscs, which is a function of the detergent(s) used, temperature, identity of the membrane protein, phospholipid(s), cholesterol, etc. and the details of detergent removal that initiates assembly. Despite this lacuna in fundamental knowledge, there has been tremendous success in the use of nanodiscs by the scientific community. The ready availability of the genes for the membrane scaffold protein through AddGene (over 1300 shipments worldwide), detailed protocols provided in many reviews, and critical improvements by many laboratories have yielded a system of broad applicability to a plethora of problems in biochemistry, chemistry, pharmacology, and materials science. This review cites over 500 publications that have nanodiscs as a central feature. We look forward to next few years when even more dramatic successes can be realized.

AUTHOR INFORMATION

Corresponding Authors

*E-mail: denisov@illinois.edu. Phone: 217-244-6094.
*E-mail: s-sligar@illinois.edu. Phone: 217-244-7395.

ORCID

Stephen G. Sligar: 0000-0002-5548-2866

Notes

The authors declare no competing financial interest.

Biographies

Ilia G. Denisov graduated in molecular physics and spectroscopy from the Department of Physics, Leningrad State University (now Saint-Petersburg) in 1981. In 1991 he received his Ph.D. degree in Polymer Physics from the Institute of Macromolecular Compounds, Russian Academy of Sciences. He was a visiting scientist at the University of Milan, Italy, where he worked on hemoglobin ligand binding intermediates with Professor M. Perrella. In 1996 he moved to Washington University to continue his work with Professor G. K. Ackers. Since 1999 he has been in Professor S. G. Sligar's laboratory, currently as a senior research scientist. His main interests are in the field of spectroscopic studies of reaction intermediates in heme enzymes and in biophysics and biochemistry of membrane bound human cytochromes P450 with specific focus on their allosteric properties and role in drug-drug interactions.

Stephen G. Sligar received his Ph.D. in Physics from the University of Illinois in 1975. Dr. Sligar served on the faculty in the Department of Molecular Biophysics and Biochemistry at Yale University and returned to the University of Illinois in 1982 where he was the I. C. Gunsalus Professor of Biochemistry, the William and Janet Lycan Professor, and Director of the School of Chemical Sciences. He now holds the University of Illinois Swanlund Endowed Chair and is Director of the School of Molecular and Cellular Biology. He is also a faculty member in the Department of Chemistry and the Center for Biophysics and Quantitative Biology. Dr. Sligar holds affiliate appointments in the Beckman Institute for Advanced Science and Technology, the Institute for Genomic Biology, and the Micro and Nano Technology Laboratory on the Illinois campus. He is an elected Fellow of the Biophysical Society and the American Association for the Advancement of Science and was an Academic Leadership Program Fellow with the Committee on Institutional Cooperation. Awards include the 2016 Sober Award from the American Society of Biochemistry and Molecular Biology, a Fulbright Research Scholarship, Senior Fellowship from the Japan Society for the Promotion of Science, NIH Merit and MIRA Awards, and the Bert L. and Kuggie Vallee Visiting Professorship in Inorganic Chemistry at Oxford where he was a Fellow of Queens College. He is also a Fellow in the Jerome Karle Nobel Laureate World Innovation Foundation. Dr. Sligar's research has been supported by grants from the National Science Foundation, the National Institutes of Health, and the Human Frontiers Program. His research centers on understanding the structure and mechanistic function of membrane proteins, including those metalloenzymes involved in human drug metabolism and steroid hormone biosynthesis, the molecular mechanisms of neurodegenerative diseases, and cancer signaling pathways. His work uses a combination of experimental and theoretical methods with a goal of revealing structural and functional information of value in developing new methods of therapeutic intervention. He is the founder of several

DOI: 10.1021/acs.chemrev.6b00690
Chem. Rev. 2017, 117, 4669−4713

start-up companies and was recognized by the Champaign County Economic Development Corporation's 2014 Innovation Celebration.

ACKNOWLEDGMENTS

Discovery and development of the nanodisc technology and applications in the Sligar laboratory was accomplished by a plethora of individuals including: Timothy Bayburt, Joe Carlson, Yelena Grinkova, Mark McLean, Aditi Das, Steve Grimme, Natanya Civjan, Bradley Baas, Aleksandra Kijac, Andrew Leitz, Andrew Shaw, Amy Shih, Stephanie Gantt, Yogan Khatri, Daniel Frank, Catherine Baker, Michael Marty, Abhinav Luthra, Michael Gregory, Ivan Lenov, Xin Ye, and Ruchia Duggal. Collaborations over the years have enabled new avenues of exploration. These have included Ana Jonas (UIUC), Barry Springer (Johnson&Johnson Pharmaceuticals), James Morrissey (UIUC), Chad Rienstra (UIUC), Mary Schuler (UIUC), Klaus Schulten (UIUC), Emad Tajkhorshid (UIUC), Ryan Bailey (UIUC), Robert Gennis (UIUC), William Atkins (University of Washington), James Kincaid and Piotr Mak (Marquette University), Richard Van Duyne, George Schatz, Vinayak Dravid, Chang Liu (Northwestern University), Vsevolod Gurevich (Vanderbilt University), Mark Ginsberg (UCSD), Lisa Arleth and Birger Lindberg Moller (University of Copenhagen), Milan Mrksich (Northwestern University), Michael Gross (Washington University in Saint-Louis), Frank Duong (University of British Columbia), Dennis Voelker (National Jewish Health Center), William Klein (Northwestern University), Dan Oprian (Brandeis University), Tom Laue (University of New Hampshire), Gerald Hazelbauer (University of Missouri-Columbia), Phil Dawson (Scripps Research Institute), Tom Meade (Northwestern University), Tom Poulos (UC Irvine), John Dawson (University of South Carolina), and Brian Hoffman (Northwestern University) together with their many talented students and researchers in their laboratories. We want to especially acknowledge the Frederick National Laboratory for Cancer Research led by Dave Heimbrook and the Ras collaborations led by Andy Stephen. Research in the Sligar laboratory has been supported for the past 40 years by grants from the National Institutes of Health, including NIH GM33775, GM31756, GM110428, and GM118145. We want to especially acknowledge receipt of an NIGMS MIRA award that is allowing us to fully explore the opportunities for fundamental discovery in the application of nanodiscs to human health issues.

REFERENCES

(1) Baker, L. A.; Baldus, M. Characterization of membrane protein function by solid-state NMR spectroscopy. *Curr. Opin. Struct. Biol.* **2014**, *27*, 48−55.
(2) Brown, L. S.; Ladizhansky, V. Membrane proteins in their native habitat as seen by solid-state NMR spectroscopy. *Protein Sci.* **2015**, *24*, 1333−1346.
(3) Cross, T. A.; Murray, D. T.; Watts, A. Helical membrane protein conformations and their environment. *Eur. Biophys. J.* **2013**, *42*, 731−755.
(4) Koehler Leman, J.; Ulmschneider, M. B.; Gray, J. J. Computational modeling of membrane proteins. *Proteins: Struct., Funct., Genet.* **2015**, *83*, 1−24.
(5) Maler, L. Solution NMR studies of peptide-lipid interactions in model membranes. *Mol. Membr. Biol.* **2012**, *29*, 155−176.
(6) Planchard, N.; Point, E.; Dahmane, T.; Giusti, F.; Renault, M.; Le Bon, C.; Durand, G.; Milon, A.; Guittet, E.; Zoonens, M.; et al. The Use of amphipols for solution NMR studies of membrane proteins: Advantages and constraints as compared to other solubilizing media. *J. Membr. Biol.* **2014**, *247*, 827−842.
(7) Popot, J. L. Amphipols, nanodiscs, and fluorinated surfactants: three nonconventional approaches to studying membrane proteins in aqueous solutions. *Annu. Rev. Biochem.* **2010**, *79*, 737−775.
(8) Zhou, H. X.; Cross, T. A. Influences of membrane mimetic environments on membrane protein structures. *Annu. Rev. Biophys.* **2013**, *42*, 361−392.
(9) Warschawski, D. E.; Arnold, A. A.; Beaugrand, M.; Gravel, A.; Chartrand, E.; Marcotte, I. Choosing membrane mimetics for NMR structural studies of transmembrane proteins. *Biochim. Biophys. Acta, Biomembr.* **2011**, *1808*, 1957−1974.
(10) Noguchi, H. Structure formation in binary mixtures of lipids and detergents: Self-assembly and vesicle division. *J. Chem. Phys.* **2013**, *138*, 024907.
(11) Bayburt, T. H.; Sligar, S. G. Membrane protein assembly into nanodisks. *FEBS Lett.* **2010**, *584*, 1721−1727.
(12) Denisov, I. G.; Sligar, S. G. Nanodiscs for structural and functional studies of membrane proteins. *Nat. Struct. Mol. Biol.* **2016**, *23*, 481−486.
(13) Brouillette, C. G.; Anantharamaiah, G. M.; Engler, J. A.; Borhani, D. W. Structural models of human apolipoprotein A-I: a critical analysis and review. *Biochim. Biophys. Acta, Mol. Cell Biol. Lipids* **2001**, *1531*, 4−46.
(14) *Apolipoprotein mimetics in the management of human disease*; Anantharamaiah, G. M., Goldberg, D., Ed.; Springer International Publishing: Switzerland, 2015.
(15) Midtgaard, S. R.; Pedersen, M. C.; Kirkensgaard, J. J. K.; Sorensen, K. K.; Mortensen, K.; Jensen, K. J.; Arleth, L. Self-assembling peptides form nanodiscs that stabilize membrane proteins. *Soft Matter* **2014**, *10*, 738−752.
(16) Kondo, H.; Ikeda, K.; Nakano, M. Formation of size-controlled, denaturation-resistant lipid nanodiscs by an amphiphilic self-polymerizing peptide. *Colloids Surf., B* **2016**, *146*, 423−430.
(17) Jonas, A.; Steinmetz, A.; Churgay, L. The number of amphipathic alpha-helical segments of apolipoproteins A-I, E, and A-IV determines the size and functional properties of their reconstituted lipoprotein particles. *J. Biol. Chem.* **1993**, *268*, 1596−1602.
(18) Narayanaswami, V.; Maiorano, J. N.; Dhanasekaran, P.; Ryan, R. O.; Phillips, M. C.; Lund-Katz, S.; Davidson, W. S. Helix orientation of the functional domains in apolipoprotein E in discoidal high density lipoprotein particles. *J. Biol. Chem.* **2004**, *279*, 14273−14279.
(19) Chromy, B. A.; Arroyo, E.; Blanchette, C. D.; Bench, G.; Benner, H.; Cappuccio, J. A.; Coleman, M. A.; Henderson, P. T.; Hinz, A. K.; Kuhn, E. A.; et al. Different apolipoproteins impact nanolipoprotein particle formation. *J. Am. Chem. Soc.* **2007**, *129*, 14348−14354.
(20) Ryan, R. O. Nanobiotechnology applications of reconstituted high density lipoprotein. *J. Nanobiotechnol.* **2010**, *8*, 28.
(21) Brisbois, C. A.; Lee, J. C. Apolipoprotein C-III nanodiscs studied by site-specific tryptophan fluorescence. *Biochemistry* **2016**, *55*, 4939.
(22) Baker, C. J.; Denisov, I. G.; Sligar, S. G. Nanoscale membrane mimetics for biophysical studies of membrane proteins. In *Liposomes, LIpid Bilayers and Model Membranes*; Pabst, G., Kucerka, N., Nieh, M.-P., Katsaras, J., Eds.; CRC Press: Boca Raton, FL, 2014, pp. 167−177.
(23) Borch, J.; Hamann, T. The nanodisc: a novel tool for membrane protein studies. *Biol. Chem.* **2009**, *390*, 805−814.
(24) Luthra, A.; Gregory, M.; Grinkova, Y. V.; Denisov, I. G.; Sligar, S. G. Nanodiscs in the studies of membrane-bound cytochrome p450 enzymes. *Methods Mol. Biol.* **2013**, *987*, 115−127.
(25) Malhotra, K.; Alder, N. N. Advances in the use of nanoscale bilayers to study membrane protein structure and function. *Biotechnol. Genet. Eng. Rev.* **2014**, *30*, 79−93.
(26) Nath, A.; Atkins, W. M.; Sligar, S. G. Applications of phospholipid bilayer Nanodiscs in the study of membranes and membrane proteins. *Biochemistry* **2007**, *46*, 2059−2069.
(27) Nath, A.; Trexler, A. J.; Koo, P.; Miranker, A. D.; Atkins, W. M.; Rhoades, E. Single-molecule fluorescence spectroscopy using phospholipid bilayer nanodiscs. *Methods Enzymol.* **2010**, *472*, 89−117.

DOI: 10.1021/acs.chemrev.6b00690
Chem. Rev. 2017, 117, 4669−4713

(28) Ritchie, T. K.; Grinkova, Y. V.; Bayburt, T. H.; Denisov, I. G.; Zolnerciks, J. K.; Atkins, W. M.; Sligar, S. G. Reconstitution of membrane proteins in phospholipid bilayer nanodiscs. *Methods Enzymol.* **2009**, *464*, 211−231.
(29) Viegas, A.; Viennet, T.; Etzkorn, M. The power, pitfalls and potential of the nanodisc system for NMR-based studies. *Biol. Chem.* **2016**, *397*, 1335−1354.
(30) Kontush, A.; Chapman, J. M. *High-Density Lipoproteins: Structure, Metabolism, Function, and Therapeutics*; Wiley & Sons: Hoboken, NJ, 2012.
(31) Denisov, I. G.; McLean, M. A.; Shaw, A. W.; Grinkova, Y. V.; Sligar, S. G. Thermotropic phase transition in soluble nanoscale lipid bilayers. *J. Phys. Chem. B* **2005**, *109*, 15580−15588.
(32) Bayburt, T. H.; Grinkova, Y. V.; Sligar, S. G. Self-assembly of discoidal phospholipid bilayer nanoparticles with membrane scaffold proteins. *Nano Lett.* **2002**, *2*, 853−856.
(33) Roos, C.; Kai, L.; Proverbio, D.; Ghoshdastider, U.; Filipek, S.; Dotsch, V.; Bernhard, F. Co-translational association of cell-free expressed membrane proteins with supplied lipid bilayers. *Mol. Membr. Biol.* **2013**, *30*, 75−89.
(34) Moers, K.; Roos, C.; Scholz, F.; Wachtveitl, J.; Doetsch, V.; Bernhard, F.; Glaubitz, C. Modified lipid and protein dynamics in nanodiscs. *Biochim. Biophys. Acta, Biomembr.* **2013**, *1828*, 1222−1229.
(35) Jonas, A. Reconstitution of high-density lipoproteins. *Methods Enzymol.* **1986**, *128*, 553−582.
(36) Matz, C. E.; Jonas, A. Micellar complexes of human apolipoprotein A-I with phosphatidylcholines and cholesterol prepared from cholate-lipid dispersions. *J. Biol. Chem.* **1982**, *257*, 4535−4540.
(37) Jonas, A.; Phillips, M. C. In *Biochemistry of Lipids, Lipoproteins and Membranes*, 5th ed.; Vance, D. E., Vance, J. E., Eds.; Elsevier: Amsterdam, The Netherlands, 2008.
(38) Durbin, D. M.; Jonas, A. The effect of apolipoprotein A-II on the structure and function of apolipoprotein A-I in a homogeneous reconstituted high density lipoprotein particle. *J. Biol. Chem.* **1997**, *272*, 31333−31339.
(39) Li, L.; Chen, J.; Mishra, V. K.; Kurtz, J. A.; Cao, D.; Klon, A. E.; Harvey, S. C.; Anantharamaiah, G. M.; Segrest, J. P. Double belt structure of discoidal high density lipoproteins: molecular basis for size heterogeneity. *J. Mol. Biol.* **2004**, *343*, 1293−1311.
(40) Leroy, A.; Toohill, K. L.; Fruchart, J. C.; Jonas, A. Structural properties of high density lipoprotein subclasses homogeneous in protein composition and size. *J. Biol. Chem.* **1993**, *268*, 4798−4805.
(41) Calabresi, L.; Vecchio, G.; Frigerio, F.; Vavassori, L.; Sirtori, C. R.; Franceschini, G. Reconstituted high-density lipoproteins with a disulfide-linked apolipoprotein A-I dimer: Evidence for restricted particle size heterogeneity. *Biochemistry* **1997**, *36*, 12428−12433.
(42) Rye, K.-A.; Barter, P. J. Regulation of high-density lipoprotein metabolism. *Circ. Res.* **2014**, *114*, 143−156.
(43) Segrest, J. P.; Cheung, M. C.; Jones, M. K. Volumetric determination of apolipoprotein stoichiometry of circulating HDL subspecies. *J. Lipid Res.* **2013**, *54*, 2733−2744.
(44) Denisov, I. G.; Grinkova, Y. V.; Lazarides, A. A.; Sligar, S. G. Directed self-assembly of monodisperse phospholipid bilayer Nanodiscs with controlled Size. *J. Am. Chem. Soc.* **2004**, *126*, 3477−3487.
(45) Scanu, A. M. Structure of human serum lipoproteins. *Ann. N. Y. Acad. Sci.* **1972**, *195*, 390−406.
(46) Morrisett, J. D.; Jackson, R. L.; Gotto, A. M., Jr. Lipoproteins: structure and function. *Annu. Rev. Biochem.* **1975**, *44*, 183−207.
(47) Leslie, R. B. Some physical and physico-chemical approaches to the structure of serum high density lipoproteins (HDL). *Biochem. Soc. Sympos.* **1971**, *33*, 47−85.
(48) Lux, S. E.; Hirz, R.; Shrager, R. I.; Gotto, A. M. The influence of lipid on the conformation of human plasma high density apolipoproteins. *J. Biol. Chem.* **1972**, *247*, 2598−2606.
(49) Segrest, J. P.; Jackson, R. L.; Morrisett, J. D.; Gotto, A. M., Jr. A molecular theory of lipid-protein interactions in the plasma lipoproteins. *FEBS Lett.* **1974**, *38*, 247−258.
(50) Gotto, A. M., Jr.; Pownall, H. J.; Havel, R. J. Introduction to the plasma lipoproteins. *Methods Enzymol.* **1986**, *128*, 3−41.
(51) Atkinson, D.; Small, D. M. Recombinant lipoproteins: implications for structure and assembly of native lipoproteins. *Annu. Rev. Biophys. Biophys. Chem.* **1986**, *15*, 403−456.
(52) Phillips, M. C. New insights into the determination of HDL structure by apolipoproteins: Thematic review series: high density lipoprotein structure, function, and metabolism. *J. Lipid Res.* **2013**, *54*, 2034−2048.
(53) Segrest, J. P. Molecular packing of high density lipoproteins: a postulated functional role. *FEBS Lett.* **1976**, *69*, 111−115.
(54) Atkinson, D.; Smith, H. M.; Dickson, J.; Austin, J. P. Interaction of apoprotein from porcine high-density lipoprotein with dimyristoyl lecithin. 1. The structure of the complexes. *Eur. J. Biochem.* **1976**, *64*, 541−547.
(55) Segrest, J. P. Why high density lipoprotein: phospholipid recombinants cannot be spherical micelles. *FEBS Lett.* **1979**, *106*, 169−170.
(56) Wlodawer, A.; Segrest, J. P.; Chung, B. H.; Chiovetti, R., Jr.; Weinstein, J. N. High-density lipoprotein recombinants: evidence for a bicycle tire micelle structure obtained by neutron scattering and electron microscopy. *FEBS Lett.* **1979**, *104*, 231−235.
(57) Forte, T. M.; Nichols, A. V.; Gong, E. L.; Levy, R. I.; Lux, S. Electron microscopic study on reassembly of plasma high density apoprotein with various lipids. *Biochim. Biophys. Acta, Lipids Lipid Metab.* **1971**, *248*, 381−386.
(58) Garda, H. A.; Arrese, E. L.; Soulages, J. L. Structure of apolipophorin-III in discoidal lipoproteins. Interhelical distances in the lipid-bound state and conformational change upon binding to lipid. *J. Biol. Chem.* **2002**, *277*, 19773−19782.
(59) Lee, J. W.; Kim, H. Fragmentation of dimyristoylphosphatidylcholine vesicles by apomyoglobin. *Arch. Biochem. Biophys.* **1992**, *297*, 354−361.
(60) Frauenfeld, J.; Loving, R.; Armache, J. P.; Sonnen, A. F.; Guettou, F.; Moberg, P.; Zhu, L.; Jegerschold, C.; Flayhan, A.; Briggs, J. A.; et al. A saposin-lipoprotein nanoparticle system for membrane proteins. *Nat. Methods* **2016**, *13*, 345−351.
(61) Leney, A. C.; Rezaei Darestani, R.; Li, J.; Nikjah, S.; Kitova, E. N.; Zou, C.; Cairo, C. W.; Xiong, Z. J.; Prive, G. G.; Klassen, J. S. Picodiscs for facile protein-glycolipid interaction analysis. *Anal. Chem.* **2015**, *87*, 4402−4408.
(62) Li, J.; Fan, x.; Kitova, E. N.; Zou, C.; Cairo, C. W.; Eugenio, L.; Ng, K. K. S.; Xiong, Z. J.; Prive, G. G.; Klassen, J. S. Screening glycolipids against proteins in vitro using picodiscs and catch-and-release electrospray ionization mass spectrometry. *Anal. Chem.* **2016**, *88*, 4742−4750.
(63) Popovic, K.; Holyoake, J.; Pomès, R.; Privé, G. G. Structure of saposin A lipoprotein discs. *Proc. Natl. Acad. Sci. U. S. A.* **2012**, *109*, 2908−2912.
(64) Eichmann, C.; Campioni, S.; Kowal, J.; Maslennikov, I.; Gerez, J.; Liu, X.; Verasdonck, J.; Nespovitaya, N.; Choe, S.; Meier, B. H.; et al. Preparation and characterization of stable α-synuclein lipoprotein particles. *J. Biol. Chem.* **2016**, *291*, 8516−8527.
(65) Varkey, J.; Mizuno, N.; Hegde, B. G.; Cheng, N.; Steven, A. C.; Langen, R. alpha-Synuclein oligomers with broken helical conformation form lipoprotein nanoparticles. *J. Biol. Chem.* **2013**, *288*, 17620−17630.
(66) Imura, T.; Tsukui, Y.; Sakai, K.; Sakai, H.; Taira, T.; Kitamoto, D. Minimum amino acid residues of an α-helical peptide leading to lipid nanodisc formation. *J. Oleo Sci.* **2014**, *63*, 1203−1208.
(67) Imura, T.; Tsukui, Y.; Taira, T.; Aburai, K.; Sakai, K.; Sakai, H.; Abe, M.; Kitamoto, D. Surfactant-like properties of an amphiphilic α-helical peptide leading to lipid Nanodisc formation. *Langmuir* **2014**, *30*, 4752−4759.
(68) Anantharamaiah, G. M.; Brouillette, C. G.; Engler, J. A.; De Loof, H.; Venkatachalapathi, Y. V.; Boogaerts, J.; Segrest, J. P. Role of amphipathic helixes in HDL structure/function. *Adv. Exp. Med. Biol.* **1990**, *285*, 131−140.
(69) Chung, B. H.; Anatharamaiah, G. M.; Brouillette, C. G.; Nishida, T.; Segrest, J. P. Studies of synthetic peptide analogs of the

DOI: 10.1021/acs.chemrev.6b00690
Chem. Rev. 2017, 117, 4669−4713

amphipathic helix. Correlation of structure with function. *J. Biol. Chem.* **1985**, *260*, 10256−10262.
(70) Kariyazono, H.; Nadai, R.; Miyajima, R.; Takechi-Haraya, Y.; Baba, T.; Shigenaga, A.; Okuhira, K.; Otaka, A.; Saito, H. Formation of stable nanodiscs by bihelical apolipoprotein A-I mimetic peptide. *J. Pept. Sci.* **2016**, *22*, 116−122.
(71) Larsen, A. N.; Sorensen, K. K.; Johansen, N. T.; Martel, A.; Kirkensgaard, J. J.; Jensen, K. J.; Arleth, L.; Midtgaard, S. R. Dimeric peptides with three different linkers self-assemble with phospholipids to form peptide nanodiscs that stabilize membrane proteins. *Soft Matter* **2016**, *12*, 5937−5949.
(72) Zhang, M.; Huang, R.; Ackermann, R.; Im, S.-C.; Waskell, L.; Schwendeman, A.; Ramamoorthy, A. Reconstitution of the Cytb5-CytP450 Complex in Nanodiscs for Structural Studies using NMR Spectroscopy. *Angew. Chem., Int. Ed.* **2016**, *55*, 4497−4499.
(73) Bayburt, T. H.; Grinkova, Y. V.; Sligar, S. G. Assembly of single bacteriorhodopsin trimers in bilayer nanodiscs. *Arch. Biochem. Biophys.* **2006**, *450*, 215−222.
(74) Bayburt, T. H.; Sligar, S. G. Self-assembly of single integral membrane proteins into soluble nanoscale phospholipid bilayers. *Protein Sci.* **2003**, *12*, 2476−2481.
(75) Xu, H.; Hill, J. J.; Michelsen, K.; Yamane, H.; Kurzeja, R. J.; Tam, T.; Isaacs, R. J.; Shen, F.; Tagari, P. Characterization of the direct interaction between KcsA-Kv1.3 and its inhibitors. *Biochim. Biophys. Acta, Biomembr.* **2015**, *1848*, 1974−1980.
(76) Tark, S.-H.; Das, A.; Sligar, S.; Dravid, V. P. Nanomechanical detection of cholera toxin using microcantilevers functionalized with ganglioside nanodiscs. *Nanotechnology* **2010**, *21*, 435502.
(77) Bayburt, T. H.; Carlson, J. W.; Sligar, S. G. Reconstitution and imaging of a membrane protein in a nanometer-size phospholipid bilayer. *J. Struct. Biol.* **1998**, *123*, 37−44.
(78) Carlson, J. W.; Jonas, A.; Sligar, S. G. Imaging and manipulation of high-density lipoproteins. *Biophys. J.* **1997**, *73*, 1184−1189.
(79) Bayburt, T. H.; Sligar, S. G. Single-molecule height measurements on microsomal cytochrome P450 in nanometer-scale phospholipid bilayer disks. *Proc. Natl. Acad. Sci. U. S. A.* **2002**, *99*, 6725−6730.
(80) Xu, X.-P.; Kim, E.; Swift, M.; Smith, J. W.; Volkmann, N.; Hanein, D. Three-dimensional structures of full-length, membrane-embedded human αIIbβ3 integrin complexes. *Biophys. J.* **2016**, *110*, 798−809.
(81) Bayburt, T. H.; Leitz, A. J.; Xie, G.; Oprian, D. D.; Sligar, S. G. Transducin activation by nanoscale lipid bilayers containing one and two rhodopsins. *J. Biol. Chem.* **2007**, *282*, 14875−14881.
(82) Duggal, R.; Liu, Y.; Gregory, M. C.; Denisov, I. G.; Kincaid, J. R.; Sligar, S. G. Evidence that cytochrome b5 acts as a redox donor in CYP17A1 mediated androgen synthesis. *Biochem. Biophys. Res. Commun.* **2016**, *477*, 202−208.
(83) Gregory, M.; Mak, P. J.; Sligar, S. G.; Kincaid, J. R. Differential hydrogen bonding in human CYP17 dictates hydroxylation versus lyase chemistry. *Angew. Chem., Int. Ed.* **2013**, *52*, 5342−5345.
(84) Gregory, M. C.; Denisov, I. G.; Grinkova, Y. V.; Khatri, Y.; Sligar, S. G. Kinetic solvent isotope effect in human P450 CYP17A1-mediated androgen formation: Evidence for a reactive peroxoanion intermediate. *J. Am. Chem. Soc.* **2013**, *135*, 16245−16247.
(85) Grinkova, Y. V.; Denisov, I. G.; McLean, M. A.; Sligar, S. G. Oxidase uncoupling in heme monooxygenases: Human cytochrome P450 CYP3A4 in Nanodiscs. *Biochem. Biophys. Res. Commun.* **2013**, *430*, 1223−1227.
(86) Grinkova, Y. V.; Denisov, I. G.; Waterman, M. R.; Arase, M.; Kagawa, N.; Sligar, S. G. The ferrous-oxy complex of human aromatase. *Biochem. Biophys. Res. Commun.* **2008**, *372*, 379−382.
(87) Mak, P. J.; Denisov, I. G.; Grinkova, Y. V.; Sligar, S. G.; Kincaid, J. R. Defining CYP3A4 structural responses to substrate binding. Raman spectroscopic studies of a Nanodisc-incorporated mammalian cytochrome P450. *J. Am. Chem. Soc.* **2011**, *133*, 1357−1366.
(88) Mak, P. J.; Gregory, M. C.; Denisov, I. G.; Sligar, S. G.; Kincaid, J. R. Unveiling the crucial intermediates in androgen production. *Proc. Natl. Acad. Sci. U. S. A.* **2015**, *112*, 15856−15861.
(89) Mak, P. J.; Gregory, M. C.; Sligar, S. G.; Kincaid, J. R. Resonance Raman spectroscopy reveals that substrate structure selectively impacts the heme-bound diatomic ligands of CYP17. *Biochemistry* **2014**, *53*, 90−100.
(90) Mak, P. J.; Luthra, A.; Sligar, S. G.; Kincaid, J. R. Resonance Raman spectroscopy of the oxygenated intermediates of human CYP19A1 implicates a compound I intermediate in the final lyase step. *J. Am. Chem. Soc.* **2014**, *136*, 4825−4828.
(91) Nakatani-Webster, E.; Hu, S. L.; Atkins, W. M.; Catalano, C. E. Assembly and characterization of gp160-nanodiscs: A new platform for biochemical characterization of HIV envelope spikes. *J. Virol. Methods* **2015**, *226*, 15−24.
(92) Shaw, A. W.; Pureza, V. S.; Sligar, S. G.; Morrissey, J. H. The local phospholipid environment modulates the activation of blood clotting. *J. Biol. Chem.* **2006**, *282*, 6556−6563.
(93) Ye, X.; McLean, M. A.; Sligar, S. G. Conformational equilibrium of talin is regulated by anionic lipids. *Biochim. Biophys. Acta, Biomembr.* **2016**, *1858*, 1833−1840.
(94) Zhang, P.; Ye, F.; Bastidas, A. C.; Kornev, A. P.; Wu, J.; Ginsberg, M. H.; Taylor, S. S. An isoform-specific myristylation switch targets Type II PKA holoenzymes to membranes. *Structure* **2015**, *23*, 1563−1572.
(95) Boettcher, J. M.; Davis-Harrison, R. L.; Clay, M. C.; Nieuwkoop, A. J.; Ohkubo, Y. Z.; Tajkhorshid, E.; Morrissey, J. H.; Rienstra, C. M. Atomic view of calcium-induced clustering of phosphatidylserine in mixed lipid bilayers. *Biochemistry* **2011**, *50*, 2264−2273.
(96) Her, C.; Filoti, D. I.; McLean, M. A.; Sligar, S. G.; Alexander Ross, J. B.; Steele, H.; Laue, T. M. The charge properties of phospholipid Nanodiscs. *Biophys. J.* **2016**, *111*, 989−998.
(97) Ye, X.; McLean, M. A.; Sligar, S. G. PIP2 modulates the affinity of talin-1 for phospholipid bilayers and activates its auto- inhibited form. *Biochemistry* **2016**, *55*, 5038.
(98) Yao, Y.; Nisan, D.; Antignani, A.; Barnes, A.; Tjandra, N.; Youle, R. J.; Marassi, F. M.; Fujimoto, L. M. Characterization of the membrane-inserted C-terminus of cytoprotective BCL-XL. *Protein Expression Purif.* **2016**, *122*, 56−63.
(99) Nath, A.; Koo, P. K.; Rhoades, E.; Atkins, W. M. Allosteric effects on substrate dissociation from cytochrome P450 3A4 in Nanodiscs observed by ensemble and single-molecule fluorescence spectroscopy. *J. Am. Chem. Soc.* **2008**, *130*, 15746−15747.
(100) Yin, L.; Kim, J.; Shin, Y.-K. Complexin splits the membrane-proximal region of a single SNAREpin. *Biochem. J.* **2016**, *473*, 2219−2224.
(101) Bender, G.; Schexnaydre, E. E.; Murphy, R. C.; Uhlson, C.; Newcomer, M. E. Membrane-dependent activities of human 15-LOX-2 and its murine counterpart: Implications for murine models of atherosclerosis. *J. Biol. Chem.* **2016**, *291*, 19413−19424.
(102) Eggensperger, S.; Fisette, O.; Parcej, D.; Schafer, L. V.; Tampe, R. An annular lipid belt is essential for allosteric coupling and viral inhibition of the antigen translocation complex TAP (Transporter Associated with Antigen Processing). *J. Biol. Chem.* **2014**, *289*, 33098−33108.
(103) Finkenwirth, F.; Sippach, M.; Landmesser, H.; Kirsch, F.; Ogienko, A.; Grunzel, M.; Kiesler, C.; Steinhoff, H. J.; Schneider, E.; Eitinger, T. ATP-dependent conformational changes trigger substrate capture and release by an ECF-type biotin transporter. *J. Biol. Chem.* **2015**, *290*, 16929−16942.
(104) Hornschemeyer, P.; Liss, V.; Heermann, R.; Jung, K.; Hunke, S. Interaction analysis of a two-component system using Nanodiscs. *PLoS One* **2016**, *11*, e0149187.
(105) Dominik, P. K.; Borowska, M. T.; Dalmas, O.; Kim, S. S.; Perozo, E.; Keenan, R. J.; Kossiakoff, A. A. Conformational chaperones for structural studies of membrane proteins using antibody phage display with Nanodiscs. *Structure* **2016**, *24*, 300−309.
(106) Mi, L. Z.; Grey, M. J.; Nishida, N.; Walz, T.; Lu, C. F.; Springer, T. A. Functional and structural stability of the epidermal growth factor receptor in detergent micelles and phospholipid nanodiscs. *Biochemistry* **2008**, *47*, 10314−10323.

DOI: 10.1021/acs.chemrev.6b00690
Chem. Rev. 2017, 117, 4669−4713

(107) Bajaj, R.; Bruce, K. E.; Davidson, A. L.; Rued, B. E.; Stauffacher, C. V.; Winkler, M. E. Biochemical characterization of essential cell division proteins FtsX and FtsE that mediate peptidoglycan hydrolysis by PcsB in Streptococcus pneumoniae. *MicrobiologyOpen* **2016**, *5*, 738.
(108) Mitra, N.; Liu, Y.; Liu, J.; Serebryany, E.; Mooney, V.; DeVree, B. T.; Sunahara, R. K.; Yan, E. C. Y. Calcium dependent ligand binding and G-protein signaling of family B GPCR parathyroid hormone 1 receptor purified in Nanodiscs. *ACS Chem. Biol.* **2013**, *8*, 617−625.
(109) Shirzad-Wasei, N.; Oostrum, J. V.; Bovee-Geurts, P. H.; Kusters, L. J.; Bosman, G. J.; DeGrip, W. J. Rapid transfer of overexpressed integral membrane protein from the host membrane into soluble lipid nanodiscs without previous purification. *Biol. Chem.* **2015**, *396*, 903−916.
(110) Gregersen, J. L.; Fedosova, N. U.; Nissen, P.; Boesen, T. Reconstitution of Na(+),K(+)-ATPase in Nanodiscs. *Methods Mol. Biol.* **2016**, *1377*, 403−409.
(111) Marty, M. T.; Wilcox, K. C.; Klein, W. L.; Sligar, S. G. Nanodisc-solubilized membrane protein library reflects the membrane proteome. *Anal. Bioanal. Chem.* **2013**, *405*, 4009−4016.
(112) Wilcox, K. C.; Marunde, M. R.; Das, A.; Velasco, P. T.; Kuhns, B. D.; Marty, M. T.; Jiang, H.; Luan, C. H.; Sligar, S. G.; Klein, W. L. Nanoscale synaptic membrane mimetic allows unbiased high throughput screen that targets binding sites for Alzheimer's-associated Abeta oligomers. *PLoS One* **2015**, *10*, e0125263.
(113) Hoi, K. K.; Robinson, C. V.; Marty, M. T. Unraveling the composition and behavior of heterogeneous lipid Nanodiscs by mass spectrometry. *Anal. Chem.* **2016**, *88*, 6199−6204.
(114) Landreh, M.; Marty, M. T.; Gault, J.; Robinson, C. V. A sliding selectivity scale for lipid binding to membrane proteins. *Curr. Opin. Struct. Biol.* **2016**, *39*, 54−60.
(115) Civjan, N. R.; Bayburt, T. H.; Schuler, M. A.; Sligar, S. G. Direct solubilization of heterologously expressed membrane proteins by incorporation into nanoscale lipid bilayers. *BioTechniques* **2003**, *35*, 556−558; *560*, 562−563.
(116) Civjan, N. R. Regulation and functionality of stress-induced cytochrome P450 monooxygenases: A functional genomic approach. Ph.D. Thesis, University of Illinois: Urbana, IL, 2005.
(117) Duan, H.; Civjan, N. R.; Sligar, S. G.; Schuler, M. A. Co-incorporation of heterologously expressed Arabidopsis cytochrome P450 and P450 reductase into soluble nanoscale lipid bilayers. *Arch. Biochem. Biophys.* **2004**, *424*, 141−153.
(118) Li, F.; Kummel, D.; Coleman, J.; Reinisch, K. M.; Rothman, J. E.; Pincet, F. A half-zippered SNARE complex represents a functional intermediate in membrane fusion. *J. Am. Chem. Soc.* **2014**, *136*, 3456−3464.
(119) Li, F.; Tiwari, N.; Rothman, J. E.; Pincet, F. Kinetic barriers to SNAREpin assembly in the regulation of membrane docking/priming and fusion. *Proc. Natl. Acad. Sci. U. S. A.* **2016**, *113*, 10536.
(120) Puthenveetil, R.; Vinogradova, O. Optimization of the design and preparation of nanoscale phospholipid bilayers for its application to solution NMR. *Proteins: Struct., Funct., Genet.* **2013**, *81*, 1222−1231.
(121) Vishnivetskiy, S. A.; Ostermaier, M. K.; Singhal, A.; Panneels, V.; Homan, K. T.; Glukhova, A.; Sligar, S. G.; Tesmer, J. J. G.; Schertler, G. F. X.; Standfuss, J.; et al. Constitutively active rhodopsin mutants causing night blindness are effectively phosphorylated by GRKs but differ in arrestin-1 binding. *Cell. Signalling* **2013**, *25*, 2155−2162.
(122) Alami, M.; Dalal, K.; Lelj-Garolla, B.; Sligar, S. G.; Duong, F. Nanodiscs unravel the interaction between the SecYEG channel and its cytosolic partner SecA. *EMBO J.* **2007**, *26*, 1995−2004.
(123) Dalal, K.; Duong, F. Reconstitution of the SecY translocon in nanodiscs. *Methods Mol. Biol.* **2010**, *619*, 145−156.
(124) Heuveling, J.; Frochaux, V.; Ziomkowska, J.; Wawrzinek, R.; Wessig, P.; Herrmann, A.; Schneider, E. Conformational changes of the bacterial type I ATP-binding cassette importer HisQMP2 at distinct steps of the catalytic cycle. *Biochim. Biophys. Acta, Biomembr.* **2014**, *1838*, 106−116.
(125) D'Antona, A. M.; Xie, G.; Sligar, S. G.; Oprian, D. D. Assembly of an activated rhodopsin-transducin complex in nanoscale lipid bilayers. *Biochemistry* **2014**, *53*, 127−134.
(126) Shenkarev, Z. O.; Lyukmanova, E. N.; Butenko, I. O.; Petrovskaya, L. E.; Paramonov, A. S.; Shulepko, M. A.; Nekrasova, O. V.; Kirpichnikov, M. P.; Arseniev, A. S. Lipid-protein nanodiscs promote in vitro folding of transmembrane domains of multi-helical and multimeric membrane proteins. *Biochim. Biophys. Acta, Biomembr.* **2013**, *1828*, 776−784.
(127) Etzkorn, M.; Raschle, T.; Hagn, F.; Gelev, V.; Rice, A. J.; Walz, T.; Wagner, G. Cell-free expressed bacteriorhodopsin in different soluble membrane mimetics: Biophysical properties and NMR accessibility. *Structure* **2013**, *21*, 394−401.
(128) Hagn, F.; Etzkorn, M.; Raschle, T.; Wagner, G. Optimized phospholipid bilayer Nanodiscs facilitate high-resolution structure determination of membrane proteins. *J. Am. Chem. Soc.* **2013**, *135*, 1919−1925.
(129) Frey, L.; Lakomek, N. A.; Riek, R.; Bibow, S. Micelles, bicelles, and nanodiscs: Comparing the impact of membrane mimetics on membrane protein backbone dynamics. *Angew. Chem., Int. Ed.* **2017**, *56*, 380−383.
(130) Boldog, T.; Li, M.; Hazelbauer, G. L. Using Nanodiscs to create water-soluble transmembrane chemoreceptors inserted in lipid bilayers. *Methods Enzymol.* **2007**, *423*, 317−335.
(131) Goddard, A. D.; Dijkman, P. M.; Adamson, R. J.; Inacio dos Reis, R.; Watts, A. Reconstitution of membrane proteins: a GPCR as an example. *Methods Enzymol.* **2015**, *556*, 405−424.
(132) Boldog, T.; Grimme, S.; Li, M.; Sligar, S. G.; Hazelbauer, G. L. Nanodiscs separate chemoreceptor oligomeric states and reveal their signaling properties. *Proc. Natl. Acad. Sci. U. S. A.* **2006**, *103*, 11509−11514.
(133) Bao, H.; Duong, F.; Chan, C. S. A step-by-step method for the reconstitution of an ABC transporter into nanodisc lipid particles. *J. Visualized Exp.* **2012**, 3911−3916.
(134) Shenkarev, Z. O.; Lyukmanova, E. N.; Paramonov, A. S.; Shingarova, L. N.; Chupin, V. V.; Kirpichnikov, M. P.; Blommers, M. J.; Arseniev, A. S. Lipid-protein nanodiscs as reference medium in detergent screening for high-resolution NMR studies of integral membrane proteins. *J. Am. Chem. Soc.* **2010**, *132*, 5628−5629.
(135) Mineev, K. S.; Goncharuk, S. A.; Kuzmichev, P. K.; Vilar, M.; Arseniev, A. S. NMR dynamics of transmembrane and intracellular domains of p75NTR in lipid-protein Nanodiscs. *Biophys. J.* **2015**, *109*, 772−782.
(136) Akkaladevi, N.; Mukherjee, S.; Katayama, H.; Janowiak, B.; Patel, D.; Gogol, E. P.; Pentelute, B. L.; John Collier, R.; Fisher, M. T. Following natures lead: On the construction of membrane-inserted toxins in lipid bilayer Nanodiscs. *J. Membr. Biol.* **2015**, *248*, 595−607.
(137) Gogol, E. P.; Akkaladevi, N.; Szerszen, L.; Mukherjee, S.; Chollet-Hinton, L.; Katayama, H.; Pentelute, B. L.; Collier, R. J.; Fisher, M. T. Three dimensional structure of the anthrax toxin translocon-lethal factor complex by cryo-electron microscopy. *Protein Sci.* **2013**, *22*, 586−594.
(138) Matthies, D.; Dalmas, O.; Borgnia; Mario, J.; Dominik; Pawel, K.; Merk, A.; Rao, P.; Reddy; Bharat, G.; Islam, S.; Bartesaghi, A.; Perozo, E.; et al. Cryo-EM structures of the magnesium channel CorA reveal symmetry break upon gating. *Cell* **2016**, *164*, 747−756.
(139) Stam, N. J.; Wilkens, S. Structure of Nanodisc reconstituted vacuolar ATPase proton channel: Definition of the interaction of rotor and stator and implications for enzyme regulation by reversible dissociation. *J. Biol. Chem.* **2017**, *292*, 1749−1761.
(140) Puthenveetil, R., Nguyen, K., Vinogradova, O. Nanodiscs and solution NMR: preparation, application and challenges. *Nanotechnol. Rev.* **2017**, *6*, DOI: 10.1515/ntrev-2016-0076
(141) Viegas, A.; Viennet, T.; Etzkorn, M. The power, pitfalls and potential of the nanodisc system for NMR-based studies. *Biol. Chem.* **2016**, *397*, 1335−1354.
(142) Jo, S.; Cheng, X.; Lee, J.; Kim, S.; Park, S.-J.; Patel, D. S.; Beaven, A. H.; Lee, K. I.; Rui, H.; Park, S.; et al. CHARMM-GUI 10

DOI: 10.1021/acs.chemrev.6b00690
Chem. Rev. 2017, 117, 4669−4713

years for biomolecular modeling and simulation. *J. Comput. Chem.* **2016**, DOI: 10.1002/jcc.24660.
(143) Grinkova, Y. V.; Denisov, I. G.; Sligar, S. G. Engineering extended membrane scaffold proteins for self-assembly of soluble nanoscale lipid bilayers. *Protein Eng., Des. Sel.* **2010**, *23*, 843−848.
(144) Miyazaki, M.; Nakano, M.; Fukuda, M.; Handa, T. Smaller discoidal high-density lipoprotein particles form saddle surfaces, but not planar bilayers. *Biochemistry* **2009**, *48*, 7756−7763.
(145) Catte, A.; Patterson, J. C.; Jones, M. K.; Jerome, W. G.; Bashtovyy, D.; Su, Z.; Gu, F.; Chen, J.; Aliste, M. P.; Harvey, S. C.; et al. Novel changes in discoidal high density lipoprotein morphology: a molecular dynamics study. *Biophys. J.* **2006**, *90*, 4345−4360.
(146) Justesen, B. H.; Laursen, T.; Weber, G.; Fuglsang, A. T.; Moeller, B. L.; Gunther Pomorski, T. Isolation of monodisperse Nanodisc-reconstituted membrane proteins using free flow electrophoresis. *Anal. Chem.* **2013**, *85*, 3497−3500.
(147) Marty, M. T.; Zhang, H.; Cui, W.; Blankenship, R. E.; Gross, M. L.; Sligar, S. G. Native mass spectrometry characterization of intact nanodisc lipoprotein complexes. *Anal. Chem.* **2012**, *84*, 8957−8960.
(148) Marty, M. T.; Baldwin, A. J.; Marklund, E. G.; Hochberg, G. K.; Benesch, J. L.; Robinson, C. V. Bayesian deconvolution of mass and ion mobility spectra: from binary interactions to polydisperse ensembles. *Anal. Chem.* **2015**, *87*, 4370−4376.
(149) Stoilova-McPhie, S.; Grushin, K.; Dalm, D.; Miller, J. Lipid nanotechnologies for structural studies of membrane-associated proteins. *Proteins: Struct., Funct., Genet.* **2014**, *82*, 2902−2909.
(150) Marty, M. T.; Zhang, H.; Cui, W.; Gross, M. L.; Sligar, S. G. Interpretation and deconvolution of Nanodisc native mass spectra. *J. Am. Soc. Mass Spectrom.* **2014**, *25*, 269−277.
(151) Phillips, J. C.; Wriggers, W.; Li, Z.; Jonas, A.; Schulten, K. Predicting the structure of apolipoprotein A-I in reconstituted high-density lipoprotein disks. *Biophys. J.* **1997**, *73*, 2337−2346.
(152) Li, Y.; Kijac, A. Z.; Sligar, S. G.; Rienstra, C. M. Structural analysis of nanoscale self-assembled discoidal lipid bilayers by solid-state NMR spectroscopy. *Biophys. J.* **2006**, *91*, 3819−3828.
(153) Koppaka, V.; Silvestro, L.; Engler, J. A.; Brouillette, C. G.; Axelsen, P. H. The structure of human lipoprotein A-I. Evidence for the "belt" model. *J. Biol. Chem.* **1999**, *274*, 14541−14544.
(154) Bibow, S.; Polyhach, Y.; Eichmann, C.; Chi, C. N.; Kowal, J.; Albiez, S.; McLeod, R. A.; Henning Stahlberg, H.; Jeschke, G.; Güntert, P.; Riek, R. Solution structure of discoidal high-density lipoprotein particles with a shortened apolipoprotein A-I. *Nat. Struct. Mol. Biol.* **2017**, *24*,10.1038/nsmb.3345
(155) Ozawa, M.; Handa, T.; Nakano, M. Effect of cholesterol on binding of amphipathic helices to lipid emulsions. *J. Phys. Chem. B* **2012**, *116*, 476−482.
(156) Tanaka, M.; Hosotani, A.; Tachibana, Y.; Nakano, M.; Iwasaki, K.; Kawakami, T.; Mukai, T. Preparation and characterization of reconstituted lipid-synthetic polymer discoidal particles. *Langmuir* **2015**, *31*, 12719−12726.
(157) Smirnova, I. A.; Sjostrand, D.; Li, F.; Bjorck, M.; Schafer, J.; Ostbye, H.; Hogbom, M.; von Ballmoos, C.; Lander, G. C.; Adelroth, P.; et al. Isolation of yeast complex IV in native lipid nanodiscs. *Biochim. Biophys. Acta, Biomembr.* **2016**, *1858*, 2984−2992.
(158) Benedetti, E.; Di Blasio, B.; Pavone, V.; Pedone, C.; Toniolo, C.; Crisma, M. Characterization at atomic resolution of peptide helical structures. *Biopolymers* **1992**, *32*, 453−456.
(159) Forte, T. M.; Nordhausen, R. W. Electron microscopy of negatively stained lipoproteins. *Methods Enzymol.* **1986**, *128*, 442−457.
(160) Zhang, L.; Tong, H.; Garewal, M.; Ren, G. Optimized negative-staining electron microscopy for lipoprotein studies. *Biochim. Biophys. Acta, Gen. Subj.* **2013**, *1830*, 2150−2159.
(161) Xu, X. P.; Zhai, D.; Kim, E.; Swift, M.; Reed, J. C.; Volkmann, N.; Hanein, D. Three-dimensional structure of Bax-mediated pores in membrane bilayers. *Cell Death Dis.* **2013**, *4*, e683.
(162) Justesen, B. H.; Hansen, R. W.; Martens, H. J.; Theorin, L.; Palmgren, M. G.; Martinez, K. L.; Pomorski, T. G.; Fuglsang, A. T. Active plasma membrane P-type H+-ATPase reconstituted into nanodisks is a monomer. *J. Biol. Chem.* **2013**, *288*, 26419−26429.
(163) Nakano, M.; Fukuda, M.; Kudo, T.; Miyazaki, M.; Wada, Y.; Matsuzaki, N.; Endo, H.; Handa, T. Static and dynamic properties of phospholipid bilayer Nanodiscs. *J. Am. Chem. Soc.* **2009**, *131*, 8308−8312.
(164) Skar-Gislinge, N.; Simonsen, J. B.; Mortensen, K.; Feidenhans'l, R.; Sligar, S. G.; Moeller, B. L.; Bjoernholm, T.; Arleth, L. Elliptical structure of phospholipid bilayer Nanodiscs encapsulated by scaffold proteins: Casting the roles of the lipids and the protein. *J. Am. Chem. Soc.* **2010**, *132*, 13713−13722.
(165) Skar-Gislinge, N.; Arleth, L. Small-angle scattering from phospholipid nanodiscs: derivation and refinement of a molecular constrained analytical model form factor. *Phys. Chem. Chem. Phys.* **2011**, *13*, 3161−3170.
(166) Huda, P.; Binderup, T.; Pedersen, M. C.; Midtgaard, S. R.; Elema, D. R.; Kjaer, A.; Jensen, M.; Arleth, L. PET/CT based In vivo evaluation of 64Cu labelled Nanodiscs in tumor bearing mice. *PLoS One* **2015**, *10*, e0129310.
(167) Midtgaard, S. R.; Pedersen, M. C.; Arleth, L. Small-angle X-ray scattering of the cholesterol incorporation into human ApoA1-POPC discoidal particles. *Biophys. J.* **2015**, *109*, 308−318.
(168) Wadsater, M.; Barker, R.; Mortensen, K.; Feidenhans'l, R.; Cardenas, M. Effect of phospholipid composition and phase on Nanodisc films at the solid-liquid interface as studied by neutron reflectivity. *Langmuir* **2013**, *29*, 2871−2880.
(169) Wadsater, M.; Simonsen, J. B.; Lauridsen, T.; Tveten, E. G.; Naur, P.; Bjoernholm, T.; Wacklin, H.; Mortensen, K.; Arleth, L.; Feidenhans'l, R.; et al. Aligning Nanodiscs at the air-water interface, a neutron reflectivity study. *Langmuir* **2011**, *27*, 15065−15073.
(170) Justesen, B. H.; Guenther-Pomorski, T. Chromatographic and electrophoretic methods for nanodisc purification and analysis. *Rev. Anal. Chem.* **2014**, *33*, 165−172.
(171) Inagaki, S.; Ghirlando, R.; Grisshammer, R. Biophysical characterization of membrane proteins in nanodiscs. *Methods* **2013**, *59*, 287−300.
(172) Kijac, A.; Shih, A. Y.; Nieuwkoop, A. J.; Schulten, K.; Sligar, S. G.; Rienstra, C. M. Lipid-protein correlations in nanoscale phospholipid bilayers determined by solid-state nuclear Mmagnetic resonance. *Biochemistry* **2010**, *49*, 9190−9198.
(173) Shaw, A. W.; McLean, M. A.; Sligar, S. G. Phospholipid phase transitions in homogeneous nanometer scale bilayer discs. *FEBS Lett.* **2004**, *556*, 260−264.
(174) Morrissey, J. H.; Pureza, V.; Davis-Harrison, R. L.; Sligar, S. G.; Rienstra, C. M.; Kijac, A. Z.; Ohkubo, Y. Z.; Tajkhorshid, E. Protein-membrane interactions: blood clotting on nanoscale bilayers. *J. Thromb. Haemostasis* **2009**, *7*, 169−172.
(175) Sivashanmugam, A.; Yang, Y.; Murray, V.; McCullough, C.; Chen, B.; Ren, X.; Li, Q.; Wang, J. Structural basis of human high-density lipoprotein formation and assembly at sub nanometer resolution. *Methods Cell Biol.* **2008**, *90*, 327−364.
(176) Chen, B.; Ren, X.; Neville, T.; Jerome, W. G.; Hoyt, D. W.; Sparks, D.; Ren, G.; Wang, J. Apolipoprotein AI tertiary structures determine stability and phospholipid-binding activity of discoidal high-density lipoprotein particles of different sizes. *Protein Sci.* **2009**, *18*, 921−935.
(177) Cavigiolio, G.; Shao, B.; Geier, E. G.; Ren, G.; Heinecke, J. W.; Oda, M. N. The interplay between size, morphology, stability, and functionality of high-density lipoprotein subclasses. *Biochemistry* **2008**, *47*, 4770−4779.
(178) Brouillette, C. G.; Jones, J. L.; Ng, T. C.; Kercret, H.; Chung, B. H.; Segrest, J. P. Structural studies of apolipoprotein A-I/phosphatidylcholine recombinants by high-field proton NMR, non-denaturing gradient gel electrophoresis, and electron microscopy. *Biochemistry* **1984**, *23*, 359−367.
(179) Wald, J. H.; Krul, E. S.; Jonas, A. Structure of apolipoprotein A-I in three homogeneous, reconstituted high density lipoprotein particles. *J. Biol. Chem.* **1990**, *265*, 20037−20043.
(180) Shenkarev, Z. O.; Lyukmanova, E. N.; Solozhenkin, O. I.; Gagnidze, I. E.; Nekrasova, O. V.; Chupin, V. V.; Tagaev, A. A.; Yakimenko, Z. A.; Ovchinnikova, T. V.; Kirpichnikov, M. P.; et al.

DOI: 10.1021/acs.chemrev.6b00690
Chem. Rev. 2017, 117, 4669−4713

Lipid-protein nanodiscs: Possible application in high-resolution NMR investigations of membrane proteins and membrane-active peptides. *Biochemistry (Moscow)* **2009**, *74*, 756−765.
(181) Tavoosi, N.; Davis-Harrison, R. L.; Pogorelov, T. V.; Ohkubo, Y. Z.; Arcario, M. J.; Clay, M. C.; Rienstra, C. M.; Tajkhorshid, E.; Morrissey, J. H. Molecular determinants of phospholipid synergy in blood clotting. *J. Biol. Chem.* **2011**, *286*, 23247−23253.
(182) Marty, M. T.; Hoi, K. K.; Gault, J.; Robinson, C. V. Probing the lipid annular belt by gas-phase dissociation of membrane proteins in Nanodiscs. *Angew. Chem., Int. Ed.* **2016**, *55*, 550−554.
(183) Hopper, J. T. S.; Yu, Y. T.-C.; Li, D.; Raymond, A.; Bostock, M.; Liko, I.; Mikhailov, V.; Laganowsky, A.; Benesch, J. L. P.; Caffrey, M.; et al. Detergent-free mass spectrometry of membrane protein complexes. *Nat. Methods* **2013**, *10*, 1206−1208.
(184) Zhang, Y.; Liu, L.; Daneshfar, R.; Kitova, E. N.; Li, C.; Jia, F.; Cairo, C. W.; Klassen, J. S. Protein-glycosphingolipid interactions revealed using catch-and-release mass spectrometry. *Anal. Chem.* **2012**, *84*, 7618−7621.
(185) Lin, H.; Kitova, E. N.; Klassen, J. S. Quantifying protein-ligand interactions by direct electrospray ionization-MS analysis: Evidence of nonuniform response factors induced by high molecular weight molecules and complexes. *Anal. Chem.* **2013**, *85*, 8919−8922.
(186) Shih, A. Y.; Denisov, I. G.; Phillips, J. C.; Sligar, S. G.; Schulten, K. Molecular dynamics simulations of discoidal bilayers assembled from truncated human lipoproteins. *Biophys. J.* **2005**, *88*, 548−556.
(187) Shih, A. Y.; Arkhipov, A.; Freddolino, P. L.; Sligar, S. G.; Schulten, K. Assembly of lipids and proteins into lipoprotein particles. *J. Phys. Chem. B* **2007**, *111*, 11095−11104.
(188) Shih, A. Y.; Freddolino, P. L.; Sligar, S. G.; Schulten, K. Disassembly of Nanodiscs with cholate. *Nano Lett.* **2007**, *7*, 1692−1696.
(189) Shih, A. Y.; Arkhipov, A.; Freddolino, P. L.; Schulten, K. Coarse grained protein-lipid model with application to lipoprotein particles. *J. Phys. Chem. B* **2006**, *110*, 3674−3684.
(190) Shih, A. Y.; Freddolino, P. L.; Arkhipov, A.; Schulten, K. Assembly of lipoprotein particles revealed by coarse-grained molecular dynamics simulations. *J. Struct. Biol.* **2007**, *157*, 579−592.
(191) Aksimentiev, A.; Brunner, R.; Cohen, J.; Comer, J.; Cruz-Chu, E.; Hardy, D.; Rajan, A.; Shih, A.; Sigalov, G.; Yin, Y.; et al. Computer modeling in biotechnology: a partner in development. *Methods Mol. Biol.* **2008**, *474*, 181−234.
(192) Shih, A. Y.; Freddolino, P. L.; Arkhipov, A.; Sligar, S. G.; Schulten, K. Molecular modeling of the structural properties and formation of high-density lipoprotein particles. *Curr. Top. Membr.* **2008**, *60*, 313−342.
(193) Shih, A. Y.; Sligar, S. G.; Schulten, K. Maturation of high-density lipoproteins. *J. R. Soc., Interface* **2009**, *6*, 863−871.
(194) Debnath, A.; Schafer, L. V. Structure and dynamics of phospholipid Nanodiscs from all-atom and coarse-grained simulations. *J. Phys. Chem. B* **2015**, *119*, 6991−7002.
(195) Siuda, I.; Tieleman, D. P. Molecular Models of Nanodiscs. *J. Chem. Theory Comput.* **2015**, *11*, 4923−4932.
(196) Vestergaard, M.; Kraft, J. F.; Vosegaard, T.; Thogersen, L.; Schiott, B. Bicelles and other membrane mimics: Comparison of structure, properties, and dynamics from MD simulations. *J. Phys. Chem. B* **2015**, *119*, 15831−15843.
(197) Skar-Gislinge, N.; Kynde, S. A.; Denisov, I. G.; Ye, X.; Lenov, I.; Sligar, S. G.; Arleth, L. Small-angle scattering determination of the shape and localization of human cytochrome P450 embedded in a phospholipid nanodisc environment. *Acta Crystallogr., Sect. D: Biol. Crystallogr.* **2015**, *71*, 2412−2421.
(198) Pan, L.; Segrest, J. P. Computational studies of plasma lipoprotein lipids. *Biochim. Biophys. Acta, Biomembr.* **2016**, *1858*, 2401−2420.
(199) Morgan, C. R.; Hebling, C. M.; Rand, K. D.; Stafford, D. W.; Jorgenson, J. W.; Engen, J. R. Conformational transitions in the membrane scaffold protein of phospholipid bilayer nanodiscs. *Mol. Cell. Proteomics* **2011**, *10*, 010876.
(200) Parasassi, T.; De Stasio, G.; d'Ubaldo, A.; Gratton, E. Phase fluctuation in phospholipid membranes revealed by Laurdan fluorescence. *Biophys. J.* **1990**, *57*, 1179−1186.
(201) Parasassi, T.; Gratton, E. Membrane lipid domains and dynamics as detected by Laurdan fluorescence. *J. Fluoresc.* **1995**, *5*, 59−69.
(202) Bacalum, M.; Zorila, B.; Radu, M. Fluorescence spectra decomposition by asymmetric functions: Laurdan spectrum revisited. *Anal. Biochem.* **2013**, *440*, 123−129.
(203) Jamshad, M.; Grimard, V.; Idini, I.; Knowles, T. J.; Dowle, M. R.; Schofield, N.; Sridhar, P.; Lin, Y.; Finka, R.; Wheatley, M.; et al. Structural analysis of a nanoparticle containing a lipid bilayer used for detergent-free extraction of membrane proteins. *Nano Res.* **2015**, *8*, 774−789.
(204) Orwick, M. C.; Judge, P. J.; Procek, J.; Lindholm, L.; Graziadei, A.; Engel, A.; Groebner, G.; Watts, A. Detergent-free formation and physicochemical characterization of nanosized lipid-polymer complexes: Lipodisq. *Angew. Chem., Int. Ed.* **2012**, *51*, 4653−4657.
(205) Arenas, R. C.; Klingler, J.; Vargas, C.; Keller, S. Influence of lipid bilayer properties on nanodisc formation mediated by styrene/maleic acid copolymers. *Nanoscale* **2016**, *8*, 15016−15026.
(206) Wadsaeter, M.; Maric, S.; Simonsen, J. B.; Mortensen, K.; Cardenas, M. The effect of using binary mixtures of zwitterionic and charged lipids on nanodisc formation and stability. *Soft Matter* **2013**, *9*, 2329−2337.
(207) Lai, G.; Forti, K. M.; Renthal, R. Kinetics of lipid mixing between bicelles and nanolipoprotein particles. *Biophys. Chem.* **2015**, *197*, 47−52.
(208) Lee, J.; Lentz, B. R. Evolution of lipidic structures during model membrane fusion and the relation of this process to cell membrane fusion. *Biochemistry* **1997**, *36*, 6251−6259.
(209) Amin, D. N.; Hazelbauer, G. L. Influence of membrane lipid composition on a transmembrane bacterial chemoreceptor. *J. Biol. Chem.* **2012**, *287*, 41697−41705.
(210) Schwall, C. T.; Greenwood, V. L.; Alder, N. N. The stability and activity of respiratory Complex II is cardiolipin-dependent. *Biochim. Biophys. Acta, Bioenerg.* **2012**, *1817*, 1588−1596.
(211) Orlando, B. J.; McDougle, D. R.; Lucido, M. J.; Eng, E. T.; Graham, L. A.; Schneider, C.; Stokes, D. L.; Das, A.; Malkowski, M. G. Cyclooxygenase-2 catalysis and inhibition in lipid bilayer nanodiscs. *Arch. Biochem. Biophys.* **2014**, *546*, 33−40.
(212) Lee, T. Y.; Yeh, V.; Chuang, J.; Chung Chan, J. C.; Chu, L. K.; Yu, T. Y. Tuning the photocycle kinetics of bacteriorhodopsin in lipid Nanodiscs. *Biophys. J.* **2015**, *109*, 1899−1906.
(213) Bocquet, N.; Kohler, J.; Hug, M. N.; Kusznir, E. A.; Rufer, A. C.; Dawson, R. J.; Hennig, M.; Ruf, A.; Huber, W.; Huber, S. Real-time monitoring of binding events on a thermostabilized human A2A receptor embedded in a lipid bilayer by surface plasmon resonance. *Biochim. Biophys. Acta, Biomembr.* **2015**, *1848*, 1224−1233.
(214) Casiraghi, M.; Damian, M.; Lescop, E.; Point, E.; Moncoq, K.; Morellet, N.; Levy, D.; Marie, J.; Guittet, E.; Baneres, J. L.; et al. Functional modulation of a G protein-coupled receptor conformational landscape in a lipid bilayer. *J. Am. Chem. Soc.* **2016**, *138*, 11170−11175.
(215) Rues, R.-B.; Doetsch, V.; Bernhard, F. Co-translational formation and pharmacological characterization of beta1-adrenergic receptor/nanodisc complexes with different lipid environments. *Biochim. Biophys. Acta, Biomembr.* **2016**, *1858*, 1306−1316.
(216) Henrich, E.; Ma, Y.; Engels, I.; Munch, D.; Otten, C.; Schneider, T.; Henrichfreise, B.; Sahl, H. G.; Dotsch, V.; Bernhard, F. Lipid requirements for the enzymatic activity of MraY translocases and in vitro reconstitution of Lipid II synthesis pathway. *J. Biol. Chem.* **2016**, *291*, 2535−2546.
(217) Henrich, E.; Dotsch, V.; Bernhard, F. Screening for lipid requirements of membrane proteins by combining cell-free expression with nanodiscs. *Methods Enzymol.* **2015**, *556*, 351−369.
(218) Martens, C.; Stein, R. A.; Masureel, M.; Roth, A.; Mishra, S.; Dawaliby, R.; Konijnenberg, A.; Sobott, F.; Govaerts, C.; McHaourab,

DOI: 10.1021/acs.chemrev.6b00690
Chem. Rev. 2017, 117, 4669−4713

H. S. Lipids modulate the conformational dynamics of a secondary multidrug transporter. *Nat. Struct. Mol. Biol.* **2016**, *23*, 744−751.
(219) Chung, K. Y.; Day, P. W.; Velez-Ruiz, G.; Sunahara, R. K.; Kobilka, B. K. Identification of GPCR-interacting cytosolic proteins using HDL particles and mass spectrometry-based proteomic approach. *PLoS One* **2013**, *8*, e54942.
(220) Rasmussen, S. G.; Choi, H. J.; Fung, J. J.; Pardon, E.; Casarosa, P.; Chae, P. S.; Devree, B. T.; Rosenbaum, D. M.; Thian, F. S.; Kobilka, T. S.; et al. Structure of a nanobody-stabilized active state of the βeta(2) adrenoceptor. *Nature* **2011**, *469*, 175−180.
(221) Rosenbaum, D. M.; Zhang, C.; Lyons, J. A.; Holl, R.; Aragao, D.; Arlow, D. H.; Rasmussen, S. G.; Choi, H. J.; Devree, B. T.; Sunahara, R. K.; et al. Structure and function of an irreversible agonist-beta(2) adrenoceptor complex. *Nature* **2011**, *469*, 236−240.
(222) Kahsai, A. W.; Wisler, J. W.; Lee, J.; Ahn, S.; Cahill Iii, T. J.; Dennison, S. M.; Staus, D. P.; Thomsen, A. R.; Anasti, K. M.; Pani, B.; et al. Conformationally selective RNA aptamers allosterically modulate the beta2-adrenoceptor. *Nat. Chem. Biol.* **2016**, *12*, 709−716.
(223) DeVree, B. T.; Mahoney, J. P.; Velez-Ruiz, G. A.; Rasmussen, S. G.; Kuszak, A. J.; Edwald, E.; Fung, J. J.; Manglik, A.; Masureel, M.; Du, Y.; et al. Allosteric coupling from G protein to the agonist-binding pocket in GPCRs. *Nature* **2016**, *535*, 182−186.
(224) Segrest, J. P.; Jones, M. K.; Catte, A.; Thirumuruganandham, S. P. Validation of previous computer models and MD simulations of discoidal HDL by a recent crystal structure of apoA-I. *J. Lipid Res.* **2012**, *53*, 1851−1863.
(225) Goldie, K. N.; Abeyrathne, P.; Kebbel, F.; Chami, M.; Ringler, P.; Stahlberg, H. Cryo-electron microscopy of membrane proteins. *Methods Mol. Biol.* **2014**, *1117*, 325−341.
(226) Gingras, A. R.; Ye, F.; Ginsberg, M. H. Reconstructing integrin activation in vitro. *Methods Mol. Biol.* **2013**, *1046*, 1−17.
(227) Dai, A.; Ye, F.; Taylor, D. W.; Hu, G.; Ginsberg, M. H.; Taylor, K. A. The structure of a full-length membrane-embedded integrin bound to a physiological ligand. *J. Biol. Chem.* **2015**, *290*, 27168−27175.
(228) Efremov, R. G.; Leitner, A.; Aebersold, R.; Raunser, S. Architecture and conformational switch mechanism of the ryanodine receptor. *Nature* **2014**, *517*, 39−43.
(229) Gao, Y.; Cao, E.; Julius, D.; Cheng, Y. TRPV1 structures in nanodiscs reveal mechanisms of ligand and lipid action. *Nature* **2016**, *534*, 347−351.
(230) Gatsogiannis, C.; Merino, F.; Prumbaum, D.; Roderer, D.; Leidreiter, F.; Meusch, D.; Raunser, S. Membrane insertion of a Tc toxin in near-atomic detail. *Nat. Struct. Mol. Biol.* **2016**, *23*, 884−890.
(231) Kumar, R. B.; Zhu, L.; Idborg, H.; Radmark, O.; Jakobsson, P. J.; Rinaldo-Matthis, A.; Hebert, H.; Jegerschold, C. Structural and functional analysis of calcium ion mediated binding of 5-lipoxygenase to Nanodiscs. *PLoS One* **2016**, *11*, e0152116.
(232) Daury, L.; Orange, F.; Taveau, J.-C.; Verchere, A.; Monlezun, L.; Gounou, C.; Marreddy, R. K. R.; Picard, M.; Broutin, I.; Pos, K. M.; et al. Tripartite assembly of RND multidrug efflux pumps. *Nat. Commun.* **2016**, *7*, 10731.
(233) Frauenfeld, J.; Gumbart, J.; van der Sluis, E. O.; Funes, S.; Gartmann, M.; Beatrix, B.; Mielke, T.; Berninghausen, O.; Becker, T.; Schulten, K.; et al. Cryo-EM structure of the ribosome-SecYE complex in the membrane environment. *Nat. Struct. Mol. Biol.* **2011**, *18*, 614−621.
(234) Grushin, K.; Miller, J.; Dalm, D.; Stoilova-McPhie, S. Factor VIII organisation on nanodiscs with different lipid composition. *Thromb. Haemostasis* **2015**, *113*, 741−749.
(235) Katayama, H.; Wang, J.; Tama, F.; Chollet, L.; Gogol, E. P.; Collier, R. J.; Fisher, M. T. Three-dimensional structure of the anthrax toxin pore inserted into lipid nanodiscs and lipid vesicles. *Proc. Natl. Acad. Sci. U. S. A.* **2010**, *107*, 3453−3457.
(236) Akkaladevi, N.; Hinton-Chollet, L.; Katayama, H.; Mitchell, J.; Szerszen, L.; Mukherjee, S.; Gogol, E. P.; Pentelute, B. L.; Collier, R. J.; Fisher, M. T. Assembly of anthrax toxin pore: Lethal-factor complexes into lipid nanodiscs. *Protein Sci.* **2013**, *22*, 492−501.
(237) Reichart, T. M.; Baksh, M. M.; Rhee, J.-K.; Fiedler, J. D.; Sligar, S. G.; Finn, M. G.; Zwick, M. B.; Dawson, P. E. Trimerization of the HIV transmembrane domain in lipid bilayers modulates broadly neutralizing antibody binding. *Angew. Chem., Int. Ed.* **2016**, *55*, 2688−2692.
(238) Lee, H.; Shingler, K. L.; Organtini, L. J.; Ashley, R. E.; Makhov, A. M.; Conway, J. F.; Hafenstein, S. The novel asymmetric entry intermediate of a picornavirus captured with nanodiscs. *Sci. Adv.* **2016**, *2*, e1501929.
(239) Nasr, M. L.; Baptista, D.; Strauss, M.; Sun, Z. J.; Grigoriu, S.; Huser, S.; Pluckthun, A.; Hagn, F.; Walz, T.; Hogle, J. M.; et al. Covalently circularized nanodiscs for studying membrane proteins and viral entry. *Nat. Methods* **2016**, *14*, 49−52.
(240) Bax, A. Two-dimensional NMR and protein structure. *Annu. Rev. Biochem.* **1989**, *58*, 223−256.
(241) Bax, A.; Grishaev, A. Weak alignment NMR: a hawk-eyed view of biomolecular structure. *Curr. Opin. Struct. Biol.* **2005**, *15*, 563−570.
(242) *Protein NMR spectroscopy: Practical techniques and applications*; Lian, L.-Y., Roberts, G., Eds.; John Wiley & Sons: Chichester, U.K., 2011.
(243) Rosenzweig, R.; Kay, L. E. Bringing dynamic molecular machines into focus by methyl-TROSY NMR. *Annu. Rev. Biochem.* **2014**, *83*, 291−315.
(244) Xu, Y.; Matthews, S. TROSY NMR spectroscopy of large soluble proteins. *Top. Curr. Chem.* **2011**, *335*, 97−119.
(245) McDermott, A. Structure and dynamics of membrane proteins by magic angle spinning solid-state NMR. *Annu. Rev. Biophys.* **2009**, *38*, 385−403.
(246) McDermott, A.; Polenova, T. Solid state NMR: new tools for insight into enzyme function. *Curr. Opin. Struct. Biol.* **2007**, *17*, 617−622.
(247) Sun, S.; Han, Y.; Paramasivam, S.; Yan, S.; Siglin, A. E.; Williams, J. C.; Byeon, I.-J.L.; Ahn, J.; Angela, M.; Gronenborn, A. M.; Polenova, T. In *Protein NMR Techniques, Methods in Molecular Biology*; Shekhtman, A., Burz, D. S., Eds.; Springer Science+Business Media: Berlin, 2012; Vol. *831*, pp. 303−331.
(248) Comellas, G.; Rienstra, C. M. Protein structure determination by magic-angle spinning solid-state NMR, and insights into the formation, structure, and stability of amyloid fibrils. *Annu. Rev. Biophys.* **2013**, *42*, 515−536.
(249) Tang, M.; Comellas, G.; Rienstra, C. M. Advanced solid-state NMR approaches for structure determination of membrane proteins and amyloid fibrils. *Acc. Chem. Res.* **2013**, *46*, 2080−2088.
(250) Mazhab-Jafari, M. T.; Marshall, C. B.; Smith, M. J.; Gasmi-Seabrook, G. M.; Stathopulos, P. B.; Inagaki, F.; Kay, L. E.; Neel, B. G.; Ikura, M. Oncogenic and RASopathy-associated K-RAS mutations relieve membrane-dependent occlusion of the effector-binding site. *Proc. Natl. Acad. Sci. U. S. A.* **2015**, *112*, 6625−6630.
(251) Wang, G. NMR of membrane proteins. *Adv. Protein Pept. Sci.* **2013**, *1*, 128−188.
(252) Wang, X.; Mu, Z.; Li, Y.; Bi, Y.; Wang, Y. Smaller Nanodiscs are suitable for studying protein lipid interactions by solution NMR. *Protein J.* **2015**, *34*, 205−211.
(253) LaGuerre, A.; Lohr, F.; Bernhard, F.; Dotsch, V. Labeling of membrane proteins by cell-free expression. *Methods Enzymol.* **2015**, *565*, 367−388.
(254) Mineev, K. S.; Lesovoy, D. M.; Usmanova, D. R.; Goncharuk, S. A.; Shulepko, M. A.; Lyukmanova, E. N.; Kirpichnikov, M. P.; Bocharov, E. V.; Arseniev, A. S. NMR-based approach to measure the free energy of transmembrane helix-helix interactions. *Biochim. Biophys. Acta, Biomembr.* **2014**, *1838*, 164−172.
(255) Shenkarev, Z. O.; Lyukmanova, E. N.; Paramonov, A. S.; Panteleev, P. V.; Balandin, S. V.; Shulepko, M. A.; Mineev, K. S.; Ovchinnikova, T. V.; Kirpichnikov, M. P.; Arseniev, A. S. Lipid-protein nanodiscs offer new perspectives for structural and functional studies of water-soluble membrane-active peptides. *Acta Naturae* **2014**, *6*, 84−94.

DOI: 10.1021/acs.chemrev.6b00690
Chem. Rev. 2017, 117, 4669−4713

(256) Mineev, K. S., Nadezhdin, K. D. Membrane mimetics for solution NMR studies of membrane proteins. *Nanotechnol. Rev.* **2017**, *6*, 10.1515/ntrev-2016-0074
(257) Hagn, F.; Wagner, G. Structure refinement and membrane positioning of selectively labeled OmpX in phospholipid nanodiscs. *J. Biomol. NMR* **2015**, *61*, 249−260.
(258) Kucharska, I.; Edrington, T. C.; Liang, B.; Tamm, L. K. Optimizing nanodiscs and bicelles for solution NMR studies of two beta-barrel membrane proteins. *J. Biomol. NMR* **2015**, *61*, 261−274.
(259) Morgado, L.; Zeth, K.; Burmann, B. M.; Maier, T.; Hiller, S. Characterization of the insertase BamA in three different membrane mimetics by solution NMR spectroscopy. *J. Biomol. NMR* **2015**, *61*, 333−345.
(260) Yao, Y.; Fujimoto, L. M.; Hirshman, N.; Bobkov, A. A.; Antignani, A.; Youle, R. J.; Marassi, F. M. Conformation of BCL-XL upon membrane integration. *J. Mol. Biol.* **2015**, *427*, 2262−2270.
(261) Alvarez, F. J.; Orelle, C.; Huang, Y.; Bajaj, R.; Everly, R. M.; Klug, C. S.; Davidson, A. L. Full engagement of liganded maltose-binding protein stabilizes a semi-open ATP-binding cassette dimer in the maltose transporter. *Mol. Microbiol.* **2015**, *98*, 878−894.
(262) Alvarez, F. J. D.; Orelle, C.; Davidson, A. L. Functional reconstitution of an ABC transporter in Nanodiscs for use in electron paramagnetic resonance spectroscopy. *J. Am. Chem. Soc.* **2010**, *132*, 9513−9515.
(263) Kang, Y.; Zhou, X. E.; Gao, X.; He, Y.; Liu, W.; Ishchenko, A.; Barty, A.; White, T. A.; Yefanov, O.; Han, G. W.; et al. Crystal structure of rhodopsin bound to arrestin by femtosecond X-ray laser. *Nature* **2015**, *523*, 561−567.
(264) Shin, J.; Lou, X.; Kweon, D.-H.; Shin, Y.-K. Multiple conformations of a single SNAREpin between two nanodisc membranes reveal diverse pre-fusion states. *Biochem. J.* **2014**, *459*, 95−102.
(265) Kofuku, Y.; Ueda, T.; Okude, J.; Shiraishi, Y.; Kondo, K.; Mizumura, T.; Suzuki, S.; Shimada, I. Functional dynamics of deuterated beta2 -adrenergic receptor in lipid bilayers revealed by NMR spectroscopy. *Angew. Chem., Int. Ed.* **2014**, *53*, 13376−13379.
(266) Okude, J.; Ueda, T.; Kofuku, Y.; Sato, M.; Nobuyama, N.; Kondo, K.; Shiraishi, Y.; Mizumura, T.; Onishi, K.; Natsume, M.; et al. Identification of a conformational equilibrium that determines the efficacy and functional selectivity of the mu-opioid receptor. *Angew. Chem., Int. Ed.* **2015**, *54*, 15771−15776.
(267) Yoshiura, C.; Ueda, T.; Kofuku, Y.; Matsumoto, M.; Okude, J.; Kondo, K.; Shiraishi, Y.; Shimada, I. Elucidation of the CCR1- and CCR5-binding modes of MIP-1alpha by application of an NMR spectra reconstruction method to the transferred cross-saturation experiments. *J. Biomol. NMR* **2015**, *63*, 333−340.
(268) Nath, A.; Rhoades, E. In *Encyclopedia of Biophysics*; Roberts, G. C. K., Ed.; Springer: Berlin, 2013, pp. 1856−1859.
(269) Laursen, T.; Singha, A.; Rantzau, N.; Tutkus, M.; Borch, J.; Hedegard, P.; Stamou, D.; Moller, B. L.; Hatzakis, N. S. Single molecule activity measurements of cytochrome P450 oxidoreductase reveal the existence of two discrete functional states. *ACS Chem. Biol.* **2014**, *9*, 630−634.
(270) Lamichhane, R.; Liu, J. J.; Pljevaljcic, G.; White, K. L.; van der Schans, E.; Katritch, V.; Stevens, R. C.; Wuthrich, K.; Millar, D. P. Single-molecule view of basal activity and activation mechanisms of the G protein-coupled receptor β2AR. *Proc. Natl. Acad. Sci. U. S. A.* **2015**, *112*, 14254−14259.
(271) Bayburt, T. H.; Vishnivetskiy, S. A.; McLean, M. A.; Morizumi, T.; Huang, C.-C.; Tesmer, J. J. G.; Ernst, O. P.; Sligar, S. G.; Gurevich, V. V. Monomeric rhodopsin is sufficient for normal rhodopsin kinase (GRK1) phosphorylation and arrestin-1 binding. *J. Biol. Chem.* **2011**, *286*, 1420−1428.
(272) Sadler, E. E.; Kapanidis, A. N.; Tucker, S. J. Solution-based single-molecule FRET studies of K(+) channel gating in a lipid bilayer. *Biophys. J.* **2016**, *110*, 2663−2670.
(273) Ishmukhametov, R.; Hornung, T.; Spetzler, D.; Frasch, W. D. Direct observation of stepped proteolipid ring rotation in E. coli F0F1-ATP synthase. *EMBO J.* **2010**, *29*, 3911−3923.
(274) Martin, J.; Hudson, J.; Hornung, T.; Frasch, W. D. Fo-driven rotation in the ATP synthase direction against the force of F1 ATPase in the FoF1 ATP synthase. *J. Biol. Chem.* **2015**, *290*, 10717−10728.
(275) Zocher, M.; Roos, C.; Wegmann, S.; Bosshart, P. D.; Dotsch, V.; Bernhard, F.; Muller, D. J. Single-molecule force spectroscopy from Nanodiscs: An assay to quantify folding, stability, and interactions of native membrane proteins. *ACS Nano* **2012**, *6*, 961−971.
(276) Taufik, I.; Kedrov, A.; Exterkate, M.; Driessen, A. J. M. Monitoring the activity of single translocons. *J. Mol. Biol.* **2013**, *425*, 4145−4153.
(277) Osborne, A. R.; Rapoport, T. A. Protein translocation is mediated by oligomers of the SecY complex with one SecY copy forming the channel. *Cell (Cambridge, MA, U. S.)* **2007**, *129*, 97−110.
(278) Koch, S.; de Wit, J. G.; Vos, I.; Birkner, J. P.; Gordiichuk, P.; Herrmann, A.; van Oijen, A. M.; Driessen, A. J. Lipids activate SecA for high affinity binding to the SecYEG complex. *J. Biol. Chem.* **2016**, *291*, 22534−22543.
(279) Morrissey, J. H.; Tajkhorshid, E.; Sligar, S. G.; Rienstra, C. M. Tissue factor/factor VIIa complex: role of the membrane surface. *Thromb. Res.* **2012**, *129*, S8−10.
(280) Gajsiewicz, J. M.; Morrissey, J. H. Structure-function relationship of the interaction between tissue factor and factor VIIa. *Semin. Thromb. Hemostasis* **2015**, *41*, 682−690.
(281) Zhang, X. X.; Chan, C. S.; Bao, H.; Fang, Y.; Foster, L. J.; Duong, F. Nanodiscs and SILAC-based mass spectrometry to identify a membrane protein interactome. *J. Proteome Res.* **2012**, *11*, 1454−1459.
(282) Schuler, M. A.; Denisov, I. G.; Sligar, S. G. Nanodiscs as a new tool to examine lipid-protein interactions. *Methods Mol. Biol.* **2013**, *974*, 415−433.
(283) Borch, J.; Torta, F.; Sligar, S. G.; Roepstorff, P. Nanodiscs for immobilization of lipid bilayers and membrane receptors: Kinetic analysis of cholera toxin binding to a glycolipid receptor. *Anal. Chem.* **2008**, *80*, 6245−6252.
(284) Borch, J.; Roepstorff, P.; Moeller-Jensen, J. Nanodisc-based co-immunoprecipitation for mass spectrometric identification of membrane-interacting proteins. *Mol. Cell. Proteomics* **2011**, *10*, O110.006775.
(285) Leney, A. C.; Fan, X.; Kitova, E. N.; Klassen, J. S. Nanodiscs and electrospray ionization mass spectrometry: A tool for screening glycolipids against proteins. *Anal. Chem.* **2014**, *86*, 5271−5277.
(286) Han, L.; Kitova, E. N.; Li, J.; Nikjah, S.; Lin, H.; Pluvinage, B.; Boraston, A. B.; Klassen, J. S. Protein-glycolipid interactions studied in vitro using ESI-MS and Nanodiscs: Insights into the mechanisms and energetics of binding. *Anal. Chem.* **2015**, *87*, 4888−4896.
(287) Wan, C.; Wu, B.; Song, Z.; Zhang, J.; Chu, H.; Wang, A.; Liu, Q.; Shi, Y.; Li, G.; Wang, J. Insights into the molecular recognition of the granuphilin C2A domain with PI(4,5)P2. *Chem. Phys. Lipids* **2015**, *186*, 61−67.
(288) Hein, C.; Henrich, E.; Orban, E.; Doetsch, V.; Bernhard, F. Hydrophobic supplements in cell-free systems: Designing artificial environments for membrane proteins. *Eng. Life Sci.* **2014**, *14*, 365−379.
(289) Baumann, A.; Kerruth, S.; Fitter, J.; Buldt, G.; Heberle, J.; Schlesinger, R.; Ataka, K. In-situ observation of membrane protein folding during cell-free expression. *PLoS One* **2016**, *11*, e0151051.
(290) Orelle, C.; Alvarez, F. J. D.; Oldham, M. L.; Orelle, A.; Wiley, T. E.; Chen, J.; Davidson, A. L. Dynamics of α-helical subdomain rotation in the intact maltose ATP-binding cassette transporter. *Proc. Natl. Acad. Sci. U. S. A.* **2010**, *107*, 20293−20298.
(291) Bartelli, N. L.; Hazelbauer, G. L. Differential backbone dynamics of companion helices in the extended helical coiled-coil domain of a bacterial chemoreceptor. *Protein Sci.* **2015**, *24*, 1764−1776.
(292) Bartelli, N. L.; Hazelbauer, G. L. Bacterial chemoreceptor dynamics: Helical stability in the cytoplasmic domain varies with functional segment and adaptational modification. *J. Mol. Biol.* **2016**, *428*, 3789−3804.

DOI: 10.1021/acs.chemrev.6b00690
Chem. Rev. 2017, 117, 4669−4713

(293) Dastvan, R.; Fischer, A. W.; Mishra, S.; Meiler, J.; Mchaourab, H. S. Protonation-dependent conformational dynamics of the multidrug transporter EmrE. *Proc. Natl. Acad. Sci. U. S. A.* **2016**, *113*, 1220−1225.
(294) Denisov, I. G.; Grinkova, Y. V.; Sligar, S. G. In *Spectroscopic Methods of Analysis: Methods and Protocols*; Bujalowski, W. M., Ed.; Springer Science: New York, 2012; Vol. *875*, pp. 375−391.
(295) Denisov, I. G.; Sligar, S. G. Cytochromes P 450 in nanodiscs. *Biochim. Biophys. Acta, Proteins Proteomics* **2011**, *1814*, 223−229.
(296) Luthra, A.; Denisov, I. G.; Sligar, S. G. Temperature derivative spectroscopy to monitor the autoxidation decay of cytochromes P450. *Anal. Chem.* **2011**, *83*, 5394−5399.
(297) Das, A.; Grinkova, Y. V.; Sligar, S. G. Redox potential control by drug binding to cytochrome P 450 3A4. *J. Am. Chem. Soc.* **2007**, *129*, 13778−13779.
(298) Das, A.; Sligar, S. G. Modulation of the cytochrome P450 reductase redox potential by the phospholipid bilayer. *Biochemistry* **2009**, *48*, 12104−12112.
(299) Baylon, J. L.; Lenov, I. L.; Sligar, S. G.; Tajkhorshid, E. Characterizing the membrane-bound state of cytochrome P450 3A4: Structure, depth of insertion, and orientation. *J. Am. Chem. Soc.* **2013**, *135*, 8542−8551.
(300) Vermaas, J. V.; Baylon, J. L.; Arcario, M. J.; Muller, M. P.; Wu, Z.; Pogorelov, T. V.; Tajkhorshid, E. Efficient exploration of membrane-associated phenomena at atomic resolution. *J. Membr. Biol.* **2015**, *248*, 563−582.
(301) Baylon, J. L.; Vermaas, J. V.; Muller, M. P.; Arcario, M. J.; Pogorelov, T. V.; Tajkhorshid, E. Atomic-level description of protein-lipid interactions using an accelerated membrane model. *Biochim. Biophys. Acta, Biomembr.* **2016**, *1858*, 1573−1583.
(302) Mayne, C. G.; Arcario, M. J.; Mahinthichaichan, P.; Baylon, J. L.; Vermaas, J. V.; Navidpour, L.; Wen, P. C.; Thangapandian, S.; Tajkhorshid, E. The cellular membrane as a mediator for small molecule interaction with membrane proteins. *Biochim. Biophys. Acta, Biomembr.* **2016**, *1858*, 2290−3204.
(303) McDougle, D. R.; Baylon, J. L.; Meling, D. D.; Kambalyal, A.; Grinkova, Y. V.; Hammernik, J.; Tajkhorshid, E.; Das, A. Incorporation of charged residues in the CYP2J2 F-G loop disrupts CYP2J2-lipid bilayer interactions. *Biochim. Biophys. Acta, Biomembr.* **2015**, *1848*, 2460−2470.
(304) Ranaghan, M. J.; Schwall, C. T.; Alder, N. N.; Birge, R. R. Green proteorhodopsin reconstituted into nanoscale phospholipid bilayers (nanodiscs) as photoactive monomers. *J. Am. Chem. Soc.* **2011**, *133*, 18318−18327.
(305) Tsukamoto, H.; Szundi, I.; Lewis, J. W.; Farrens, D. L.; Kliger, D. S. Rhodopsin in Nanodiscs has native membrane-like photointermediates. *Biochemistry* **2011**, *50*, 5086−5091.
(306) Tsukamoto, H.; Farrens, D. L. A constitutively activating mutation alters the dynamics and energetics of a key conformational change in a ligand-free G protein-coupled receptor. *J. Biol. Chem.* **2013**, *288*, 28207−28216.
(307) Yeh, V.; Hsin, Y.; Lee, T.-Y.; Chan, J. C. C.; Yu, T.-Y.; Chu, L.-K. Lipids influence the proton pump activity of photosynthetic protein embedded in Nanodiscs. *RSC Adv.* **2016**, *6*, 88300−88305.
(308) Näsvik Öjemyr, L.; von Ballmoos, C.; Gennis, R. B.; Sligar, S. G.; Brzezinski, P. Reconstitution of respiratory oxidases in membrane nanodiscs for investigation of proton-coupled electron transfer. *FEBS Lett.* **2012**, *586*, 640−645.
(309) Xu, L.; Ojemyr, L. N.; Bergstrand, J.; Brzezinski, P.; Widengren, J. Protonation dynamics on lipid Nanodiscs: Influence of the membrane surface area and external buffers. *Biophys. J.* **2016**, *110*, 1993−2003.
(310) Ojemyr, L.; Sanden, T.; Widengren, J.; Brzezinski, P. Lateral proton transfer between the membrane and a membrane protein. *Biochemistry* **2009**, *48*, 2173−2179.
(311) Periasamy, A.; Shadiac, N.; Amalraj, A.; Garajova, S.; Nagarajan, Y.; Waters, S.; Mertens, H. D. T.; Hrmova, M. Cell-free protein synthesis of membrane (1,3)-β-D-glucan (Curdlan) synthase: Co-translational insertion in liposomes and reconstitution in nanodiscs. *Biochim. Biophys. Acta, Biomembr.* **2013**, *1828*, 743−757.
(312) Maric, S.; Skar-Gislinge, N.; Midtgaard, S.; Arleth, L.; Thygesen Mikkel, B.; Schiller, J.; Frielinghaus, H.; Moulin, M.; Haertlein, M.; Forsyth, V. T.; et al. Stealth carriers for low-resolution structure determination of membrane proteins in solution. *Acta Crystallogr., Sect. D: Biol. Crystallogr.* **2014**, *70*, 317−328.
(313) Maric, S.; Thygesen, M. B.; Schiller, J.; Marek, M.; Moulin, M.; Haertlein, M.; Forsyth, V. T.; Bogdanov, M.; Dowhan, W.; Arleth, L.; et al. Biosynthetic preparation of selectively deuterated phosphatidylcholine in genetically modified Escherichia coli. *Appl. Microbiol. Biotechnol.* **2015**, *99*, 241−254.
(314) Baas, B. J.; Denisov, I. G.; Sligar, S. G. Homotropic cooperativity of monomeric cytochrome P450 3A4 in a nanoscale native bilayer environment. *Arch. Biochem. Biophys.* **2004**, *430*, 218−228.
(315) Wadsaeter, M.; Laursen, T.; Singha, A.; Hatzakis, N. S.; Stamou, D.; Barker, R.; Mortensen, K.; Feidenhans'l, R.; Moller, B. L.; Cardenas, M. Monitoring shifts in the conformation equilibrium of the membrane protein cytochrome P450 reductase (POR) in Nanodiscs. *J. Biol. Chem.* **2012**, *287*, 34596−34603.
(316) Imamoto, Y.; Kojima, K.; Oka, T.; Maeda, R.; Shichida, Y. Helical rearrangement of photoactivated rhodopsin in monomeric and dimeric forms probed by high-angle X-ray scattering. *Photochem. Photobiol. Sci.* **2015**, *14*, 1965−1973.
(317) Goricanec, D.; Stehle, R.; Egloff, P.; Grigoriu, S.; Pluckthun, A.; Wagner, G.; Hagn, F. Conformational dynamics of a G-protein alpha subunit is tightly regulated by nucleotide binding. *Proc. Natl. Acad. Sci. U. S. A.* **2016**, *113*, E3629−3638.
(318) Kiser, P. D.; Golczak, M.; Palczewski, K. Chemistry of the retinoid (visual) cycle. *Chem. Rev.* **2014**, *114*, 194−232.
(319) Latek, D.; Modzelewska, A.; Trzaskowski, B.; Palczewski, K.; Filipek, S. G protein-coupled receptors–recent advances. *Acta Biochim. Pol.* **2012**, *59*, 515−529.
(320) Ernst, O. P.; Lodowski, D. T.; Elstner, M.; Hegemann, P.; Brown, L. S.; Kandori, H. Microbial and animal rhodopsins: structures, functions, and molecular mechanisms. *Chem. Rev.* **2014**, *114*, 126−163.
(321) Ferre, S.; Casado, V.; Devi, L. A.; Filizola, M.; Jockers, R.; Lohse, M. J.; Milligan, G.; Pin, J. P.; Guitart, X. G protein-coupled receptor oligomerization revisited: functional and pharmacological perspectives. *Pharmacol. Rev.* **2014**, *66*, 413−434.
(322) Scarselli, M.; Annibale, P.; McCormick, P. J.; Kolachalam, S.; Aringhieri, S.; Radenovic, A.; Corsini, G. U.; Maggio, R. Revealing G-protein-coupled receptor oligomerization at the single-molecule level through a nanoscopic lens: methods, dynamics and biological function. *FEBS J.* **2016**, *283*, 1197−1217.
(323) Vischer, H. F.; Castro, M.; Pin, J. P. G Protein-coupled receptor multimers: A question still open despite the use of novel approaches. *Mol. Pharmacol.* **2015**, *88*, 561−571.
(324) Tsukamoto, H.; Sinha, A.; DeWitt, M.; Farrens, D. L. Monomeric rhodopsin is the minimal functional unit required for arrestin binding. *J. Mol. Biol.* **2010**, *399*, 501−511.
(325) Kim, M.; Vishnivetskiy, S. A.; Van Eps, N.; Alexander, N. S.; Cleghorn, W. M.; Zhan, X.; Hanson, S. M.; Morizumi, T.; Ernst, O. P.; Meiler, J.; et al. Conformation of receptor-bound visual arrestin. *Proc. Natl. Acad. Sci. U. S. A.* **2012**, *109*, 18407−18412.
(326) Li, M.; Hazelbauer, G. L. Selective allosteric coupling in core chemotaxis signaling complexes. *Proc. Natl. Acad. Sci. U. S. A.* **2014**, *111*, 15940−15945.
(327) Amin, D. N.; Hazelbauer, G. L. The chemoreceptor dimer is the unit of conformational coupling and transmembrane signaling. *J. Bacteriol.* **2010**, *192*, 1193−1200.
(328) Li, M.; Khursigara, C. M.; Subramaniam, S.; Hazelbauer, G. L. Chemotaxis kinase CheA is activated by three neighbouring chemoreceptor dimers as effectively as by receptor clusters. *Mol. Microbiol.* **2011**, *79*, 677−685.
(329) Li, M.; Hazelbauer, G. L. Core unit of chemotaxis signaling complexes. *Proc. Natl. Acad. Sci. U. S. A.* **2011**, *108*, 9390−9395.

DOI: 10.1021/acs.chemrev.6b00690
Chem. Rev. 2017, 117, 4669−4713

(330) Pandit, A.; Shirzad-Wasei, N.; Wlodarczyk, L. M.; van Roon, H.; Boekema, E. J.; Dekker, J. P.; de Grip, W. J. Assembly of the major light-harvesting Complex II in lipid Nanodiscs. *Biophys. J.* **2011**, *101*, 2507−2515.
(331) Natali, A.; Gruber, J. M.; Dietzel, L.; Stuart, M. C.; van Grondelle, R.; Croce, R. Light-harvesting complexes (LHCs) cluster spontaneously in membrane environment leading to shortening of their excited state lifetimes. *J. Biol. Chem.* **2016**, *291*, 16730−16739.
(332) Raschle, T.; Lin, C.; Jungmann, R.; Shih, W. M.; Wagner, G. Controlled co-reconstitution of multiple membrane proteins in lipid bilayer Nanodiscs using DNA as a scaffold. *ACS Chem. Biol.* **2015**, *10*, 2448−2454.
(333) Raschle, T.; Hiller, S.; Yu, T. Y.; Rice, A. J.; Walz, T.; Wagner, G. Structural and functional characterization of the integral membrane protein VDAC-1 in lipid bilayer Nanodiscs. *J. Am. Chem. Soc.* **2009**, *131*, 17777−17779.
(334) Fahr, A.; van Hoogevest, P.; May, S.; Bergstrand, N.; Leigh, M. L. S. Transfer of lipophilic drugs between liposomal membranes and biological interfaces: Consequences for drug delivery. *Eur. J. Pharm. Sci.* **2005**, *26*, 251−265.
(335) Gatlik-Landwojtowicz, E.; Aeaenismaa, P.; Seelig, A. Quantification and characterization of P-glycoprotein-substrate interactions. *Biochemistry* **2006**, *45*, 3020−3032.
(336) Yano, K.; Masaoka, Y.; Kataoka, M.; Sakuma, S.; Yamashita, S. Mechanisms of membrane transport of poorly soluble drugs: Role of micelles in oral absorption processes. *J. Pharm. Sci.* **2010**, *99*, 1336−1345.
(337) Zhang, Z.; Dai, C.; Bai, J.; Xu, G.; Liu, M.; Li, C. Ca(2+) modulating alpha-synuclein membrane transient interactions revealed by solution NMR spectroscopy. *Biochim. Biophys. Acta, Biomembr.* **2014**, *1838*, 853−858.
(338) Kobashigawa, Y.; Harada, K.; Yoshida, N.; Ogura, K.; Inagaki, F. Phosphoinositide-incorporated lipid-protein nanodiscs: A tool for studying protein-lipid interactions. *Anal. Biochem.* **2011**, *410*, 77−83.
(339) Yokogawa, M.; Kobashigawa, Y.; Yoshida, N.; Ogura, K.; Harada, K.; Inagaki, F. NMR analyses of the interaction between the FYVE domain of early endosome antigen 1 (EEA1) and phosphoinositide embedded in a lipid bilayer. *J. Biol. Chem.* **2012**, *287*, 34936−34945.
(340) Inagaki, S.; Ghirlando, R.; White, J. F.; Gvozdenovic-Jeremic, J.; Northup, J. K.; Grisshammer, R. Modulation of the interaction between neurotensin receptor NTS1 and Gq protein by lipid. *J. Mol. Biol.* **2012**, *417*, 95−111.
(341) Leitz, A. J.; Bayburt, T. H.; Barnakov, A. N.; Springer, B. A.; Sligar, S. G. Functional reconstitution of β2-adrenergic receptors utilizing self-assembling nanodisc technology. *BioTechniques* **2006**, *40*, 601−602 604,606,608,610,612..
(342) Whorton, M. R.; Bokoch, M. P.; Rasmussen, S. G.; Huang, B.; Zare, R. N.; Kobilka, B.; Sunahara, R. K. A monomeric G protein-coupled receptor isolated in a high-density lipoprotein particle efficiently activates its G protein. *Proc. Natl. Acad. Sci. U. S. A.* **2007**, *104*, 7682−7687.
(343) Kuszak, A. J.; Pitchiaya, S.; Anand, J. P.; Mosberg, H. I.; Walter, N. G.; Sunahara, R. K. Purification and functional reconstitution of monomeric mu-opioid receptors: allosteric modulation of agonist binding by Gi2. *J. Biol. Chem.* **2009**, *284*, 26732−26741.
(344) Calinski, D. M.; Edwald, E.; Sunahara, R. K. In *G Protein-Coupled Receptors: From Structure to Function. RCS Drug Discovery series*; Giraldo, J., Pin, J.-P., Eds.; Royal Society of Chemistry: London, 2011; Vol. *8*, pp. 179−196.
(345) Fiez-Vandal, C.; Leder, L.; Freuler, F.; Sykes, D.; Charlton, S. J.; Siehler, S.; Schopfer, U.; Duckely, M. HDL-like discs for assaying membrane proteins in drug discovery. *Biophys. Chem.* **2012**, *165−166*, 56−61.
(346) Nasr, M. L.; Singh, S. K. Radioligand binding to Nanodisc-reconstituted membrane transporters assessed by the scintillation proximity assay. *Biochemistry* **2014**, *53*, 4−6.
(347) Lee, C.-M.; He, C. H.; Nour, A. M.; Zhou, Y.; Ma, B.; Park, J. W.; Kim, K. H.; Cruz, C. D.; Sharma, L.; Nasr, M. L.; et al. IL-13Rα2 uses TMEM219 in Chitinase 3-like-1-induced signalling and effector responses. *Nat. Commun.* **2016**, *7*, 12752.
(348) Kawai, T.; Caaveiro, J. M.; Abe, R.; Katagiri, T.; Tsumoto, K. Catalytic activity of MsbA reconstituted in nanodisc particles is modulated by remote interactions with the bilayer. *FEBS Lett.* **2011**, *585*, 3533−3537.
(349) Bao, H.; Dalal, K.; Cytrynbaum, E.; Duong, F. Sequential action of MalE and maltose allows coupling ATP hydrolysis to translocation in the MalFGK2 transporter. *J. Biol. Chem.* **2015**, *290*, 25452−25460.
(350) Glueck, J. M.; Koenig, B. W.; Willbold, D. Nanodiscs allow the use of integral membrane proteins as analytes in surface plasmon resonance studies. *Anal. Biochem.* **2011**, *408*, 46−52.
(351) Goluch, E. D.; Shaw, A. W.; Sligar, S. G.; Liu, C. Microfluidic patterning of nanodisc lipid bilayers and multiplexed analysis of protein interaction. *Lab Chip* **2008**, *8*, 1723−1728.
(352) Proverbio, D.; Roos, C.; Beyermann, M.; Orban, E.; Dotsch, V.; Bernhard, F. Functional properties of cell-free expressed human endothelin A and endothelin B receptors in artificial membrane environments. *Biochim. Biophys. Acta, Biomembr.* **2013**, *1828*, 2182−2192.
(353) Tavoosi, N.; Smith, S. A.; Davis-Harrison, R. L.; Morrissey, J. H. Factor VII and Protein C are phosphatidic acid-binding proteins. *Biochemistry* **2013**, *52*, 5545−5552.
(354) Wu, Z. C.; de Keyzer, J.; Kedrov, A.; Driessen, A. J. M. Competitive binding of the SecA ATPase and ribosomes to the SecYEG translocon. *J. Biol. Chem.* **2012**, *287*, 7885−7895.
(355) Das, A.; Zhao, J.; Schatz, G. C.; Sligar, S. G.; Van Duyne, R. P. Screening of type I and II drug binding to human cytochrome P450−3A4 in nanodiscs by localized surface plasmon resonance spectroscopy. *Anal. Chem.* **2009**, *81*, 3754−3759.
(356) Plucinski, L.; Ranjan Gartia, M.; Arnold, W. R.; Ameen, A.; Chang, T.-W.; Hsiao, A.; Logan Liu, G.; Das, A. Substrate binding to cytochrome P450−2J2 in Nanodiscs detected by nanoplasmonic Lycurgus cup arrays. *Biosens. Bioelectron.* **2016**, *75*, 337−346.
(357) Trahey, M.; Li, M. J.; Kwon, H.; Woodahl, E. L.; McClary, W. D.; Atkins, W. M. Applications of lipid Nanodiscs for the study of membrane proteins by surface plasmon resonance. *Curr. Protoc. Protein Sci.* **2015**, *81*, 29.13.1−29.13.16.
(358) Jang, H.; Abraham, S. J.; Chavan, T. S.; Hitchinson, B.; Khavrutskii, L.; Tarasova, N. I.; Nussinov, R.; Gaponenko, V. Mechanisms of membrane binding of small GTPase K-Ras4B farnesylated hypervariable region. *J. Biol. Chem.* **2015**, *290*, 9465−9477.
(359) Haynes, C. L.; Van Duyne, R. P. Nanosphere lithography: A versatile nanofabrication tool for studies of size-dependent nanoparticle optics. *J. Phys. Chem. B* **2001**, *105*, 5599−5611.
(360) Willets, K. A.; Van Duyne, R. P. Localized surface plasmon resonance spectroscopy and sensing. *Annu. Rev. Phys. Chem.* **2007**, *58*, 267−297.
(361) Anker, J. N.; Hall, W. P.; Lyandres, O.; Shah, N. C.; Zhao, J.; Van Duyne, R. P. Biosensing with plasmonic nanosensors. *Nat. Mater.* **2008**, *7*, 442−453.
(362) Chen, H.; Schatz, G. C.; Ratner, M. A. Experimental and theoretical studies of plasmon-molecule interactions. *Rep. Prog. Phys.* **2012**, *75*, 096402.
(363) Sloan, C. D.; Marty, M. T.; Sligar, S. G.; Bailey, R. C. Interfacing lipid bilayer nanodiscs and silicon photonic sensor arrays for multiplexed protein-lipid and protein-membrane protein interaction screening. *Anal. Chem.* **2013**, *85*, 2970−2976.
(364) Wade, J. H.; Bailey, R. C. Applications of optical microcavity resonators in analytical chemistry. *Annu. Rev. Anal. Chem.* **2016**, *9*, 1−25.
(365) Morrissey, J. H.; Pureza, V.; Davis-Harrison, R. L.; Sligar, S. G.; Ohkubo, Y. Z.; Tajkhorshid, E. Blood clotting reactions on nanoscale phospholipid bilayers. *Thromb. Res.* **2008**, *122*, S23−S26.
(366) Nasr, M. L.; Shi, X.; Bowman, A. L.; Johnson, M.; Zvonok, N.; Janero, D. R.; Vemuri, V. K.; Wales, T. E.; Engen, J. R.; Makriyannis, A. Membrane phospholipid bilayer as a determinant of mono-

DOI: 10.1021/acs.chemrev.6b00690
Chem. Rev. 2017, 117, 4669−4713

acylglycerol lipase kinetic profile and conformational repertoire. *Protein Sci.* **2013**, *22*, 774−787.
(367) Marty, M. T.; Das, A.; Sligar, S. G. Ultra-thin layer MALDI mass spectrometry of membrane proteins in nanodiscs. *Anal. Bioanal. Chem.* **2012**, *402*, 721−729.
(368) Marin, V. L.; Bayburt, T. H.; Sligar, S. G.; Mrksich, M. Functional assays of membrane-bound proteins with SAMDI-TOF mass spectrometry. *Angew. Chem., Int. Ed.* **2007**, *46*, 8796−8798.
(369) Pikuleva, I. A.; Mast, N.; Liao, W. L.; Turko, I. V. Studies of membrane topology of mitochondrial cholesterol hydroxylases CYPs 27A1 and 11A1. *Lipids* **2008**, *43*, 1127−1132.
(370) Mast, N.; Liao, W. L.; Pikuleva, I. A.; Turko, I. V. Combined use of mass spectrometry and heterologous expression for identification of membrane-interacting peptides in cytochrome P450 46A1 and NADPH-cytochrome P450 oxidoreductase. *Arch. Biochem. Biophys.* **2009**, *483*, 81−89.
(371) Mustafa, G.; Nandekar, P. P.; Yu, X.; Wade, R. C. On the application of the MARTINI coarse-grained model to immersion of a protein in a phospholipid bilayer. *J. Chem. Phys.* **2015**, *143*, 243139.
(372) Berka, K.; Paloncyova, M.; Anzenbacher, P.; Otyepka, M. Behavior of human cytochromes P450 on lipid membranes. *J. Phys. Chem. B* **2013**, *117*, 11556−11564.
(373) Denisov, I. G.; Shih, A. Y.; Sligar, S. G. Structural differences between soluble and membrane bound cytochrome P450s. *J. Inorg. Biochem.* **2012**, *108*, 150−158.
(374) Zhang, H.; Hamdane, D.; Im, S. C.; Waskell, L. Cytochrome b5 inhibits electron transfer from NADPH-cytochrome P450 reductase to ferric cytochrome P450 2B4. *J. Biol. Chem.* **2007**, *283*, 5217−5225.
(375) Pandey, M. K.; Vivekanandan, S.; Ahuja, S.; Huang, R.; Im, S. C.; Waskell, L.; Ramamoorthy, A. Cytochrome-P450-cytochrome-b5 interaction in a membrane environment changes 15N chemical shift anisotropy tensors. *J. Phys. Chem. B* **2013**, *117*, 13851−13860.
(376) Zhang, M.; Huang, R.; Im, S. C.; Waskell, L.; Ramamoorthy, A. Effects of membrane mimetics on cytochrome P450-cytochrome b5 interactions characterized by NMR spectroscopy. *J. Biol. Chem.* **2015**, *290*, 12705−12718.
(377) Waskell, L.; Kim, J.-J. P. In *Cytochrome P450: Structure, Mechanism, and Biochemistry*; Ortiz de Montallano, P. R., Ed.; Springer International: Hedielberg, 2015, pp. 33−68.
(378) Imaoka, S.; Imai, Y.; Shimada, T.; Funae, Y. Role of phospholipids in reconstituted cytochrome P 450 3A form and mechanism of their activation of catalytic activity. *Biochemistry* **1992**, *31*, 6063−6069.
(379) Yamazaki, H.; Gillam, E. M. J.; Dong, M.-S.; Johnson, W. W.; Guengerich, F. P.; Shimada, T. Reconstitution of recombinant cytochrome P450 2C10(2C9) and comparison with cytochrome P450 3A4 and other forms: effects of cytochrome P450-P450 and cytochrome P450-b5 interactions. *Arch. Biochem. Biophys.* **1997**, *342*, 329−337.
(380) Coon, M. J. Cytochrome P450: Nature's most versatile biological catalyst. *Annu. Rev. Pharmacol. Toxicol.* **2005**, *45*, 1−25.
(381) Reed, J. R.; Brignac-Huber, L. M.; Backes, W. L. Physical incorporation of NADPH-cytochrome P450 reductase and cytochrome P450 into phospholipid vesicles using glycocholate and Bio-Beads. *Drug Metab. Dispos.* **2007**, *36*, 582−588.
(382) Reed, J. R.; Eyer, M.; Backes, W. L. Functional interactions between cytochromes P450 1A2 and 2B4 require both enzymes to reside in the same phospholipid vesicle: evidence for physical complex formation. *J. Biol. Chem.* **2010**, *285*, 8942−8952.
(383) Brignac-Huber, L. M.; Reed, J. R.; Eyer, M. K.; Backes, W. L. Relationship between CYP1A2 localization and lipid microdomain formation as a function of lipid composition. *Drug Metab. Dispos.* **2013**, *41*, 1896−1905.
(384) Davydov, D. R.; Fernando, H.; Baas, B. J.; Sligar, S. G.; Halpert, J. R. Kinetics of dithionite-dependent reduction of cytochrome P450 3A4: Heterogeneity of the enzyme caused by Its oligomerization. *Biochemistry* **2005**, *44*, 13902−13913.
(385) Denisov, I. G.; Baas, B. J.; Grinkova, Y. V.; Sligar, S. G. Cooperativity in cytochrome P450 3A4 - Linkages in substrate binding, spin state, uncoupling, and product formation. *J. Biol. Chem.* **2006**, *282*, 7066−7076.
(386) Denisov, I. G.; Grinkova, Y. V.; Baas, B. J.; Sligar, S. G. The ferrous-dioxygen intermediate in human cytochrome P450 3A4 - Substrate dependence of formation and decay kinetics. *J. Biol. Chem.* **2006**, *281*, 23313−23318.
(387) Denisov, I. G.; Grinkova, Y. V.; McLean, M. A.; Sligar, S. G. The one-electron autoxidation of human cytochrome P450 3A4. *J. Biol. Chem.* **2007**, *282*, 26865−26873.
(388) Frank, D. J.; Denisov, I. G.; Sligar, S. G. Mixing apples and oranges: Analysis of heterotropic cooperativity in cytochrome P450 3A4. *Arch. Biochem. Biophys.* **2009**, *488*, 146−152.
(389) Frank, D. J.; Denisov, I. G.; Sligar, S. G. Analysis of heterotropic cooperativity in cytochrome P450 3A4 using α-naphthoflavone and testosterone. *J. Biol. Chem.* **2011**, *286*, 5540−5545.
(390) Grinkova, Y. V.; Denisov, I. G.; Sligar, S. G. Functional reconstitution of monomeric CYP3A4 with multiple cytochrome P450 reductase molecules in Nanodiscs. *Biochem. Biophys. Res. Commun.* **2010**, *398*, 194−198.
(391) Kijac, A. Z.; Li, Y.; Sligar, S. G.; Rienstra, C. M. Magic-angle spinning solid-state NMR spectroscopy of Nanodisc-embedded human CYP3A4. *Biochemistry* **2007**, *46*, 13696−13703.
(392) Nath, A.; Grinkova, Y. V.; Sligar, S. G.; Atkins, W. M. Ligand binding to cytochrome P450 3A4 in phospholipid bilayer Nanodiscs: The effect of model membranes. *J. Biol. Chem.* **2007**, *282*, 28309−28320.
(393) Harlow, G. R.; Halpert, J. R. Analysis of human cytochrome P450 3A4 cooperativity: construction and characterization of a site-directed mutant that displays hyperbolic steroid hydroxylation kinetics. *Proc. Natl. Acad. Sci. U. S. A.* **1998**, *95*, 6636−6641.
(394) Davydov, D. R.; Halpert, J. R.; Renaud, J. P.; Hui Bon Hoa, G. Conformational heterogeneity of cytochrome P450 3A4 revealed by high pressure spectroscopy. *Biochem. Biophys. Res. Commun.* **2003**, *312*, 121−130.
(395) Roberts, A. G.; Campbell, A. P.; Atkins, W. M. The thermodynamic landscape of testosterone binding to cytochrome P450 3A4: ligand binding and spin state equilibria. *Biochemistry* **2005**, *44*, 1353−1366.
(396) Tsalkova, T. N.; Davydova, N. Y.; Halpert, J. R.; Davydov, D. R. Mechanism of interactions of alpha-naphthoflavone with cytochrome P450 3A4 explored with an engineered enzyme bearing a fluorescent probe. *Biochemistry* **2007**, *46*, 106−119.
(397) Denisov, I. G.; Mak, P. J.; Grinkova, Y. V.; Bastien, D.; Bérubé, G.; Sligar, S. G.; Kincaid, J. R. The use of isomeric testosterone dimers to explore allosteric effects in substrate binding to cytochrome P450 CYP3A4. *J. Inorg. Biochem.* **2016**, *158*, 77−85.
(398) Denisov, I. G.; Grinkova, Y. V.; Baylon, J. L.; Tajkhorshid, E.; Sligar, S. G. Mechanism of drug-drug interactions mediated by human cytochrome P450 CYP3A4 monomer. *Biochemistry* **2015**, *54*, 2227−2239.
(399) Isin, E. M.; Guengerich, F. P. Kinetics and thermodynamics of ligand binding by cytochrome P450 3A4. *J. Biol. Chem.* **2006**, *281*, 9127−9136.
(400) Sevrioukova, I. F.; Poulos, T. L. Structural and mechanistic insights into the interaction of cytochrome P450 3A4 with bromoergocryptine, a type I ligand. *J. Biol. Chem.* **2012**, *287*, 3510−3517.
(401) Sligar, S. G. Coupling of spin, substrate, and redox equilibria in cytochrome P450. *Biochemistry* **1976**, *15*, 5399−5406.
(402) Denisov, I. G.; Sligar, S. G. In *Handbook of Porphyrin Science*; Kadish, K. M., Smith, K. M., Guilard, R., Eds.; World Scientific: Hoboken, NJ, 2010; Vol. *5*, pp. 165−201.
(403) Makris, T. M.; Denisov, I. G.; Schlichting, I.; Sligar, S. G. In *Cytochrome P450: Structure, Function, Genetics*, 3rd ed.; Ortiz de Montellano, P. R., Ed.; Kluwer Academic/Plenum Publishers: New York, 2004, pp. 149−182.

DOI: 10.1021/acs.chemrev.6b00690
Chem. Rev. 2017, 117, 4669−4713

(404) Fleming, B. D.; Johnson, D. L.; Bond, A. M.; Martin, L. L. Recent progress in cytochrome P450 enzyme electrochemistry. *Expert Opin. Drug Metab. Toxicol.* **2006**, *2*, 581−589.
(405) Johnson, D. L.; Conley, A. J.; Martin, L. L. Direct electrochemistry of human, bovine and porcine cytochrome P450c17. *J. Mol. Endocrinol.* **2006**, *36*, 349−359.
(406) Fisher, M. T.; Scarlata, S. F.; Sligar, S. G. High-pressure investigations of cytochrome P-450 spin and substrate binding equilibria. *Arch. Biochem. Biophys.* **1985**, *240*, 456−463.
(407) Treuheit, N. A.; Redhair, M.; Kwon, H.; McClary, W. D.; Guttman, M.; Sumida, J. P.; Atkins, W. M. Membrane interactions, ligand-dependent dynamics, and stability of cytochrome P4503A4 in lipid Nanodiscs. *Biochemistry* **2016**, *55*, 1058−1069.
(408) Liao, W. L.; Dodder, N. G.; Mast, N.; Pikuleva, I. A.; Turko, I. V. Steroid and protein ligand binding to cytochrome P450 46A1 as assessed by hydrogen-deuterium exchange and mass spectrometry. *Biochemistry* **2009**, *48*, 4150−4158.
(409) Anderson, K. W.; Mast, N.; Hudgens, J. W.; Lin, J. B.; Turko, I. V.; Pikuleva, I. A. Mapping of the allosteric site in cholesterol hydroxylase CYP46A1 for Efavirenz, a drug that stimulates enzyme activity. *J. Biol. Chem.* **2016**, *291*, 11876−11886.
(410) Di Nardo, G.; Breitner, M.; Sadeghi, S. J.; Castrignano, S.; Mei, G.; Di Venere, A.; Nicolai, E.; Allegra, P.; Gilardi, G. Dynamics and flexibility of human aromatase probed by FTIR and time resolved fluorescence spectroscopy. *PLoS One* **2013**, *8*, e82118.
(411) Wilderman, P. R.; Halpert, J. R. Plasticity of CYP2B enzymes: structural and solution biophysical methods. *Curr. Drug Metab.* **2012**, *13*, 167−176.
(412) Wilderman, P. R.; Shah, M. B.; Liu, T.; Li, S.; Hsu, S.; Roberts, A. G.; Goodlett, D. R.; Zhang, Q.; Woods, V. L., Jr.; Stout, C. D.; et al. Plasticity of cytochrome P450 2B4 as investigated by hydrogen-deuterium exchange mass spectrometry and X-ray crystallography. *J. Biol. Chem.* **2010**, *285*, 38602−38611.
(413) Hamuro, Y.; Molnar, K. S.; Coales, S. J.; OuYang, B.; Simorellis, A. K.; Pochapsky, T. C. Hydrogen-deuterium exchange mass spectrometry for investigation of backbone dynamics of oxidized and reduced cytochrome P450cam. *J. Inorg. Biochem.* **2008**, *102*, 364−370.
(414) Pochapsky, S. S.; Dang, M.; OuYang, B.; Simorellis, A. K.; Pochapsky, T. C. Redox-dependent dynamics in cytochrome P450cam. *Biochemistry* **2009**, *48*, 4254−4261.
(415) McDougle, D. R.; Palaria, A.; Magnetta, E.; Meling, D. D.; Das, A. Functional studies of N-terminally modified CYP2J2 epoxygenase in model lipid bilayers. *Protein Sci.* **2013**, *22*, 964−979.
(416) McDougle, D. R.; Kambalyal, A.; Meling, D. D.; Das, A. Endocannabinoids anandamide and 2-arachidonoylglycerol are substrates for human CYP2J2 epoxygenase. *J. Pharmacol. Exp. Ther.* **2014**, *351*, 616−627.
(417) Meling, D. D.; McDougle, D. R.; Das, A. CYP2J2 epoxygenase membrane anchor plays an important role in facilitating electron transfer from CPR. *J. Inorg. Biochem.* **2015**, *142*, 47−53.
(418) Meling, D. D.; Zelasko, S.; Kambalyal, A.; Roy, J.; Das, A. Functional role of the conserved I-helix residue I346 in CYP5A1-Nanodiscs. *Biophys. Chem.* **2015**, *200*−*201*, 34−40.
(419) Das, A.; Varma, S. S.; Mularczyk, C.; Meling, D. D. Functional investigations of thromboxane synthase (CYP5A1) in lipid bilayers of Nanodiscs. *ChemBioChem* **2014**, *15*, 892−899.
(420) Roy, J.; Adili, R.; Kulmacz, R.; Holinstat, M.; Das, A. Development of poly unsaturated fatty acid derivatives of aspirin for inhibition of platelet function. *J. Pharmacol. Exp. Ther.* **2016**, *359*, 134−141.
(421) Denisov, I. G.; Sligar, S. G. In *Cytochrome P450: Structure, Mechanism and Biochemistry*, 4th ed.; Ortiz de Montellano, P. R., Ed.; Springer International Publishing: Berlin, 2015; Vol. *1*, pp. 69−109.
(422) Davydov, R.; Gilep, A. A.; Strushkevich, N. V.; Usanov, S. A.; Hoffman, B. M. Compound I is the reactive intermediate in the first monooxygenation step during conversion of cholesterol to pregnenolone by cytochrome P450scc: EPR/ENDOR/cryoreduction/ annealing studies. *J. Am. Chem. Soc.* **2012**, *134*, 17149−17156.
(423) Davydov, R.; Im, S.; Shanmugam, M.; Gunderson, W. A.; Pearl, N. M.; Hoffman, B. M.; Waskell, L. Role of the proximal cysteine hydrogen bonding interaction in cytochrome P450 2B4 studied by cryoreduction, electron paramagnetic resonance, and electron-nuclear double resonance spectroscopy. *Biochemistry* **2016**, *55*, 869−883.
(424) Davydov, R.; Razeghifard, R.; Im, S. C.; Waskell, L.; Hoffman, B. M. Characterization of the microsomal cytochrome P450 2B4 O2 activation intermediates by cryoreduction and electron paramagnetic resonance. *Biochemistry* **2008**, *47*, 9661−9666.
(425) Davydov, R.; Strushkevich, N.; Smil, D.; Yantsevich, A.; Gilep, A.; Usanov, S.; Hoffman, B. M. Evidence that Compound I is the active species in both the hydroxylase and lyase steps by which P450scc converts cholesterol to pregnenolone: EPR/ENDOR/ cryoreduction/annealing studies. *Biochemistry* **2015**, *54*, 7089−7097.
(426) Akhtar, M.; Wright, J. N.; Lee-Robichaud, P. A review of mechanistic studies on aromatase (CYP19) and 17alpha-hydroxylase-17,20-lyase (CYP17). *J. Steroid Biochem. Mol. Biol.* **2011**, *125*, 2−12.
(427) Auchus, R. J.; Miller, W. L. In *Cytochrome P450: Structure, Mechanism and Biochemistry*; Ortiz de Montellano, P. R., Ed.; Springer International Publishing: Berlin, 2015; Vol. *2*.
(428) Akhtar, M.; Wright, J. N. Acyl-carbon bond cleaving cytochrome P450 enzymes: CYP17A1, CYP19A1 and CYP51A1. *Adv. Exp. Med. Biol.* **2015**, *851*, 107−130.
(429) Lee-Robichaud, P.; Shyadehi, A. Z.; Wright, J. N.; Akhtar, M. E.; Akhtar, M. Mechanistic kinship between hydroxylation and desaturation reactions: acyl-carbon bond cleavage promoted by pig and human CYP17 (P-450(17)alpha; 17 alpha-hydroxylase-17,20-lyase). *Biochemistry* **1995**, *34*, 14104−14113.
(430) Davydov, R.; Hoffman, B. M. Active intermediates in heme monooxygenase reactions as revealed by cryoreduction/annealing, EPR/ENDOR studies. *Arch. Biochem. Biophys.* **2011**, *507*, 36−43.
(431) Denisov, I. G. In *Physical Inorganic Chemistry: Principles, Methods, and Models*; Bakac, A., Ed.; John Wiley & Sons, Inc.: New York, 2010, pp. 109−142.
(432) Denisov, I. G.; Makris, T. M.; Sligar, S. G.; Schlichting, I. Structure and chemistry of cytochrome P 450. *Chem. Rev.* **2005**, *105*, 2253−2277.
(433) Isin, E. M.; Guengerich, F. P. Multiple sequential steps involved in the binding of inhibitors to cytochrome P450 3A4. *J. Biol. Chem.* **2006**, *282*, 6863−6874.
(434) Isin, E. M.; Guengerich, F. P. Substrate binding to cytochromes P450. *Anal. Bioanal. Chem.* **2008**, *392*, 1019−1030.
(435) Davydov, D. R.; Sineva, E. V.; Sistla, S.; Davydova, N. Y.; Frank, D. J.; Sligar, S. G.; Halpert, J. R. Electron transfer in the complex of membrane-bound human cytochrome P450 3A4 with the flavin domain of P450BM-3: The effect of oligomerization of the heme protein and intermittent modulation of the spin equilibrium. *Biochim. Biophys. Acta, Bioenerg.* **2010**, *1797*, 378−390.
(436) Haque, M. M.; Tejero, J.; Bayachou, M.; Wang, Z. Q.; Fadlalla, M.; Stuehr, D. J. Thermodynamic characterization of five key kinetic parameters that define neuronal nitric oxide synthase catalysis. *FEBS J.* **2013**, *280*, 4439−4453.
(437) Douzou, P. Cryoenzymology. *Cryobiology* **1983**, *20*, 625−635.
(438) Douzou, P.; Petsko, G. A. Proteins at work: "stop-action" pictures at subzero temperatures. *Adv. Protein Chem.* **1984**, *36*, 245−361.
(439) Denisov, I. G.; Makris, T. M.; Sligar, S. G. Cryoradiolysis for the study of P450 reaction intermediates. *Methods Enzymol.* **2002**, *357*, 103−115.
(440) Denisov, I. G.; Dawson, J. H.; Hager, L. P.; Sligar, S. G. The ferric-hydroperoxo complex of chloroperoxidase. *Biochem. Biophys. Res. Commun.* **2007**, *363*, 954−958.
(441) Nienhaus, K.; Nienhaus, G. U. Ligand dynamics in heme proteins observed by Fourier transform infrared-temperature derivative spectroscopy. *Biochim. Biophys. Acta, Proteins Proteomics* **2011**, *1814*, 1030−1041.
(442) Berendzen, J.; Braunstein, D. Temperature-derivative spectroscopy: a tool for protein dynamics. *Proc. Natl. Acad. Sci. U. S. A.* **1990**, *87*, 1−5.

DOI: 10.1021/acs.chemrev.6b00690
Chem. Rev. 2017, 117, 4669−4713

(443) Gantt, S. L.; Denisov, I. G.; Grinkova, Y. V.; Sligar, S. G. The critical iron-oxygen intermediate in human aromatase. *Biochem. Biophys. Res. Commun.* **2009**, *387*, 169−173.
(444) Davydov, R.; Laryukhin, M.; Ledbetter-Rogers, A.; Sono, M.; Dawson, J. H.; Hoffman, B. M. Electron paramagnetic resonance and electron-nuclear double resonance studies of the reactions of cryogenerated hydroperoxoferric-hemoprotein intermediates. *Biochemistry* **2014**, *53*, 4894−4903.
(445) Davydov, R.; Makris, T. M.; Kofman, V.; Werst, D. E.; Sligar, S. G.; Hoffman, B. M. Hydroxylation of camphor by reduced oxy-cytochrome P450cam: mechanistic implications of EPR and ENDOR studies of catalytic intermediates in native and mutant enzymes. *J. Am. Chem. Soc.* **2001**, *123*, 1403−1415.
(446) Davydov, R.; Perera, R.; Jin, S.; Yang, T. C.; Bryson, T. A.; Sono, M.; Dawson, J. H.; Hoffman, B. M. Substrate modulation of the properties and reactivity of the oxy-ferrous and hydroperoxo-ferric intermediates of cytochrome P450cam as shown by cryoreduction-EPR/ENDOR spectroscopy. *J. Am. Chem. Soc.* **2005**, *127*, 1403−1413.
(447) Davydov, R. M.; McLaughlin, M. P.; Bill, E.; Hoffman, B. M.; Holland, P. L. Generation of high-spin iron(I) in a protein environment using cryoreduction. *Inorg. Chem.* **2013**, *52*, 7323−7325.
(448) Makris, T. M.; Davydov, R.; Denisov, I. G.; Hoffman, B. M.; Sligar, S. G. Mechanistic enzymology of oxygen activation by the cytochromes P450. *Drug Metab. Rev.* **2002**, *34*, 691−708.
(449) Ahuja, S.; Jahr, N.; Im, S. C.; Vivekanandan, S.; Popovych, N.; Le Clair, S. V.; Huang, R.; Soong, R.; Xu, J.; Yamamoto, K.; et al. A model of the membrane-bound cytochrome b5-cytochrome P450 complex from NMR and mutagenesis data. *J. Biol. Chem.* **2013**, *288*, 22080−22095.
(450) Biggs, B. W.; Rouck, J. E.; Kambalyal, A.; Arnold, W.; Lim, C. G.; De Mey, M.; O'Neil-Johnson, M.; Starks, C. M.; Das, A.; Ajikumar, P. K. Orthogonal assays clarify the oxidative biochemistry of Taxol P450 CYP725A4. *ACS Chem. Biol.* **2016**, *11*, 1445−1451.
(451) Laursen, T.; Naur, P.; Moller, B. L. Amphipol trapping of a functional CYP system. *Biotechnol. Appl. Biochem.* **2013**, *60*, 119−127.
(452) Nielsen, K. A.; Tattersall, D. B.; Jones, P. R.; Moller, B. L. Metabolon formation in dhurrin biosynthesis. *Phytochemistry* **2008**, *69*, 88−98.
(453) Bavishi, K.; Laursen, T.; Martinez, K. L.; Moller, B. L.; Della Pia, E. A. Application of nanodisc technology for direct electrochemical investigation of plant cytochrome P450s and their NADPH P450 oxidoreductase. *Sci. Rep.* **2016**, *6*, 29459.
(454) Duan, H.; Schuler, M. A. Heterologous expression and strategies for encapsulation of membrane-localized plant P450s. *Phytochem. Rev.* **2006**, *5*, 507−523.
(455) Cruz, F.; Edmondson, D. E. Kinetic properties of recombinant MAO-A on incorporation into phospholipid nanodisks. *J. Neural Transm.* **2007**, *114*, 699−702.
(456) Seidel, S. A.; Dijkman, P. M.; Lea, W. A.; van den Bogaart, G.; Jerabek-Willemsen, M.; Lazic, A.; Joseph, J. S.; Srinivasan, P.; Baaske, P.; Simeonov, A.; et al. Microscale thermophoresis quantifies biomolecular interactions under previously challenging conditions. *Methods* **2013**, *59*, 301−315.
(457) Seidel, S. A.; Wienken, C. J.; Geissler, S.; Jerabek-Willemsen, M.; Duhr, S.; Reiter, A.; Trauner, D.; Braun, D.; Baaske, P. Label-free microscale thermophoresis discriminates sites and affinity of protein-ligand binding. *Angew. Chem., Int. Ed.* **2012**, *51*, 10656−10659.
(458) Duhr, S.; Braun, D. Why molecules move along a temperature gradient. *Proc. Natl. Acad. Sci. U. S. A.* **2006**, *103*, 19678−19682.
(459) Denisov, I. G.; Frank, D. J.; Sligar, S. G. Cooperative properties of cytochromes P450. *Pharmacol. Ther.* **2009**, *124*, 151−167.
(460) Denisov, I. G.; Sligar, S. G. A novel type of allosteric regulation: functional cooperativity in monomeric proteins. *Arch. Biochem. Biophys.* **2012**, *519*, 91−102.
(461) Sligar, S. G.; Denisov, I. G. Understanding cooperativity in Human P450 mediated drug-drug interactions. *Drug Metab. Rev.* **2007**, *39*, 567−579.
(462) Khatri, Y.; Gregory, M. C.; Grinkova, Y. V.; Denisov, I. G.; Sligar, S. G. Active site proton delivery and the lyase activity of human CYP17A1. *Biochem. Biophys. Res. Commun.* **2014**, *443*, 179−184.
(463) Springer, C. L.; Huntoon, H. P.; Peersen, O. B. Polyprotein context regulates the activity of poliovirus 2CATPase bound to bilayer Nanodiscs. *J. Virol.* **2013**, *87*, 5994−6004.
(464) Abdine, A.; Park, K. H.; Warschawski, D. E. Cell-free membrane protein expression for solid-state NMR. *Methods Mol. Biol.* **2012**, *831*, 85−109.
(465) Rues, R. B.; Orban, E.; Dotsch, V.; Bernhard, F. Cell-free expression of G-protein coupled receptors: new pipelines for challenging targets. *Biol. Chem.* **2014**, *395*, 1425−1434.
(466) Li, B.; Makino, S. I.; Beebe, E. T.; Urano, D.; Aceti, D. J.; Misenheimer, T. M.; Peters, J.; Fox, B. G.; Jones, A. M. Cell-free translation and purification of Arabidopsis thaliana regulator of G signaling 1 protein. *Protein Expression Purif.* **2016**, *126*, 33−41.
(467) Lyukmanova, E. N.; Shenkarev, Z. O.; Khabibullina, N. F.; Kopeina, G. S.; Shulepko, M. A.; Paramonov, A. S.; Mineev, K. S.; Tikhonov, R. V.; Shingarova, L. N.; Petrovskaya, L. E.; et al. Lipid-protein nanodiscs for cell-free production of integral membrane proteins in a soluble and folded state: Comparison with detergent micelles, bicelles and liposomes. *Biochim. Biophys. Acta, Biomembr.* **2012**, *1818*, 349−358.
(468) Bernhard, F.; Henrich, E.; Maertens, B. Obtaining functional membrane proteins through optimization of lipid environment in nanodiscs. *BIOspektrum* **2015**, *21*, 640−642.
(469) Johnson, P. J. M.; Halpin, A.; Morizumi, T.; Brown, L. S.; Prokhorenko, V. I.; Ernst, O. P.; Dwayne Miller, R. J. The photocycle and ultrafast vibrational dynamics of bacteriorhodopsin in lipid nanodiscs. *Phys. Chem. Chem. Phys.* **2014**, *16*, 21310−21320.
(470) Lai, G.; Renthal, R. Integral membrane protein fragment recombination after transfer from nanolipoprotein particles to bicelles. *Biochemistry* **2013**, *52*, 9405−9412.
(471) Petrache, A. I.; Machin, D. C.; Williamson, D. J.; Webb, M. E.; Beales, P. A. Sortase-mediated labelling of lipid nanodiscs for cellular tracing. *Mol. BioSyst.* **2016**, *12*, 1760−1763.
(472) Carney, C. E.; Lenov, I. L.; Baker, C. J.; MacRenaris, K. W.; Eckermann, A. L.; Sligar, S. G.; Meade, T. J. Nanodiscs as a modular platform for multimodal MR-optical imaging. *Bioconjugate Chem.* **2015**, *26*, 899−905.
(473) Skajaa, T.; Cormode, D. P.; Falk, E.; Mulder, W. J.; Fisher, E. A.; Fayad, Z. A. High-density lipoprotein-based contrast agents for multimodal imaging of atherosclerosis. *Arterioscler., Thromb., Vasc. Biol.* **2010**, *30*, 169−176.
(474) Cormode, D. P.; Skajaa, T.; van Schooneveld, M. M.; Koole, R.; Jarzyna, P.; Lobatto, M. E.; Calcagno, C.; Barazza, A.; Gordon, R. E.; Zanzonico, P.; et al. Nanocrystal core high-density lipoproteins: a multimodality contrast agent platform. *Nano Lett.* **2008**, *8*, 3715−3723.
(475) Murakami, T. Phospholipid nanodisc engineering for drug delivery systems. *Biotechnol. J.* **2012**, *7*, 762−767.
(476) Ryan, R. O. Nanodisks: hydrophobic drug delivery vehicles. *Expert Opin. Drug Delivery* **2008**, *5*, 343−351.
(477) Numata, M.; Grinkova, Y. V.; Mitchell, J. R.; Chu, H. W.; Sligar, S. G.; Voelker, D. R. Nanodiscs as a therapeutic delivery agent: inhibition of respiratory syncytial virus infection in the lung. *Int. J. Nanomed.* **2013**, *8*, 1417−1427.
(478) Simonsen, J. B. Evaluation of reconstituted high-density lipoprotein (rHDL) as a drug delivery platform - a detailed survey of rHDL particles ranging from biophysical properties to clinical implications. *Nanomedicine* **2016**, *12*, 2161−2179.
(479) Oda, M. N.; Hargreaves, P. L.; Beckstead, J. A.; Redmond, K. A.; van Antwerpen, R.; Ryan, R. O. Reconstituted high density lipoprotein enriched with the polyene antibiotic amphotericin B. *J. Lipid Res.* **2005**, *47*, 260−267.
(480) Nelson, K. G.; Bishop, J. V.; Ryan, R. O.; Titus, R. Nanodisk-associated amphotericin B clears Leishmania major cutaneous infection in susceptible BALB/c mice. *Antimicrob. Agents Chemother.* **2006**, *50*, 1238−1244.

DOI: 10.1021/acs.chemrev.6b00690
Chem. Rev. 2017, 117, 4669−4713

(481) Redmond, K. A.; Nguyen, T. S.; Ryan, R. O. All-trans-retinoic acid nanodisks. *Int. J. Pharm.* **2007**, *339*, 246−250.
(482) Crosby, N. M.; Ghosh, M.; Su, B.; Beckstead, J. A.; Kamei, A.; Simonsen, J. B.; Luo, B.; Gordon, L. I.; Forte, T. M.; Ryan, R. O. Anti-CD20 single chain variable antibody fragment-apolipoprotein A-I chimera containing nanodisks promote targeted bioactive agent delivery to CD20-positive lymphomas. *Biochem. Cell Biol.* **2015**, *93*, 343−350.
(483) Feng, M.; Cai, Q.; Huang, H.; Zhou, P. Liver targeting and anti-HBV activity of reconstituted HDL-acyclovir palmitate complex. *Eur. J. Pharm. Biopharm.* **2008**, *68*, 688−693.
(484) Duivenvoorden, R.; Tang, J.; Cormode, D. P.; Mieszawska, A. J.; Izquierdo-Garcia, D.; Ozcan, C.; Otten, M. J.; Zaidi, N.; Lobatto, M. E.; van Rijs, S. M.; et al. A statin-loaded reconstituted high-density lipoprotein nanoparticle inhibits atherosclerotic plaque inflammation. *Nat. Commun.* **2014**, *5*, 3065.
(485) Borowska, M. T.; Dominik, P. K.; Anghel, S. A.; Kossiakoff, A. A.; Keenan, R. J. A YidC-like protein in the archaeal plasma membrane. *Structure* **2015**, *23*, 1715−1724.
(486) Dominik, P. K.; Kossiakoff, A. A. Phage display selections for affinity reagents to membrane proteins in nanodiscs. *Methods Enzymol.* **2015**, *557*, 219−245.
(487) Sheng, J. R.; Grimme, S.; Bhattacharya, P.; Stowell, M. H. B.; Artinger, M.; Prabahakar, B. S.; Meriggioli, M. N. In vivo adsorption of autoantibodies in myasthenia gravis using Nanodisc-incorporated acetylcholine receptor. *Exp. Neurol.* **2010**, *225*, 320−327.
(488) Bhattacharya, P.; Grimme, S.; Ganesh, B.; Gopisetty, A.; Sheng, J. R.; Martinez, O.; Jayarama, S.; Artinger, M.; Meriggioli, M.; Prabhakar, B. S. Nanodisc-Incorporated hemagglutinin provides protective immunity against influenza virus infection. *J. Virol.* **2010**, *84*, 361−371.
(489) Frueh, V.; Zhou, Y.; Chen, D.; Loch, C.; Ab, E.; Grinkova, Y. V.; Verheij, H.; Sligar, S. G.; Bushweller, J. H.; Siegal, G. Application of fragment-based drug discovery to membrane proteins: Identification of ligands of the integral membrane enzyme DsbB. *Chem. Biol.* **2010**, *17*, 881−891.
(490) Vanwetswinkel, S.; Heetebrij, R. J.; van Duynhoven, J.; Hollander, J. G.; Filippov, D. V.; Hajduk, P. J.; Siegal, G. TINS, target immobilized NMR screening: an efficient and sensitive method for ligand discovery. *Chem. Biol.* **2005**, *12*, 207−216.
(491) Roy, J.; Pondenis, H.; Fan, T. M.; Das, A. Direct capture of functional proteins from mammalian plasma membranes into Nanodiscs. *Biochemistry* **2015**, *54*, 6299−6302.
(492) Pavlidou, M.; Haenel, K.; Moeckel, L.; Willbold, D. Nanodiscs allow phage display selection for ligands to non-linear epitopes on membrane proteins. *PLoS One* **2013**, *8*, e72272.
(493) Laursen, T.; Borch, J.; Knudsen, C.; Bavishi, K.; Torta, F.; Martens, H. J.; Silvestro, D.; Hatzakis, N. S.; Wenk, M. R.; Dafforn, T. R.; et al. Characterization of a dynamic metabolon producing the defense compound dhurrin in sorghum. *Science* **2016**, *354*, 890−893.
(494) Oertel, J.; Keller, A.; Prinz, J.; Schreiber, B.; Hubner, R.; Kerbusch, J.; Bald, I.; Fahmy, K. Anisotropic metal growth on phospholipid nanodiscs via lipid bilayer expansion. *Sci. Rep.* **2016**, *6*, 26718.
(495) Cormode, D. P.; Jarzyna, P. A.; Mulder, W. J.; Fayad, Z. A. Modified natural nanoparticles as contrast agents for medical imaging. *Adv. Drug Delivery Rev.* **2010**, *62*, 329−338.
(496) Kim, Y.; Fay, F.; Cormode, D. P.; Sanchez-Gaytan, B. L.; Tang, J.; Hennessy, E. J.; Ma, M.; Moore, K.; Farokhzad, O. C.; Fisher, E. A.; et al. Single step reconstitution of multifunctional high-density lipoprotein-derived nanomaterials using microfluidics. *ACS Nano* **2013**, *7*, 9975−9983.
(497) Lim, S. J.; McDougle, D. R.; Zahid, M. U.; Ma, L.; Das, A.; Smith, A. M. Lipoprotein nanoplatelets: Brightly fluorescent, zwitterionic probes with rapid cellular entry. *J. Am. Chem. Soc.* **2016**, *138*, 64−67.
(498) Sligar, S. G.; Salemme, F. R. Protein engineering for molecular electronics. *Curr. Opin. Biotechnol.* **1992**, *3*, 388−393.
(499) Beales, P. A.; Geerts, N.; Inampudi, K. K.; Shigematsu, H.; Wilson, C. J.; Vanderlick, T. K. Reversible assembly of stacked membrane Nanodiscs with reduced dimensionality and variable periodicity. *J. Am. Chem. Soc.* **2013**, *135*, 3335−3338.
(500) Geerts, N.; Schreck, C. F.; Beales, P. A.; Shigematsu, H.; O'Hern, C. S.; Vanderlick, T. K. Using DNA-driven assembled phospholipid Nanodiscs as a scaffold for gold nanoparticle patterning. *Langmuir* **2013**, *29*, 13089−13094.
(501) Ham, M.-H.; Choi, J. H.; Boghossian, A. A.; Jeng, E. S.; Graff, R. A.; Heller, D. A.; Chang, A. C.; Mattis, A.; Bayburt, T. H.; Grinkova, Y. V.; et al. Photoelectrochemical complexes for solar energy conversion that chemically and autonomously regenerate. *Nat. Chem.* **2010**, *2*, 929−936.
(502) Goldsmith, B. R.; Mitala, J. J., Jr.; Josue, J.; Castro, A.; Lerner, M. B.; Bayburt, T. H.; Khamis, S. M.; Jones, R. A.; Brand, J. G.; Sligar, S. G.; et al. Biomimetic chemical sensors using nanoelectronic readout of olfactory receptor proteins. *ACS Nano* **2011**, *5*, 5408−5416.

DOI: 10.1021/acs.chemrev.6b00690
Chem. Rev. 2017, 117, 4669−4713